UNIVERSITAT DE BARCELONA

Network biology identifies novel apoptosis-related proteins and synergistic drug combinations in breast cancer

Eva Capdevila Busquets

UNIVERSITAT DE BARCELONA

UNIVESITAT DE BARCELONA, FACULTAT DE BIOLOGIA

PROGRAMA DE DOCTORAT EN BIOMEDICINA

FEBRER 2016

Network biology identifies novel apoptosis-related proteins and synergistic drug combinations in breast cancer

Memòria presentada per

Eva Capdevila Busquets

Per optar al títol de doctor per la Universitat de Barcelona. Tesis realitzada a l'Institut de Recerca Biomèdica de Barcelona

Director

Dr. Patrick Aloy Calaf

Doctorand

Eva Capdevila Busquets

Table of contents

List of figures

List of tables

Abbreviations

3AT	3-aminotriazole
ADME	Absorption, distribution, metabolism and elimination
AI	Aromatase inhibitors
AIF	Apoptosis-inducing factor
Apaf-1	Apoptotic protease activating factor 1
APO-1	Apoptosis antigen 1
APS	Ammonium persulphate
AR	Androgen receptor
ATC	Anatomical Therapeutic Chemical
ATM	Ataxia telangiectasia mutated
Bad	Bcl-2-associated death promoter
BAG4	BCL2-associated athanogene 4
Bak	Bcl-2-antagonist killer
Bax	Bcl-2-associated X protein
BC	Breast cancer
Bid	BH3 interacting-domain death agonist
Bim	Bcl-2 interacting mediator of cell death
BRCA1/2	Breast cancer 1/2
BRIP1	BRCA1-interacting protein 1
BC	Breast cancer
BCAR3	Breast cancer anti-estrogen resistance 3

Bcl-2	B-cell lymphoma 2
Bcl-xL	B-cell lymphoma-extra large
BH	Bcl-2 homology
CASP	Caspase
CC	Cellular compartment
CD95	Cluster of differentiation 95
CDK	Cyclin-dependent kinase
CHEK2	Checkpoint kinase 2
ChT	Chemotherapy
CK	Cytokeratin
CP	Co-expression profile
CSC	Cancer stem cell
DC	Drug combination
DCDB	Drug combination database
DCI	Drug combination index
DIABLO	Direct inhibitor of apoptosis protein (IAP)-binding protein with low pI
DISC	Death-inducing signalling complex
DMEM	Dulbecco's modified eagle medium
DMSO	Dimethyl sulfoxide
DR	Death receptor
DTT	Dithiothreitol
ECL	Enhanced ChemiLuminiscence

EDTA	Etilendiaminotetraacetic acid
EGF	Epidermal growth factor
EGFR	Epidermal growth factor receptor
EM	Expectation-Maximization
EMT	Epithelial-mesenchymal transition
EndoG	Endonuclease G
EPSTI1	Epithelial stromal interaction 1
ER	Estrogen receptor
ERK	Extracellular signal-regulated kinases
ES	Expression similarity
ET	Endocrine therapy
ELK-1	ETS domain-containing protein
ETS-1	Protein C-ets-1
FBS	Fetal bovine serum
FADD	Fas-associated death domain
FDA	US food and drug administration
FGF	Fibroblast growth factor
Flt	Fms-like tyrosine kinase
Flk	FMS-like tyrosine kinase
HC	high-confidence
HDAC	Histone deacetylase
HER	Human epidermal growth factor receptor
HR	Hormone receptor

HRP	Horseradish peroxidase
Hsp90	Heat shock protein 90
HTRA2	High-temperature-requirement protein A2
IAP	Inhibitor of apoptosis proteins
IFN-α	Interferon alpha
IGF	Insulin growth factor
IGF1R	Insulin-like growth factor 1 receptor
IRS	Insulin receptor substrates
IHC	Immunohistochemistry
IL	Interleukin
JAK	Janus kinase
JNK	Jun NH2-terminalk kinase
KEGG	Kyoto Encyclopedia of Genes and Genomes
Leu	Leucine
MAPK	Mitogen activated protein kinase
Mcl-1	Myeloid cell leukemia 1
MEK	Mitogen-activated protein kinase/extracellular signal-regulated kinase kinase
mTOR	mammalian target of rapamycin
MTT	methyl3-[4,5-dimethylthiazol-2-il]-2,5-diphenyltetrazolium bromide
NA	Network activity
NCI	National cancer institute
NE	Network efficiency

NR3C2	Nuclear receptor subfamily 3 group C member 2
OE	Overexpressed
ORF	Open reading frame
PALB2	Partner and localizer of BRCA2
PARP	Poly (ADP-ribose) polymerase
PBS	Phosphate-buffered saline
PCI	Pathway crosstalk inhibition
PCR	Polymerase chain reaction
PDGFR	Platelet-derived growth factor receptor
PDK	Pyruvate dehydrogenase kinase
PFA	Paraformaldehyde
PI	Propidium iodide
PI3K	Phosphatidylinositol 3-kinase
PI3P	Phosphatidylinositol-3,4,5-triphosphate
PK	Pharmacokinetic
PKB/AKT	Protein kinase B
***p*NA**	*p*-nitroanilide
PPI	Protein-protein interaction
PR	Progesterone receptor
PS	Phosphatidylserine
PSMC3IP	Proteasome 26S ATPase subunit 3-interacting protein
PTEN	Phosphatase and tensin homolog

Puma	p53 upregulated modulator of apoptosis
PVDF	Polyvinylidene difluoride
RNA	Ribonucleic acid
RSE	Relative standard error
RSK	Ribosomal S6 kinase
RT	Room temperature
RTK	Receptor tyrosine kinase
SA	Specific activity
SDS	Sodium dodecyl sulphate
SDS-PAGE	SDS- polyacrylamide gel electrophoresis
SERM	selective estrogen receptor modulator
SMAC	Second mitochondria-derived activator of caspase
SOC	Super optimal broth with catabolite repression
STAT	Signal Transducer and Activator of Transcription
STK11	Serine/threonine kinase 11
T	Trastuzumab
TBS	Tris-buffered saline
TdT	terminal deoxynucleotidyl transferase
TE	Tris-EDTA
TF	Transcription factor
Tm	Melting temperature
TEMED	Tetramethylethylenediamine
TNF	Tumour necrosis factor

TNFR1	TNF receptor 1
TKI	Tyrosine kinase inhibitors
TNBC	Triple-negative breast cancer
TP53	Tumor protein p53
TRAIL	TNF-related apoptosis-inducing ligand-receptor 1
Trp	Tryptophan
TUNEL	Terminal deoxynucleotidyl transferase dUTP nick end labeling
VEGFR	Vascular endothelial growth factor receptor
XIAP	X-linked inhibitor of apoptosis protein
Y2H	Yeast two-hybrid

1. INTRODUCTION

1.1 BREAST CANCER

Breast cancer is by far the most commonly diagnosed type of cancer and the leading cause of cancer death in women worldwide, with more than 1.3 million cases each year and accounting for 15% of cancer-related deaths (Torre et al., 2015).

The vast majority of breast tumours are carcinomas (tumours developed from epithelial cells), whereas less than 1% are sarcomas (arisen from connective tissue, bone, muscle or fat). Among all breast cancer types, 75% are ductal carcinoma, which develops in the epithelial cells lining the milk ducts; less than 10% localize within the breast lobes and are called lobular carcinomas; while Paget's disease (cancer of the areola and nipple) and inflammatory carcinoma account for nearly all other forms of breast cancer.

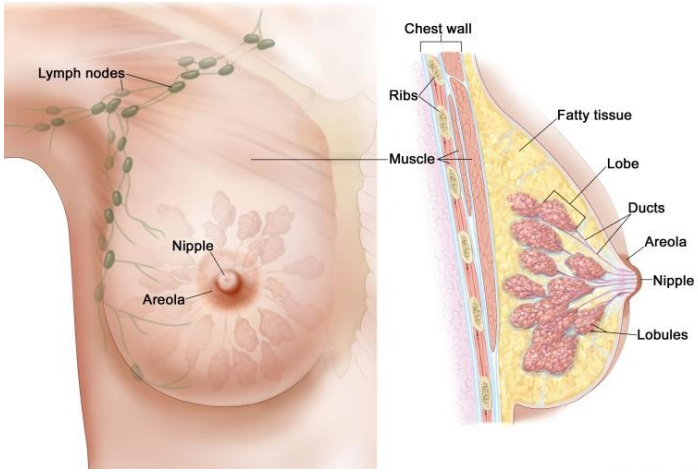

Figure 1. **Breast anatomy** (http://www.cancer.gov)

1.1.1 Risk factors

Genetic susceptibility is believed to be the primary cause of approximately 5–10% of breast cancers, up to 90% of which are due to mutations in *BRCA1* and *BRCA2* genes, whereas a substantial minority is caused by non-BRCA mutations, such as *TP53, PTEN, STK11, CHEK2, ATM, BRIP1,* and *PALB2* mutations (Gage et al., 2012, Pasche, 2010).

Additionally, several factors affecting hormonal status (i.e. early menstruation, late menopause, never having been pregnant and long-term use of hormone therapy) and lifestyle/environmental agents (i.e., fat-rich diet, alcohol consumption and ionizing radiation) are also associated to breast cancer predisposition (http://www.cancer.gov).

1.1.2 Initiation and progression

The natural history of breast cancer involves progression through defined pathological and clinical stages, starting with cell hyperproliferation that could potentially evolve into *in situ*, invasive carcinomas, and finally into metastatic disease (Allred et al., 2001, Burstein et al., 2004). The initiation of breast cancer is due to transforming (genetic and epigenetic) events in the tissue cells, and subsequent tumour progression is driven by the accumulation of additional genetic changes combined with clonal expansion and selection (Polyak, 2007).

In phenotypically normal tissue, epithelial structures consist of central luminal epithelial cells surrounded by myoepithelial cells and enclosed by a continuous basement membrane, while the primarily collagenous stroma contains fibroblasts, immune cells and blood vessels. Progression to carcinoma *in situ* is characterized by proliferative epithelial cells enclosed in a still-continuous basement membrane, increased number of fibroblasts and immune cell infiltration, and enhanced angiogenesis. Finally, invasive breast carcinoma is defined by breakdown of the basement membrane, loss of

myoepithelial cells, and invasion of the tumour cells into the surrounding stroma and the vasculature (Cichon et al., 2010) (**Figure 2**).

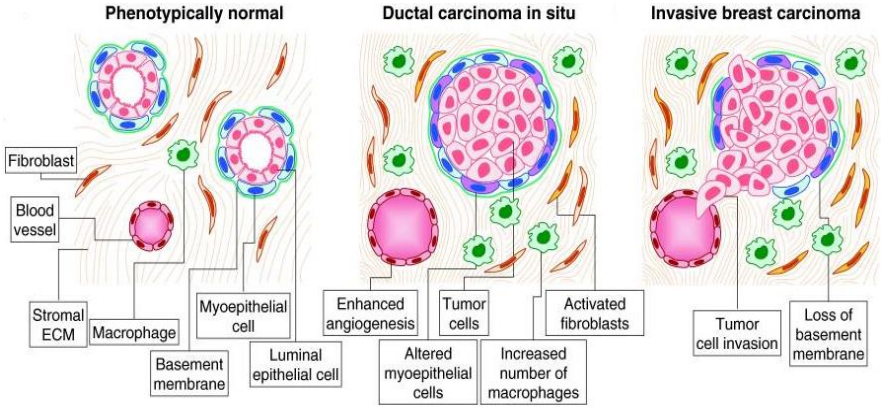

Figure 2. Breast tumourigenesis and progression. The stepwise progression from epithelial hyperplasia to invasive carcinoma and eventually metastasis (Cichon et al., 2010).

According to the progression of the disease, breast cancer may be classified into four clinical stages as defined by tumour size and spread, with stage 0 corresponding to *in situ* carcinoma and stage IV to the metastatic tumour. This classification is used to group tumours with respect to prognosis as well as to define therapeutic strategies.

1.1.3 Breast cancer subtypes

Breast cancer is a heterogeneous disease in terms of histology, therapeutic response, dissemination patterns to distant sites and patient outcomes. For this reason, breast tumours can be classified in different ways based on: (i) histology into ductal or lobular carcinomas, (ii) differentiation state/gene expression profiles into luminal and basal-like subtypes, and (iii) the expression of estrogen receptor (ER), progesterone receptor (PR) and HER2 receptor, into hormone receptor (ER and PR) positive, HER2+, ER+PR+HER2+ (triple positive) and ER−PR−HER2− (triple-negative

breast cancer, TNBC) subtypes (Polyak and Metzger Filho, 2012). At the molecular level, the analysis of breast cancer gene expression patterns derived from cDNA microarrays led to the initial definition of four major intrinsic gene signatures: luminal, HER2-enriched, basal-like and normal breast-like subtype (Perou et al., 2000). However, subsequent studies redefined these intrinsic molecular subtypes: Luminal A, Luminal B, HER2-enriched and Basal-like (Cancer Genome Atlas, 2012, Prat et al., 2012, Prat et al., 2010, Prat and Perou, 2011) (**Figure 3**).

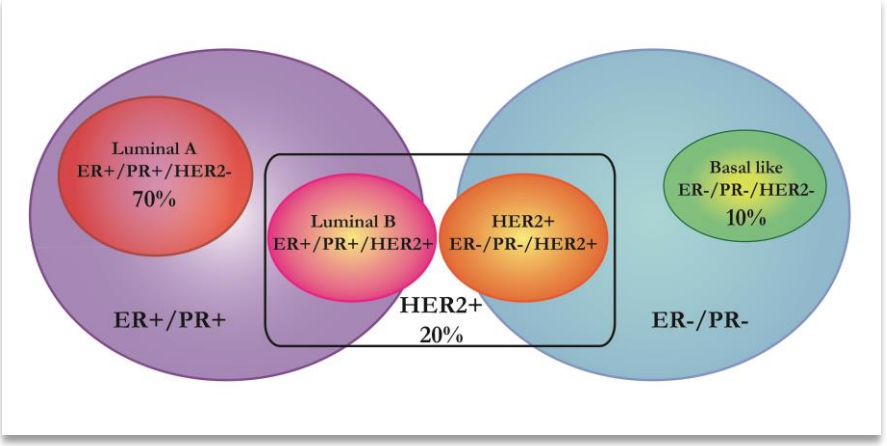

Figure 3. Breast cancer intrinsic subtypes. Receptor status and frequency of breast cancer subtypes.

TNBC is the most aggressive subtype, with high rates of relapse and the one with the worst overall survival rate. For years, the relationship between basal-like and TNBC tumours has been controversial. Indeed, not all TNBCs are identified as basal-like tumours by gene expression, and *vice versa*. Thus, basal-like tumours are characterized by the expression of genes found in normal basal/myoepithelial breast cells, including high-molecular-weight basal cytokeratins (*CK5/6, CK14, and CK17*), epidermal growth factor receptor (*EGFR*), or both, which are not expressed in all triple negative tumours (Nielsen et al., 2004).

Luminal breast cancer is the most common subtype and presents the best prognosis and low recurrence rates. These tumours are characterized by the expression of ER and represent an heterogeneous category that is divided in two subgroups according to different gene expression patterns that correlate with different patient survival, disease relapse, site of metastasis, and response to chemotherapy (Kennecke et al., 2010, Rouzier et al., 2005, Sorlie et al., 2001).

Finally, HER2-positive subtype shows HER2 protein overexpression and has been associated with poor prognosis, increased resistance to chemotherapy and, in addition, it is prone to early and frequent recurrence and metastases (Toss and Cristofanilli, 2015).

1.1.4 Deregulated processes in breast cancer

It has been suggested that the complexity of cancer can be reduced to a manifestation of ten essential physiologic changes that collectively dictate malignant grow: sustained proliferative signalling, growth suppressors evasion, immune destruction escape, limitless replicative potential, tumour-promoting inflammation, activation of invasion and metastasis, angiogenesis induction, deregulation of cellular energetics, genome instability and apoptosis evasion (**Figure 4**) (Hanahan and Weinberg, 2000, Hanahan and Weinberg, 2011).

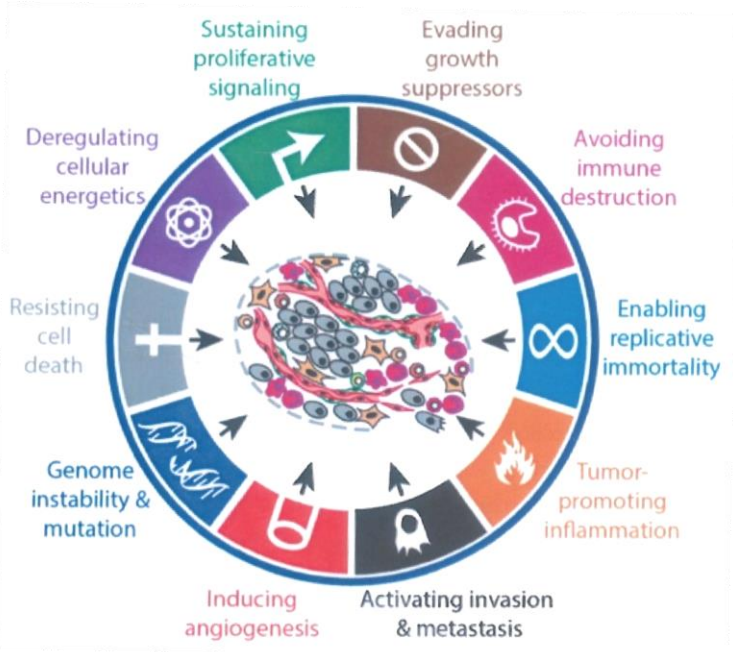

Figure 4. The hallmarks of cancer. Acquired functional capabilities necessary for tumour growth and progression. Adapted from (Hanahan and Weinberg, 2011).

Driver and passenger genes in cancer progression

Cancer progression is an example of a rapidly adapting population which exhibits a high mutation rate and rapidly change in population size (Hanahan and Weinberg, 2011, Lawrence et al., 2013). Progression is driven by a handful of mutations (Lawrence et al., 2014) and chromosomal abnormalities (Zack et al., 2013) in cancer-related genes (oncogenes and tumour suppressors), collectively called "drivers." Drivers are beneficial to cancer cells as they facilitate uncontrolled proliferation and other hallmarks of cancer. In solid tumours such as pancreatic, colorectal, breast, and brain cancers, the number of mutated driver genes is often three to six, but several tumours have only one or two driver gene mutations (Vogelstein and Kinzler, 2004).

Drivers, however, arise alongside thousands of other mutations/alterations, called "passengers," that are randomly dispersed throughout the genome, are nonrecurrent in patients, and have no immediate beneficial effect (Lawrence et al., 2014). Passengers have previously been assumed to be neutral and largely ignored in cancer research, yet growing evidence suggests that they can play an important role in both cancer progression and clinical outcomes. However, the molecular mechanisms that relate, for instance, changes in expression of the many passenger genes to breast cancer onset and progression are largely unknown.

All of the known cancer driver genes can be classified into one or more of 12 pathways that regulate three core cellular processes: cell fate, cell survival, and genome maintenance (Vogelstein et al., 2013) (**Figure 5**).

It is becoming increasingly clear that pathways rather than individual genes govern the course of tumourigenesis (Vogelstein and Kinzler, 2004), thus mutations in any of several genes of a single pathway can thereby cause an increase in cell proliferation.

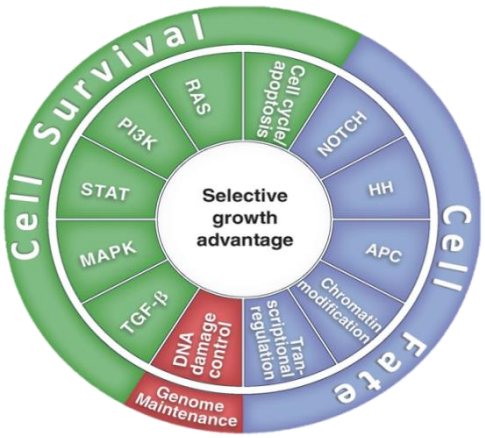

Figure 5. Cancer cell signalling pathways and the cellular processes they regulate (Vogelstein et al., 2013).

Genomic aberrations in breast carcinogenesis

The systematic characterization of breast cancer genomes has identified somatic mutations in several key signalling pathways (**Figure 6**). In particular, the expression of proteins belonging to the EGFR/PI3K/mitogen activated protein kinase (MAPK) pathways is frequently altered in breast cancer. Since these pathways play prominent roles in malignant transformation, apoptosis regulation, drug resistance and metastasis, altered proteins involved in these routes are potential therapeutic targets and markers, guiding the selection of patients who would most likely benefit from particular therapies.

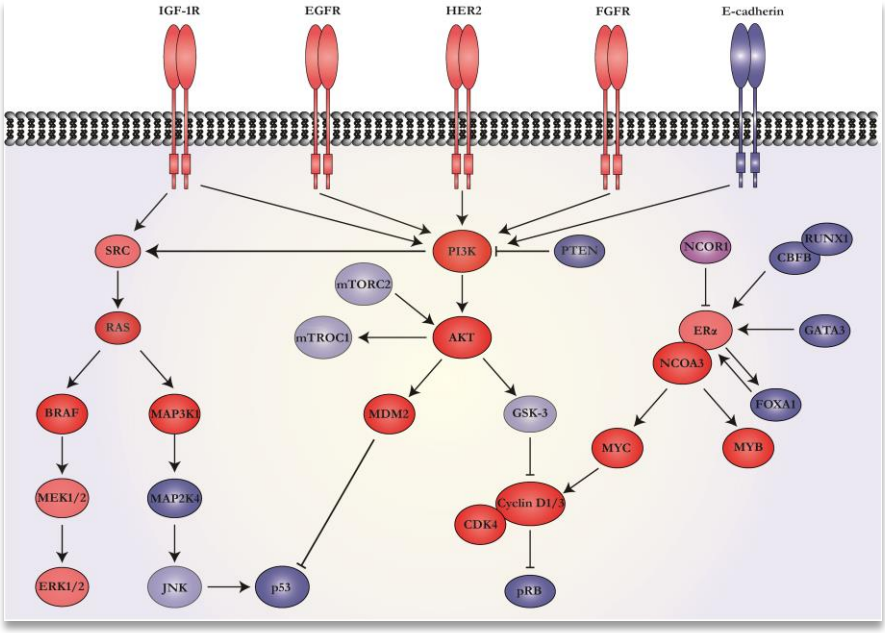

Figure 6. **Overview of the key signalling pathways involved in breast cancer based on somatic mutations.** Colours indicate tumour suppressor (blue), oncogene (red) or mutant genes with unclear role (purple) and lighter shading marks pathway components in which somatic mutations have not been identified. Adapted from (Polyak and Metzger Filho, 2012).

PI3K/AKT/mTOR pathway

The phosphatidylinositol 3-kinase (PI3K)-Akt signaling pathway is activated by many types of cellular stimuli and regulates fundamental cellular functions such as transcription, translation, proliferation, growth, and survival (Osaki et al., 2004). The PI3K/AKT signaling is the most frequently mutated pathway in breast cancer and promotes enhanced cell proliferation and survival, growth factor independence, protection from apoptosis, and drug resistance (Eichhorn et al., 2008, Isakoff et al., 2005, Samuels et al., 2005).

PI3Ks are heterodimeric kinases consisting of a catalytic subunit p110 and a regulatory subunit p85, the latter acting as an adaptor that mediates the activation of PI3K by RTKs and other kinases. PI3K phosphorylates phosphatidylinositol 4-phosphate and phosphatidylinositol 4,5-bisphosphate to generate phosphatidylinositol-3,4,5-triphosphate (PIP3), which recruits PH-domain-containing proteins, including Akt1 and PDK1, to the cell membrane. In the cell membrane, Akt is phosphorylated by PDK1 first, and fully activated by mammalian target of rapamycin C2 (mTORC2) or PDK2 (Chan and Tsichlis, 2001, Toss and Cristofanilli, 2015). Once activated, Akt may induce signals interfering with the apoptotic functions by inactivation of BAD, one of the members of the Bcl-2 family of proteins, resulting in protection from apoptosis (see Section 1.2 for more detailed information) (Peruzzi et al., 1999). Akt activation also leads to increased protein synthesis, by this means promoting cell proliferation and motility, possibly through activation of mTOR, among other mechanisms (Al-Bazz et al., 2009, Altomare and Testa, 2005, Xue and Hemmings, 2013).

The activity of PI3K is antagonized by PTEN, a tumour suppressor. PTEN is a dual-specificity phosphatase that dephosphorylates PIP3, leading to inhibition of Akt kinase activity, and can also antagonize the MAP kinase pathway via its protein phosphatase function (Song et al., 2012).

Insulin-like growth factor 1 receptor (IGF-1R)

IGF-1R is a transmembrane tyrosine receptor kinase (RTK) involved in cell growth and survival control. It is expressed in normal and malignant breast tissue and has been implicated in cell survival and resistance to cytotoxic therapies (Yerushalmi et al., 2012).

Insulin growth factor ligands (IGF1 or IGF2) bind IGF-1R resulting in its auto-phosphorylation and recruitment of insulin receptor substrates 1 and 2 (IRS1 and IRS2) (Myers et al., 1993). Subsequently, IRS1 and IRS2 initiate phosphorylation cascades that transmit the IGF-1R signal to downstream signalling pathways such as PI3K/AKT and RAS/MAPK/ERK1 promoting cancer cell proliferation (Dearth et al., 2006).

EGFR family

The EGFR family proteins are RTKs involved in the regulation of diverse cellular pathways leading to proliferation, migration, gene transcription, cell cycle progression and cell survival. Deregulation of EGFRs by overexpression, amplification or mutations is frequently linked to hyperproliferative diseases such as breast cancer (Prenzel et al., 2001).

EGFR family also called the ErbB or (HER) family comprises 4 transmembrane RTKs: EGFR (or HER1), HER2, HER3, and HER4 (also called ErbB2, ErbB3 and ErbB4 respectively) (Prenzel et al., 2001). Activation of HER receptors requires binding of growth factor ligand promoting receptor dimerization (to form both homo- and heterodimeric HER complexes) and phosphorylation on tyrosine residues. Phosphorylated tyrosine residues serve as docking sites for adaptor proteins such as Grb2 and the p85 subunit of the PI3K complex, which elicit the activation of several downstream pathways such as AKT, MAPK and STAT, thereby triggering the activation of several biologic functions, and ultimately resulting in cell survival and proliferation (Baker et al., 2014).

Vascular Endothelial Growth Factor Receptor (VEGFR) family

The VEGFR family contains three RTKs, VEGFR-1 (Flt-1), VEGFR-2 (KDR/Flk-1) and VEGFR-3 (Flt-4), that regulate blood and lymphatic vessel formation (Olsson et al., 2006). While abundantly expressed in endothelial cells, VEGFR-2 is also expressed by different cancers including breast cancer (Guo et al., 2010). Secreted by both cancer and stromal cells, VEGF preferentially binds VEGFR-2 on endothelial cells to stimulate new blood vessel formation required for cancer growth and metastasis (Chung et al., 2010). VEGF binding leads to receptor dimerization and activation of the VEGF/VEGFR-2 complex that recruits the adaptor proteins Shc, Grb2 and Nck, and protein tyrosine phosphatase SHP-1 and SHP-2, leading to the induction of downstream effects including cell survival (through the PI3K/Akt pathway) and proliferation (through the Raf/MEK/Erk pathway) (Karkkainen and Petrova, 2000). In addition of regulating angiogenesis, VEGF can also synergize with EGFR to promote autocrine growth factor-mediated tumour cell proliferation (Lichtenberger et al., 2010).

Estrogen Receptor alpha (ERa)

The estrogen receptor alpha (ERα) is a ligand-dependent nuclear hormone receptor involved in the regulation of gene expression, which controls cellular proliferation and differentiation in target tissues. ERα is expressed in only a small subset of cells in normal breast epithelium, where it plays an important role in breast development and differentiation. In contrast, 65%–70% of breast tumours display high ERα expression levels and as well as estrogen dependency for tumour growth. The biological effects of oestrogen are mediated through at least three different pathways (**Figure 7**). (i) In the *classical pathway,* hormone binding activates ER allowing its migration to the nucleus where it recruits co-activators and finally induce gene expression (Kushner et al., 2000, Safe, 2001). (ii) In the *ligand independent pathway,* ER can also be activated as a consequence of signalling events downstream of RTKs,

such as the EGFR, HER2 and IGFR, or due to phosphorylation by the ERK or Akt serine/threonine kinases (Musgrove and Sutherland, 2009). (iii) Finally, ER signalling can also be mediated through *non-genomic* mechanisms. ER could be located at the cell membrane or in the cytoplasm and ligand binding induces the assembly of functional protein complexes that involve other signalling molecules which activate intracellular signalling cascades such as MAPK (Song et al., 2004) and PI3K/Akt (Musgrove and Sutherland, 2009), resulting in transcription factor (TF) activation.

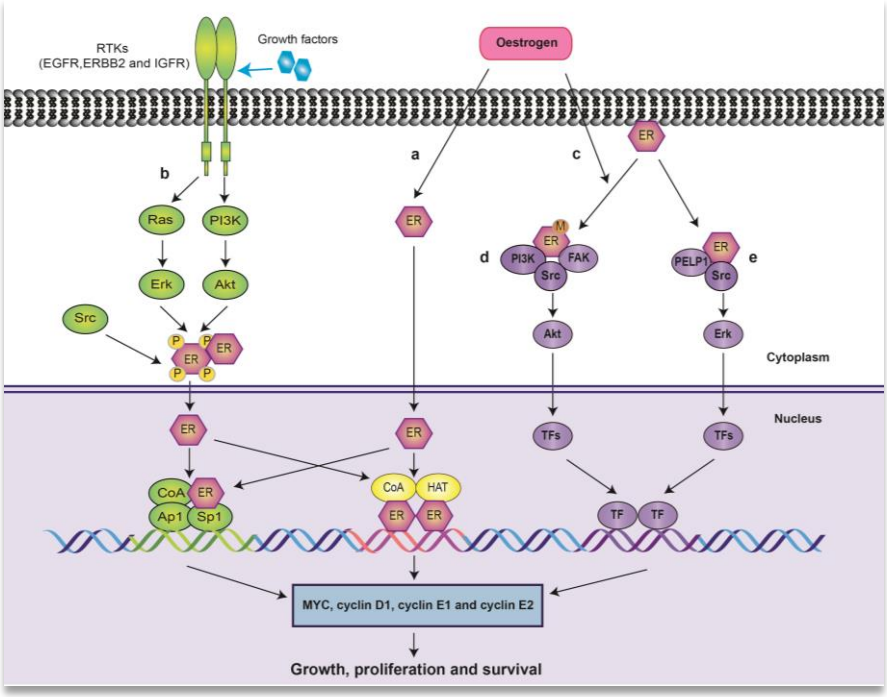

Figure 7. **Distinct pathways of oestrogen regulation of gene expression.** Classic oestrogen signalling **(a)**, ligand independent **(b)**, and non-genomic mechanisms **(c, d and e)**. Adapted from (Musgrove and Sutherland, 2009).

JAK/STAT pathway

Janus kinases (JAKs) and Signal Transducer and Activator of Transcription (STATs) are critical components of many cytokine receptor systems,

regulating growth, survival, differentiation, and pathogen resistance. STAT3, one of the seven members of the STAT family is constitutively activated in all breast cancer subtypes promoting cell proliferation, angiogenesis and metastasis (Yue and Turkson, 2009).

The binding of a cytokine to its cell-surface receptor results in receptor dimerization and the subsequent activation of JAK tyrosine kinases, which are constitutively associated with the receptor. Specific tyrosine residues on the receptor are then phosphorylated by activated JAKs and serve as docking sites for STATs family. STATs are phosphorylated by JAKs, then dimerize and subsequently leave the receptor and translocate to the nucleus, where they activate gene transcription (Darnell, 1997, Levy and Darnell, 2002).

Additionally STATs, in particular STAT3, may also be phosphorylated directly by receptor tyrosine kinases as well as by non-receptor tyrosine kinases such as c-Src (Banerjee and Resat, 2015).

Ras/MAPK pathway

Ras family members (H-Ras, K-Ras, N-Ras, M-Ras) are small GTPases that are indirectly activated via external stimuli, such as ligand-dependent activation of RTKs (Montagut and Settleman, 2009). Signals emanating from Ras are relayed through Raf, MEK, and ERK1/2 to the nucleus, where downstream transcription factors including FOS, MYC, ETS-1, ETS-2, and ELK-1 drive transcriptional programs of cell proliferation and survival (Giltnane and Balko, 2014).

Two proteins in the MAPK pathway, MAP3K1 and MAP2K4, present somatic mutations mainly in luminal breast tumours, yet these two proteins appear almost mutually exclusive relative to one another (Cancer Genome Atlas, 2012). MAP3K1 or MEKK1 is a MAPK kinase kinase activated in response to growth factor stimulation and by expression of activated Ras. In one hand, MAP3K1 selectively phosphorylates and activates MAP2K4,

which in turn phosphorylates and activates JNK and p38 MAPKs. On the other hand, MAP3K1 also encodes an E3 ligase domain that ubiquitylates c-Jun and ERK1/2 (Derijard et al., 1995, Lin et al., 1995, Su et al., 1998).

1.2 APOPTOSIS

Overall, all proteins and pathways mentioned in section 1.1.4 are directly or indirectly related to the apoptotic machinery regulation, thus conferring to the tumour cells the capacity to escape cell death and promote tumour proliferation. Therefore, promoting apoptosis is a promising strategy for breast cancer treatment that allows devising novel therapies to induce cancer cells death or sensitize them to an established treatment.

Programmed cell death (apoptosis) is a tightly controlled self-renovation process that promotes the elimination of undesired cells such as those with potentially harmful mutations, aberrant substratum attachment, or alterations in cell-cycle control, in order to maintain the healthy balance between cell survival and cell death, playing a critical role in the development and homeostasis in normal tissues (Bauer and Helfand, 2006, Kerr JF, 1991, Wong, 2011).

1.2.1 Morphological changes in apoptotic cells

Morphological hallmarks of apoptosis in the nucleus are chromatin condensation and nuclear fragmentation, which are accompanied by rounding up of the cell, reduction in cellular volume and retraction of pseudopods. At the later stage of apoptosis, some of the morphological features include membrane blebbing, ultrastructural modification of cytoplasmic organelles and loss of membrane integrity (Kroemer et al., 2005).

1.2.2 Biochemical changes in apoptotic cells

Broadly, three main types of biochemical changes can be observed in apoptosis: (i) activation of caspases, (ii) DNA and protein breakdown and (iii) membrane changes and recognition by phagocytic cells (Kumar V, 2010).

Early in apoptosis, there is expression of phosphatidylserine (PS) in the outer layers of the cell membrane, which has been "flipped out" from the inner layers. This allows early recognition of dead cells by macrophages, resulting in their phagocytosis without the release of harmful pro-inflammatory cellular components (Hengartner, 2001). This is followed by a characteristic breakdown of DNA into large 50 to 300 kilobase pieces, which is later cleaved into oligonucleosomes by endonucleases (Vaux and Silke, 2003). Although this feature is characteristic of apoptosis, it is not specific for this process, since it can also be observed in necrotic cells (McCarthy and Evan, 1998).

A specific feature of apoptosis is the activation of a group of enzymes belonging to the cysteine protease family named caspases. The apoptotic caspases are generally divided into two classes: the initiator caspases, which include caspase-2, -8, -9 and -10, and the effector caspases, including caspase-3, -6 and -7. All caspases are produced in cells as catalytically inactive zymogens, and must undergo proteolytic cleavage to become active during apoptosis. The activation of an effector caspase is carried out by an initiator caspase through the cleavage at specific internal Asp residues. By contrast, initiator caspases are autoactivated under apoptotic conditions, a process usually requiring and facilitated by multi-component complexes (Shi, 2002). In the end, activated caspases cleave many essential cellular proteins, breaking up the nuclear scaffold and cytoskeleton, and finally activate DNAses, which will further degrade nuclear DNA (Lavrik et al., 2005).

1.2.3 Apoptotic pathways

There are two major apoptotic pathways, the mitochondria-mediated (or intrinsic pathway) and the death receptor-mediated (extrinsic pathway). In both pathways, caspases are the central players since they are the initiators and the executioners of the apoptotic response **(Figure 8).**

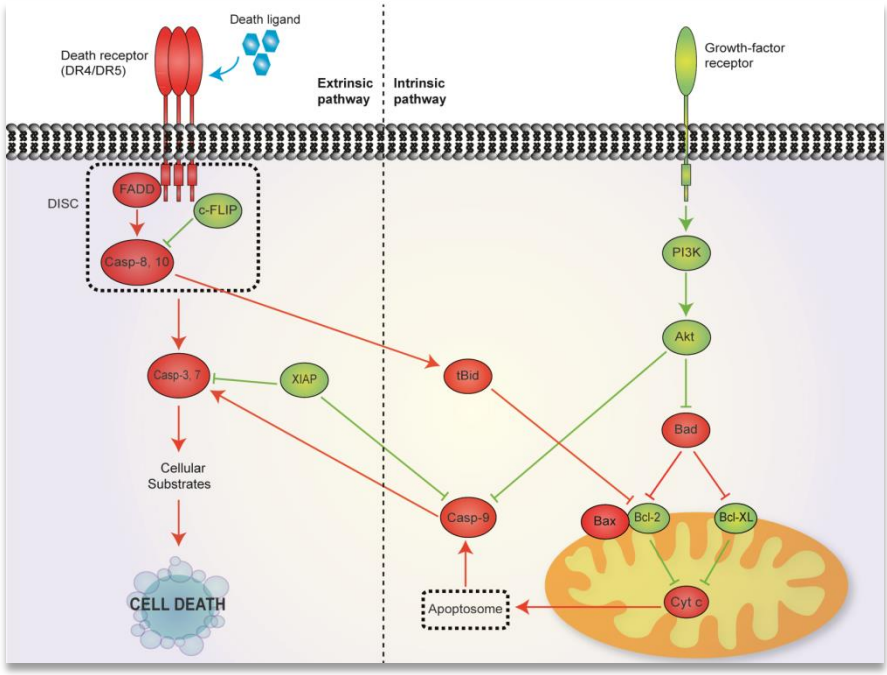

Figure 8. Simplified overview of the apoptotic mechanisms. Colours indicate pro-apoptotic proteins (red) and anti-apoptotic proteins (green).

Intrinsic pathway of apoptosis

In the intrinsic apoptotic pathway, caspase activation is closely linked to permeabilization of the outer mitochondrial membrane. Numerous cytotoxic stimuli and proapoptotic signal-transducing molecules converge to mitochondria to induce outer mitochondrial membrane permeabilization (Decaudin et al., 1998, Green and Kroemer, 2004). This permeabilization is

regulated by proteins from the Bcl-2 family, mitochondrial lipids, proteins that regulate bioenergetic metabolite flux and components of the permeability transition pore (Green and Kroemer, 2004). Upon disruption of the outer mitochondrial membrane, a set of proteins normally found in the space between the inner and outer mitochondrial membranes is released, including Cytochrome c, SMAC (second mitochondria-derived activator of caspases)/DIABLO (direct inhibitor of apoptosis (IAP)-binding protein with low pI), AIF (apoptosis-inducing factor), EndoG (endonuclease G) and Omi/HTRA2 (high-temperature-requirement protein A2) (Cande et al., 2002, Saelens et al., 2004). Once in the cytosol, the binding of cytochrome c to APAF1 induces a conformational change that allows APAF1 to bind to ATP/dATP and to form the apoptosome, which mediates the activation of caspase-9, and thereby triggering the cascade of caspases activation (Jiang and Wang, 2000, Li et al., 1997, Rodriguez and Lazebnik, 1999, Saleh et al., 1999, Zou et al., 1999).

Extrinsic pathway of apoptosis

The extrinsic apoptosis pathway is mediated by death receptors, members of the tumour necrosis factor (TNF) receptor gene superfamily which are involved in a broad range of biological functions, including regulation of cell death and survival, differentiation and immune regulation (Ashkenazi, 2002, Saelens et al., 2004). The best-characterized death receptors include TNF-related apoptosis-inducing ligand-receptor 1 (TRAIL-R1 or DR4), TRAIL-R2 (or DR5), CD95 (APO-1/Fas) and TNF receptor 1 (TNFR1) (Saelens et al., 2004). Activation of death receptors through ligand binding (i.e. TRAIL and TNF-α) leads to the formation of a homotrimeric ligand-receptor complex that recruits further cytosolic factors such as Fas-associated death domain (FADD), which in turn recruits the initiator caspase-8 to form an oligomeric death-inducing signalling complex (DISC) (Kischkel et al., 1995, Peter and Krammer, 2003). Oligomerization of caspase-8 upon DISC

formation drives its activation through self-cleavage, which subsequently cleaves effector caspases, like caspase-3 and caspase-7, resulting in activation or inactivation (as well as translocation), of several substrates such as the poly ADP ribose polymerase (PARP), with the consequent induction of cell death (Juo et al., 1998, Varfolomeev et al., 1998).

Additionally, the extrinsic pathway may crosstalk with the intrinsic pathway through the caspase-8-mediated cleavage of BID, a BH3-only member of the BCL2 family of proteins (Li et al., 1998, Luo et al., 1998), which then triggers the release of mitochondrial proteins.

1.3 APOPTOSIS AND CANCER

Defects in programmed cell death mechanisms play important roles in tumour pathogenesis, allowing neoplastic cells to survive over intended lifespans, subverting the need for exogenous survival factors and providing protection from oxidative stress and hypoxia as the tumour mass expands. This allows time enough for genetic alterations accumulation which will result in the deregulation of cell proliferation, interferences in the differentiation process, angiogenesis promotion, and increased invasiveness during tumour progression (Reed et al., 1998).

There are many ways by which a malignant cell can acquire a reduction of, or resistance to apoptosis. Generally, the mechanisms by which evasion of apoptosis occurs can be broadly divided into: (i) disrupted balance of pro-apoptotic and anti-apoptotic proteins, (ii) reduced caspase function and (iii) impaired death receptor signalling (Wong, 2011) (see **Figure 9** and following sections).

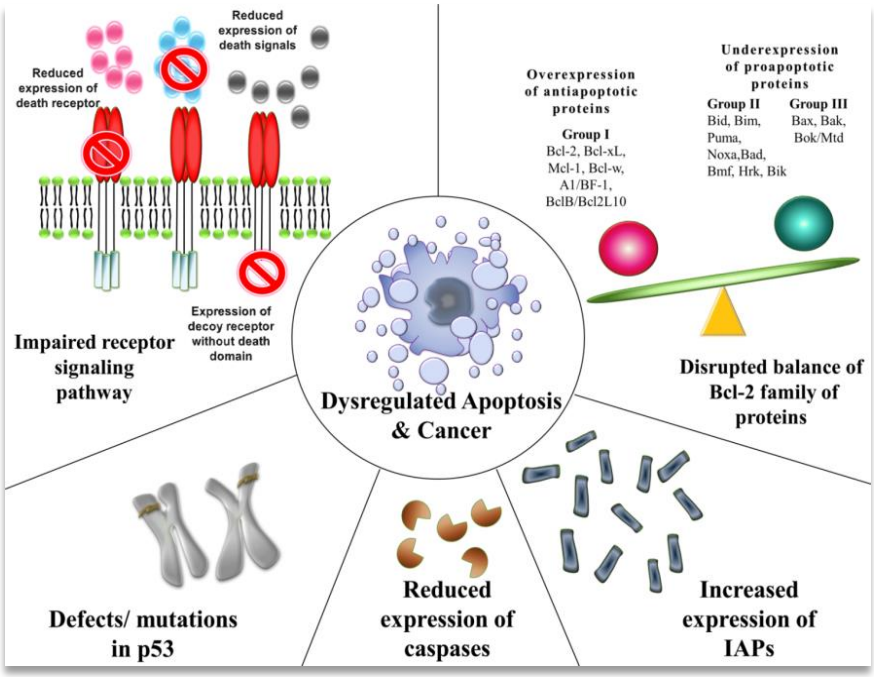

Figure 9. **Dysregulated apoptosis and cancer.** (Wong, 2011)

1.3.1Disrupted balance of pro-apoptotic and anti-apoptotic proteins

Many proteins have been reported to exert pro- or anti-apoptotic activity in the cell. It is not the absolute quantity but rather the ratio of these pro- and anti-apoptotic proteins that plays an important role in the regulation of cell death.

The Bcl-2 family of proteins

The Bcl-2 family of proteins is constituted of pro-apoptotic and anti-apoptotic proteins that play a pivotal role in the regulation of apoptosis, especially via the intrinsic pathway (Gross et al., 1999). They are responsible for the mitochondrial membrane permeability (Minn et al., 1997) and based on their function and the Bcl-2 homology (BH) domains, the Bcl-2 family members are further divided into three groups: (i) anti-apoptotic proteins

that have all four BH domains (i.e. Bcl-2, Bcl-xL, Mcl-1), (ii) pro-apoptotic proteins containing all four BH domains (i.e. Bax and Bak) and (iii) pro-apoptotic BH3-only proteins (i.e. Bid, Bim, Puma, Noxa and Bad) that function either by directly inducing the oligomerization of Bak and Bax or by inhibiting the anti-apoptotic BCL2 proteins (Huang and Strasser, 2000, Wei et al., 2001).

The disruption in the balance between anti-apoptotic and pro-apoptotic members of the Bcl-2 family may be due to overexpression of one or more anti-apoptotic proteins, underexpression of one or more pro-apoptotic proteins, or a combination of both.

p53 protein

The p53 protein is one of the best known tumour suppressor proteins, and it is encoded by the tumour suppressor gene TP53. The mutation of p53 oncogene has been linked to more than 50% of human cancers (Bai, 2006). Since its discovery, many studies have looked into its function and role in cancer, and have reported that it is not only involved in the induction of apoptosis but it is also a key player in cell cycle regulation, development, differentiation, gene amplification, DNA recombination, chromosomal segregation and cellular senescence (Bai, 2006).

Inhibitor of apoptosis proteins (IAPs)

The inhibitor of apoptosis proteins are a group of structurally and functionally related proteins that regulate apoptosis, cytokinesis and signal transduction, whose expression is dysregulated in many cancers. IAPs are endogenous inhibitors of caspase activity by binding through their conserved BIR domains to the active sites of caspases, thereby promoting degradation of active caspases or keeping them away from their substrates (Wei, 2008).

1.3.2 Reduced caspase activity

As mentioned above, caspases are one of the more important players in the initiation and execution of apoptosis. It is therefore reasonable to assume that lowering the levels of caspases or impairing their function may lead to a decrease in apoptosis and carcinogenesis.

Of note, it has been described that caspases-3 mRNA levels in total RNA samples from breast, ovarian, and cervical tumours are either undetectable (breast and cervical) or substantially decreased (ovarian). In addition, sensitivity of caspase-3-deficient breast cancer cell line (MCF-7) to undergo apoptosis in response to anticancer drug or other stimuli of apoptosis could be enhanced by restoring caspase-3 expression (Devarajan, 2002), suggesting that the loss of caspases-3 expression and function contribute to breast cancer cell survival. In some instances, more than one caspase can be downregulated, contributing to tumour cell growth and development (Devarajan, 2002).

1.3.3 Impaired death receptor signalling

Several abnormalities in the death signalling pathways that can lead to evasion of the extrinsic pathway of apoptosis have been identified (i.e. downregulation of the receptor, impairment of receptor function and reduced level in the death signals) (Wong, 2011).

In conclusion, every defect or abnormality along the apoptotic pathways can lead to tumour progression. Therefore, therapeutic strategies aimed to induce apoptosis in cancer cells are crucial for cancer treatment.

1.4 BREAST CANCER THERAPY

Depending on the tumour histological type, grade, ER/PR/HER2 status and tumour spread, different treatment strategies are applied. In general, the

primary treatment of most breast cancers is surgery, followed by chemotherapy (when indicated), radiotherapy, and targeted therapies.

1.4.1 Radiation therapy

Radiation therapy is a treatment with high-energy rays that destroy cancer cells but it has also deleterious effects in normal cells, thus causing some damage to the normal tissue surrounding the tumour. This therapy is usually performed after surgery with the aim to kill the remaining cancer cells and it is also used to treat cancer that has spread to other areas, for example to the bones or brain.

1.4.2 Systemic therapy

Systemic therapy takes advantage of drugs that reach and affect cells throughout the body. Any combination of systemic treatments may be used and it includes chemotherapy and targeted therapy.

Chemotherapy

Chemotherapy refers to the use of cytotoxic drugs which kill indiscriminately cells that divide rapidly, thus impairing cancer cells, but it also harms healthy cells such as bone marrow cells, hair follicles or digestive tract, resulting in its characteristic and strong side effects (immunodepression, inflammation of digestive tract and alopecia). There are three major types of chemotherapy:

- Neoadjuvant (given before surgery): to shrink the size of the tumour
- Adjuvant (given after surgery): to reduce the risk of recurrence, or instead of surgery for those cases in which surgery is considered unsuitable.
- As the main treatment for advanced/metastatic breast cancer

Targeted therapies

The description of well-defined molecular subtypes of breast cancer, together with the identification of the driving genetic alterations and

signalling pathways, has led to the clinical development of a number of successful molecular targeted agents. Targeted therapies are directed to specific genes, proteins, or the tissue environment that contributes to cancer growth and survival. In contrast to traditional chemotherapy, this type of treatment blocks the growth and spread of cancer cells while limiting damage to healthy cells.

The discovery of the role of the hormone estrogen in the stimulation of breast cancer growth (Beatson, 1896), paved the way for the development of therapies to treat breast cancer types that are HR-positive (ER and/or PR positive). These therapies are aimed to inhibit oestrogen synthesis or block the binding to its receptor. One example is tamoxifen, an ER antagonist that is the principal form of adjuvant treatment in premenopausal women with ER-positive disease (Howell et al., 2005). Additionally, aromatase inhibitors (AI), a class of drugs that decrease the production of estrogen by blocking the aromatase enzyme, have been approved as the first line treatment in the adjuvant therapy of HR-positive postmenopausal breast cancer (i.e. letrozole, anastrozole and exemestaneare) (Burstein et al., 2010).

Besides hormone therapy, other targeted therapies have been discovered, among them are tyrosine kinase inhibitors (TKIs), which are directed to HER1/2/3, IGFR, C-MET, FGF receptor (FGFR), inhibitors of intracellular signalling pathways (PI3K, AKT, mTOR, ERK), angiogenesis inhibitors, and agents that interfere with the DNA repair process (Higgins and Baselga, 2011). Some of these agents have become part of the standard therapies for breast cancer and one example is the treatment of patients overexpressing HER2 protein with monoclonal antibodies (trastuzumab and lapatinib) which are used to block the activity of the HER2 protein in breast cancer cells, slowing their growth (Blackwell et al., 2009, Vogel et al., 2002).

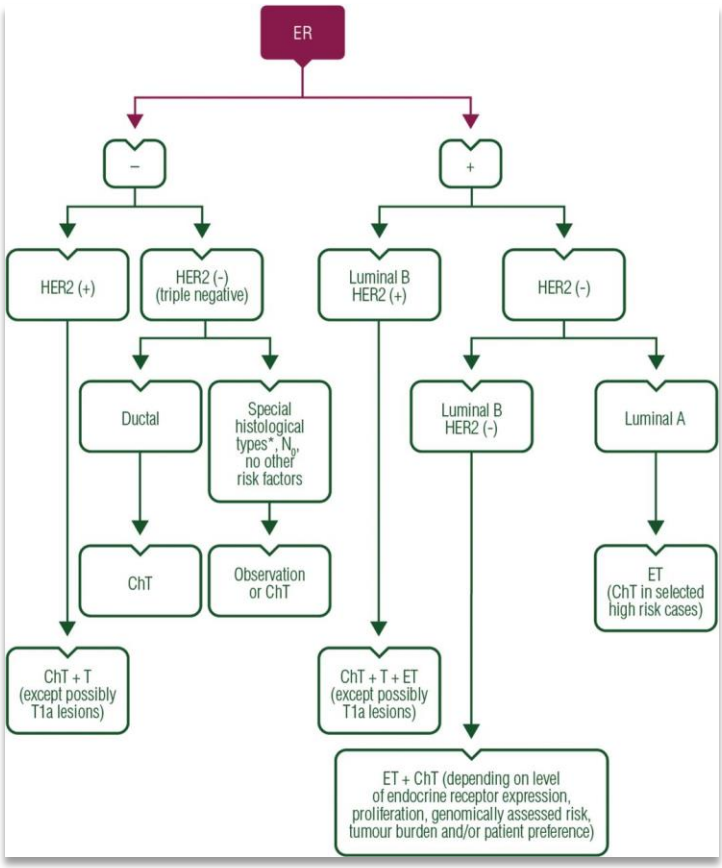

Figure 10. **(Neo)adjuvant systemic treatment choice by biomarker expression and intrinsic phenotype.** (ER=estrogen receptor, ChT=chemotherapy, T=Trastuzumab, ET=endocrine therapy) (Senkus et al., 2013).

1.4.3 Drug resistance

Despite the progress in the discovery of novel cancer therapies, resistance to chemotherapy and molecularly targeted therapies is a major problem in current cancer research. In one hand, pharmacokinetic (PK) factors such as drug absorption, distribution, metabolism and elimination (ADME) limit the amount of a systemically administered drug that reaches the tumour. On the other hand, genetic and epigenetic alterations in cancer cells can induce drug resistance, which can be divided into two categories: intrinsic (pre-existent) or acquired (induced by drugs) (**Figure 11**).

The intrinsic resistance can be caused by mutations in drug targets or lack of target dependency. In contrast, acquired resistance could be induced by several factors including loss of target expression, activating mutations downstream of the target, alteration of target regulator proteins and modulation of alternative compensatory signalling pathways (Holohan et al., 2013).

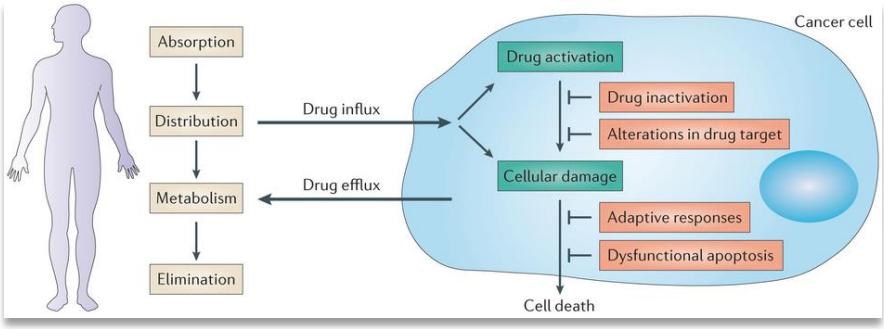

Figure 11. General principles of drug resistance. Several factors are described to modulate drug resistance before and after the drug reaches the tumour (Holohan et al., 2013).

In recent years, one of the most studied mechanisms of acquired resistance is the ability of cancer cells to rewire their internal signalling and gene-regulatory network after anticancer treatment.

In this regard, several studies have shown novel mechanisms by which breast cancer cells are able to counterbalance the therapeutic effects by multiple compensatory mechanisms. For instance, multiple mechanisms responsible for acquired endocrine resistance have been described, including the amplification or overexpression of *HER2* and the hyperactivation of the PI3K/AKT/mTOR pathway (Fu et al., 2013).

In a similar way, several mechanisms of resistance to trastuzumab have been identified, including alternative signalling from IGF-1R, other HER family members, or MET; and the activation of downstream signalling pathways such as PI3K-Akt, MEK, MAPK and mTOR (Tortora, 2011).

1.4.4 Drug combination treatment

Since tumour genetic complexity suggests that ablation of a single target or pathway is unlikely to produce a sustained effect, one solution to counteract drug resistance would be a combinatorial targeted therapy interfering with a range of different, although interrelated mechanisms by using multiple drugs, thus optimizing the success of targeted anticancer agents.

In addition, to impede compensatory mechanisms, drug combinations may also overcome toxicity and other adverse effects that are commonly associated with higher doses of single drugs, indispensable for tackling such mechanisms (Lehar et al., 2009). Several hundreds of drug combinations have been already reported (Jia et al., 2009). A large fraction of these investigational combinational therapies aims for treating various types of cancer. For instance, novel therapeutic strategies in HER-2-positive metastatic breast cancer are focused on circumventing frequently emerging primary and secondary resistance to trastuzumab therapy by combining trastuzumab with other HER2 antibodies (i.e. pertuzumab), cytotoxic agents and PI3K, IGF1R or mTOR inhibitors (Gianni et al., 2012, Nahta and Esteva, 2006, Tsang and Finn, 2012). Additionally, many molecular-targeted drugs (i.e. mTOR, histone deacetylase (HDAC) and cyclin-dependent kinase 4/6 inhibitors) in combination with endocrine therapy are currently in the evaluation process for phase II/III clinical trials in order to overcome endocrine resistance (Baselga et al., 2012, Osborne and Schiff, 2011, Saji and Kimura-Tsuchiya, 2015, Yardley et al., 2013).

These examples indicate that synergistic drug combinations either target the same or different proteins from the same or related pathways as well as from cross-talking routes are promising strategies for breast cancer treatment. However, the rationale for selecting drug combinations and the process used to demonstrate clinical effectiveness has primarily followed trial and error methodology. This implies that this approach, although sometimes effective,

is empiric and it does not take advantage of the underlying molecular mechanisms which are often not elucidated, thus hindering the design of effective combinatorial therapies.

Therefore, identifying novel drug combinations aimed to improve treatment responses while reducing drug concentrations remains a challenge in cancer treatment.

1.5 SYSTEMS AND NETWORK BIOLOGY

Molecular biology has uncovered a multitude of biological facts, such as genome sequences and protein properties, but this alone is not sufficient for interpreting biological systems. Cells, tissues, organs and organisms are systems of components whose specific interactions have been defined by evolution, thus a system-level understanding should be the prime goal of biology.

Understanding of complex biological systems requires the integration of experimental and computational research — in other words a systems biology approach. Systems biology analyses the relationships among the different elements of a system with the objective of understanding its properties (Kitano, 2002).

Systems biology complements the classic reductionist approaches in the biomedical sciences by enabling integration of available molecular, physiological, and clinical information, focusing on understanding not only on the components of a given system, but also in the effect of interactions among them and the interaction of the system with its environment.

In order to understand systems biology we need to build biomolecular maps to show the relative location and movement, the paths and ways, the links and crosstalks between the constitutive entities. The aim of achieving such

'relational maps' defines the new research field called 'network biology' (Barabasi and Oltvai, 2004).

Although much of our understanding of cellular networks is derived from model organisms, the past decade has seen an exceptional growth in human-specific molecular interaction data (Ideker and Sharan, 2008). Most attention has been directed towards molecular networks, including protein interaction networks (Rual et al., 2005, Stelzl et al., 2005); metabolic networks (Duarte et al., 2007, Jeong et al., 2000); gene regulatory networks (Carninci et al., 2005, Linding et al., 2008) and RNA networks (Lewis et al., 2005, Reynolds et al., 2004). The use of molecular networks offers a global perspective to explore links between the components of a given system (i.e. driver and passenger genes), thus providing further evidence for their molecular functions (Arroyo et al., 2015).

1.5.1 Protein-protein interactions (PPI) networks

Biochemical and biomolecular research for over a century have produced a remarkable compendium of knowledge about the function and properties of many individual proteins. But as previously mentioned, proteins do not act alone, they interact with each other in a highly specific manner to undertake specific functions, playing a key role in many cellular processes.

The complete map of protein interactions that take place in a living organism is called the 'interactome' (Cusick et al., 2005). Certainly, interactions will not occur all the time and under all conditions. Nevertheless, understanding which proteins interact with one another will give us deeper insights into the molecular machinery underlying complex phenotypes (Stumpf et al., 2007).

PPI are understood as physical contacts with molecular docking between proteins that occur in a cell or in a living organism *in vivo*. The definition of

PPI has to consider (i) the interaction interface should be intentional and not accidental (i.e. the result of specific selected biomolecular events) and (ii) the interaction interface should be non-generic (i.e. evolved for a specific purpose distinct from totally generic functions such as protein production, degradation, and others) (De Las Rivas and Fontanillo, 2010).

A critical step towards unravelling the complex molecular relationships in living systems is the mapping of PPI, which has become one of the main scopes of current biological research. In recent years, given an explosive development of high-throughput experimental technologies, the number of reported PPIs has increased substantially. In large-scale high-throughput studies, the most common binary methods to detect PPIs are the two-hybrid systems, being the yeast two-hybrid (Y2H) the most widely and successfully used methodology (Dreze et al., 2010, Fields and Song, 1989).

Protein interaction data can be represented as a network diagram where nodes correspond to proteins and edges to physical interactions between protein pairs. Despite being incomplete (Yu et al., 2008), systematic studies of protein interaction networks have been proven to be particularly important for deciphering the relationships between network structure and function (Yook et al., 2004), discovering novel protein function (Sharan et al., 2007) and identifying functionally coherent modules (Dittrich et al., 2008, Spirin and Mirny, 2003). In addition, interaction networks have become essential and powerful tools for associating proteins with distinct phenotypes and diseases (Goh et al., 2007, Ideker and Sharan, 2008), as well as for studying pharmacological drug-target relationships (Berger and Iyengar, 2009, Pujol et al., 2010).

Therefore, identifying and characterizing PPIs and their networks is essential for understanding the mechanisms of biological processes on a molecular level.

1.5.2 Protein-protein interaction networks and disease

Given the functional interdependencies between the molecular components in a human cell, a disease is rarely a consequence of an abnormality in a single gene, but reflects the perturbations of the complex intracellular and intercellular network that links tissue and organ systems (Barabasi et al., 2011). In particular, the full molecular complexity of common human diseases, such as cardiovascular diseases, diabetes, cancer, or neurological disorder, do not obey the standard Mendelian patterns of inheritance, and can only be anticipated by the study of the processes that interact in a complex network (Jaeger and Aloy, 2012). The inter- and intracellular interconnectivity implies that the impact of a specific genetic abnormality is not restricted to the activity of the gene product that carries it, but can spread along the links of the network and alter the activity of gene products that otherwise carry no defects. Therefore, an understanding of a gene's network context is essential in determining the phenotypic impact of defects that affect it (Goldstein, 2009, Schadt, 2009).

In context of understanding disease mechanisms at a molecular level, several observations motivate the usage of protein interaction networks (Ideker and Sharan, 2008). Recent studies indicated that gene products associated with a particular phenotype: (i) interact preferentially with proteins involved in the same disease (Musgrove and Sutherland, 2009), (ii) often exhibit a higher connectivity within the interaction network than nondisease gene products (Jonsson and Bates, 2006, Soler-Lopez et al., 2011), (iii) occur in central network locations, and (iv) often share characteristic topological network features with each other (Gandhi et al., 2006, Xu and Li, 2006). Therefore, the study of PPI networks allows the elucidation of the underlying disease mechanisms.

1.5.3 Network biology and cancer therapy

Despite the advances in the discovery of novel therapeutic targets, treatment failure remains a major challenge in the management of most solid cancers, such as breast cancer (Osborne and Schiff, 2011, Tsang and Finn, 2012). The main reason for this treatment failure is that traditional drug design approaches are focused on the design of maximally selective compounds binding exclusively one target (Hopkins, 2008).

Given the complexity of cancer, the classical view on drug action and therapeutic targets started to shift. Instead of focusing on individual targets or drugs, recent approaches consider the cellular context of therapeutic targets in terms of their underlying pathways and networks (Jaeger and Aloy, 2012).

As previously discussed, novel pharmacological approaches are currently focused on finding multitarget compounds (i.e. new drugs and combinations) that target particular groups of proteins involved in disrupted complexes or pathways (Hopkins, 2008). In contrast to conventional treatments, network biology approaches are aimed to increase the complexity of therapeutic strategies, improving clinical efficacies through synergistic effects while tackling critical aspects such as toxicity and drug resistance. In this regard, protein interaction networks are the perfect framework to investigate drug-induced perturbations on the different levels of molecular networks thus facilitating the understanding of the various drug effects while increasing the currently limited scope of potential drug targets (Berger and Iyengar, 2009).

Hence, emerging network biology approaches provide complementary and high quality interaction data that allows a deeper understanding of the molecular mechanisms contributing to the disease by identifying altered pathways or functional modules that in turn suggest potential therapeutic targets.

2. OBJECTIVES

The purpose of this thesis can be divided in two main objectives, the first one aimed at the identification and validation of new breast cancer genes related to apoptosis and the second focuses on the validation of new drug combinations for the treatment of breast cancer.

Objective I: The molecular mechanisms that relate changes in the expression of most passenger genes with the onset and progression of breast cancer are largely unknown. Accordingly, the first objective of this thesis is to identify the role of certain proteins in breast cancer apoptosis, which function in the disease is unknown.

Objective II: Combinatorial therapies currently approved are the result of empirical clinical experience, this means that this approach, although often effective, do not analyse in detail the underlying molecular mechanisms, which hampers the design of effective combinatorial therapies. Accordingly, our second goal is to implement a network biology approach to predict and validate novel drug combinations for the treatment of breast cancer, which achieve greater clinical efficacy and minimize side effects.

3. RESULTS AND DISCUSSION

3.1 IDENTIFICATION OF NOVEL APOPTOTIC GENES IN BREAST CANCER

As mentioned in **section 1.4**, the relatively poor prognostic outcome of breast cancer is largely due to its resistance to current cancer therapies, where the balance between cell proliferation and apoptosis plays a critical role and is crucial in determining the overall growth or regression of the tumour in response to treatments (Wong, 2011). Hence, identifying proteins involved in resistance to apoptosis developed by tumorigenic cells has an essential importance in order to find new therapeutic approaches.

3.1.1 Gene selection

PSMC3IP and EPSTI1 present relevant transcriptomics/genomics aberrations in breast cancer (de Neergaard et al., 2010, Gudjonsson et al., 2003, Li et al., 2014, Nielsen et al., 2002, Rommens et al., 1995, Sircoulomb et al., 2010), although the molecular mechanisms by which they drive breast tumour development and/or progression are still unknown.

Since cell proliferation and apoptosis are crucial for breast tumourigenesis, we sought to explore the eventual implication of the PSMC3IP and EPSTI1 genes in the regulation of these processes. To this end, we exploited the high interconnectivity observed among disease genes (Oti and Brunner, 2007) to reveal novel direct relationships between well-established breast cancer-apoptotic genes and PSMC3IP/EPSTI1, which could provide a molecular rationale for the implication of these genes in the disease.

An important factor when performing interaction discovery strategies is the selection of the core genes. With this aim, we mined the literature and the OMIM database (McKusick, 2007) to select the most relevant breast cancer

genes that are involved in apoptosis or cell proliferation: AKT1, BAG4, BCAR3, CASP8, CDKN2A, CDKN2C, CHEK2, IGF1R and PARP1.

We then performed pair-wise yeast two-hybrid (Y2H) assays (see **Material and Methods**) to identify novel interactions between BC-apoptosis genes and PSMC3IP/EPSTI1 (see **Table 1**).

Bait	Prey	Confidence
AKT1	EPSTI1	High
BAG4	EPSTI1	High
BCAR3	EPSTI1	High
BCAR3	PSMC3IP	High
CASP8	EPSTI1	High
CASP8	PSMC3IP	High
CHEK2	PSMC3IP	High
BAG4	PSMC3IP	Low
CDKN2C	EPSTI1	Low
CHEK2	EPSTI1	Low

Table 1. List of interactions detected by Y2H matrix screenings. Interacting pairs are reported as gene symbols taken from HGNC (http://www.genenames.org). The confidence level is reported as high when interactions are able to activate at least two reporter genes or being repeatedly observed in biological replica screens.

Among the seven high-confidence interactions that were identified, those of PSMC3IP and EPSTI1 with central proteins in the extrinsic apoptosis pathway (i.e. caspase 8) appeared as the most promising ones. Interestingly, both PSMC3IP and EPSTI1 showed a strong co-expression profile (CP) (see **Material and Methods**) with CASP8 in normal and cancer tissues including breast, also reflected in higher protein levels (**Table 2**).

Interaction		**Passenger expression in healthy and cancer breast tissues**			**Driver-Passenger**		
Passenger	Driver	Normal		Cancer	Sharing CC	ES	CP
		mRNA	Protein	Protein			
PSMC3IP	CASP8	+	+	OE	+	+	+
	BCAR3	+	+		nd	+	+
EPSTI1	CASP8	+	+	OE	+	+	+
	AKT1	+	+		+	+	-
	BCAR3	+	+		+	+	-

Table 2. **Promising interactions between BC-apoptosis genes and passenger BC genes.** Passenger gene expression in healthy and carcinoma breast tissues and their co-expression with core BC-apoptotic genes. OE= overexpressed, CC= cellular compartment, ES= expression similarity, meaning expression of driver and passenger in different tissues (Skrabanek and Campagne, 2001), CP= co-expression profile, +=positive result, - =negative results and nd= not detected.

In addition, PSMC3IP and EPSTI1 also interact with Breast Cancer Anti-estrogen Resistance 3 (BCAR3) protein, which is known to regulate proliferation and induce anti-estrogen resistance in ZR75–1 and MCF-7 breast cancer cells (van Agthoven et al., 1998). Finally, we also found that

EPSTI1 interacts with AKT1, an antiapoptotic protein that in response to specific stimuli, phosphorylates and inactivates certain components of the apoptotic machinery, such as the Bcl2 antagonist of cell death (BAD) and caspase-9 (Cardone et al., 1998, Datta et al., 1997). In breast cancer, the PI3K-Akt pathway is a critical downstream effector of growth factor receptors such as HER2/ErbB2, Insulin-like Growth Factor Receptor (IGFR) and Epidermal Growth Factor Receptor (EGFR) (Lenferink et al., 2001, Lobenhofer et al., 2000, Tsai et al., 2001, Yang et al., 2001). Taken together, these findings suggest that PSMC3IP and EPSTI1 could play a role in the regulation of the apoptotic response.

3.1.2 Modulation of PSMC3IP and EPSTI1 expression in breast cancer cells

We first investigated whether PSMC3IP and EPSTI1 endogenous protein levels were indeed up-regulated in breast carcinoma cells such as MCF-7 and MDA-MB-231 (**Figure 13**), which represent common breast cancer subtypes differently graded upon hormone dependency and aggressiveness. MCF-7 is a weakly invasive luminal cell line, representative of estrogen receptor (ER)-positive tumours (Thomas et al., 1999). On the other hand, MDA-MB-231 is a highly invasive basal cell line, and it is often used as model for ER-negative tumours (Zhang et al., 2010) (see **Table 3**).

	MDA-MB-231	MCF-7
Luminal	○	⊕
Basal	⊕	○
ER	○	⊕
PR	○	⊕
HER2	○	○
Other mutations	BRAF CDKN2A KRAS NF2 TP53	CDKN2A PI3KCA
Histology Subtype	Metastatic Adeno-carcinoma	Metastatic Adeno-carcinoma

Table 3. Breast cancer cell line features

In these assays we observed that PSMC3IP was highly overexpressed in both MDA-MB-231 and MCF-7, compared to the non-tumorigenic breast cancer cell line (MCF-10A) (**Figure 12A**). Conversely, EPSTI1 showed a more moderate increase, particularly in MCF-7 cells (1.3-fold, **Figure 12B**), as previously observed (de Neergaard et al., 2010), providing evidence about the heteroclonal nature of MCF-7 sublines (Nugoli et al., 2003).

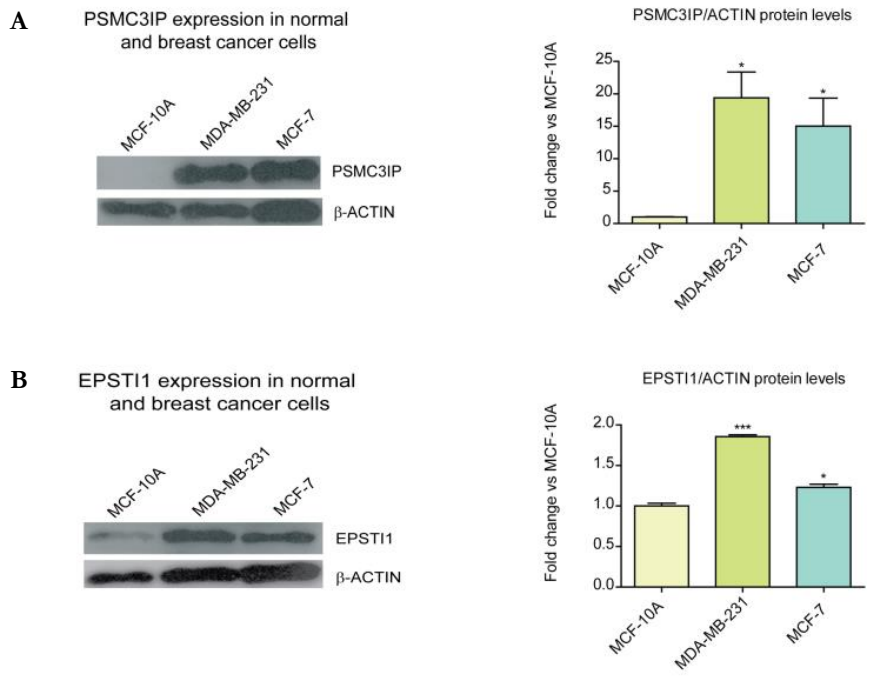

Figure 12. Expression of PSMC3IP and EPSTI1 in normal and breast cancer cell lines. We inspected the endogenous expression of PSMC3IP **(A)** and EPSTI1 **(B)** in two types of breast cancer cell lines, MDA-MB-231 and MCF-7, as compared to a normal breast epithelial cell line, MCF-10A. Protein levels were normalized based on the loading control protein β-actin. (*P <0.05, **P<0.01, ***P <0.001 vs MCF-10A cells).

We then tested whether PSMC3IP and EPSTI1 had a role on apoptosis as suggested by the interaction with caspase-8. To enhance the phenotypic response that PSMC3IP and EPSTI1 might have on apoptosis, we induced the extrinsic apoptotic pathway using TRAIL, which typically generated

about 25 and 35 % cell viability decrease in non-transfected MDA-MB-231 and MCF-7 cells, respectively (**Figure 13**), in agreement with the data reported in the literature (Rahman et al., 2009, Xu et al., 2007, Xu et al., 2010).

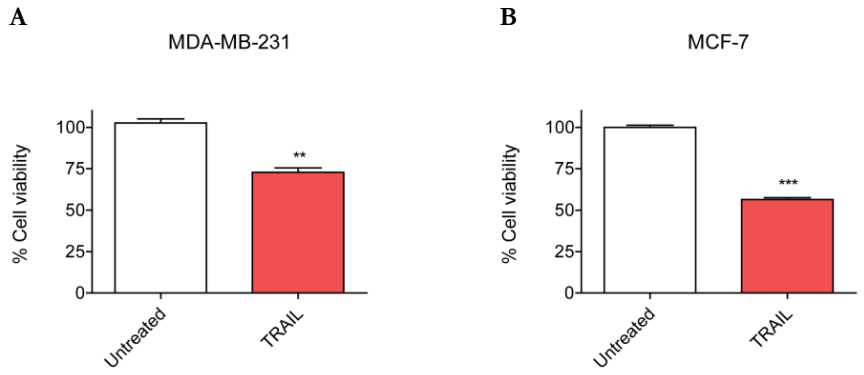

Figure 13. TRAIL-induced apoptosis in breast cancer cells. (A) MDA-MB-231 cells treated with the apoptosis inducing ligand TRAIL at 80ng/mL for 24h **(B)** MCF-7 cells treated with TRAIL at 100ng/mL for 24h. Each bar represents the mean ±SD of three experiments performed in duplicate (*P <0.05, **P <0.01, ***P <0.001 vs untreated cells).

We then modulated PSMC3IP and EPSTI1 expression by either cDNA (overexpression) or siRNA (gene silencing) cell transfection. The X-linked inhibitor of apoptosis protein (XIAP) was also included in the experiments as an anti-apoptotic reference gene, since it is a well-characterized inhibitor of caspase-3, caspase-7 and caspase-9 (Deveraux et al., 1998, Deveraux et al., 1997) (**Figure 14**). Compared to cells transfected with empty vectors, we observed a high overexpression of PSMC3IP in both cell lines (MDA-MB-231, 6.5-fold; MCF-7, 13-fold) (**Figure 14A-14B**), albeit we only achieved a moderate EPSTI1 overexpression (2.1-fold and 2.6-fold, respectively (**Figure 14A-14B**). Concerning the silencing experiment, we were able to reduce PSMC3IP levels by 70% in MDA-MB-231 and 50% in MCF-7 cells compared to cells transfected with control siRNA (siLUC) (**Figure 14C-14D**). To maximize and visualize the effect of EPSTI1 depletion, its

endogenous expression was induced with IFN-α prior to gene silencing in both cell lines (**Figure 14C-14D**), as previously reported (de Neergaard et al., 2010), obtaining an inhibition around 50% in both cell lines.

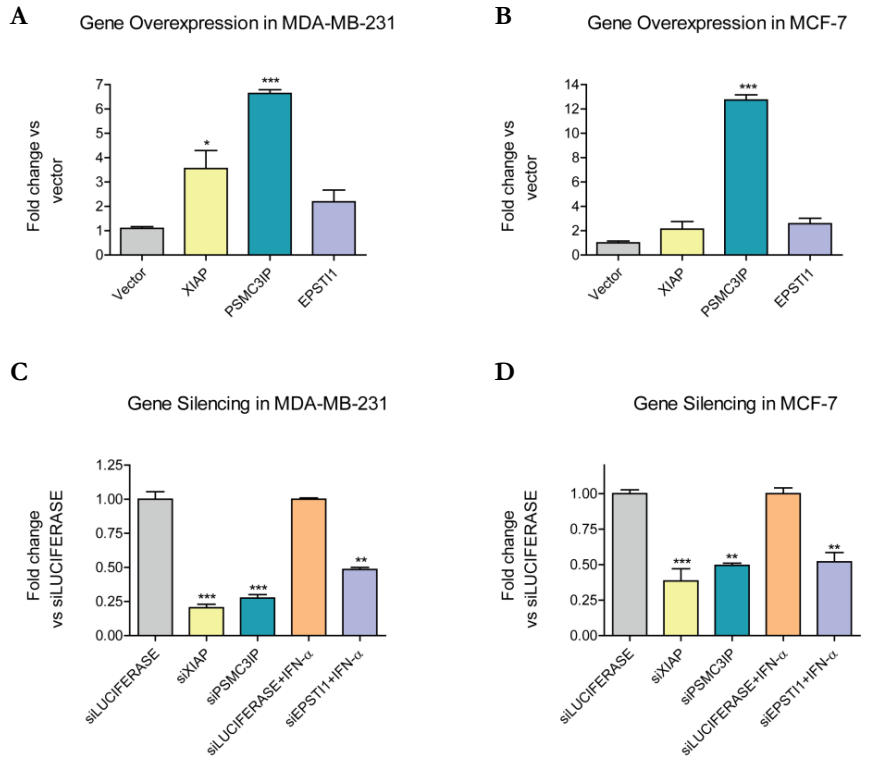

Figure 14. Modulation of PSMC3IP and EPSTI1 expression in breast cancer cells. (**A-B**) Genes were overexpressed as Myc-tagged fusion proteins in different cell lines and protein relative levels were analysed based on MYC-tag empty transfection vector (Vector). (**C-D**) Endogenous gene expression was silenced using specific siRNA and depletion levels were analysed based on siRNA against luciferase expression (siLUC) as a negative control. Prior to depletion experiments, EPSTI1 expression was induced by treating cells with IFN-α at 1000 U/ml for 8h. XIAP was used as a reference anti-apoptotic protein in all experiments. Each bar represents the mean ±SD of three experiments performed in duplicate (*P <0.05, **P <0.01, ***P <0.001 vs MYC-tag vector in overexpression assays and vs siLUC in gene silencing assays).

Subsequently, a variety of functional assays were performed to measure the

apoptotic activity of the two passenger genes in breast cancer cells under basal or apoptotic induced conditions.

3.1.3 PSMC3IP and EPSTI1 expression regulates caspase-8 activity

Since PSMC3IP and EPSTI1 both interact with caspase-8, we first sought to examine the influence of these interactions on caspase-8 activity, which is an upstream player of the apoptotic cascade. We only observed significant caspase-8 activity decrease upon PSMC3IP overexpression in MDA-MB-231 cells (1.6-fold $P<0.05$) (**Figure 15A**). But interestingly, both candidates decreased caspase-8 activity in MCF-7 cells (PSMC3IP, 1.2-fold $P<0.05$; EPSTI1, 1.5-fold $P<0.001$) (**Figure 15B**). In agreement with the overexpression results, caspase-8 activity increased after PSMC3IP or EPSTI1 gene silencing in both cell lines (**Figure 15C-D**), although predominantly in MCF-7 cells treated with TRAIL upon PSMC3IP depletion (1.3-fold, $P<0.01$) and under basal conditions upon EPSTI1 depletion (1.3-fold, $P<0.05$) (**Figure 15D**). As expected, XIAP overexpression or silencing did not affect caspase-8 activity, since the inhibitory effect of XIAP is on downstream caspases like caspase-3 or caspase-7.

Collectively, these results indicate that PSMC3IP and EPSTI1 do modulate caspase-8 activity, suggesting their involvement in the extrinsic apoptotic pathway in breast cancer cells.

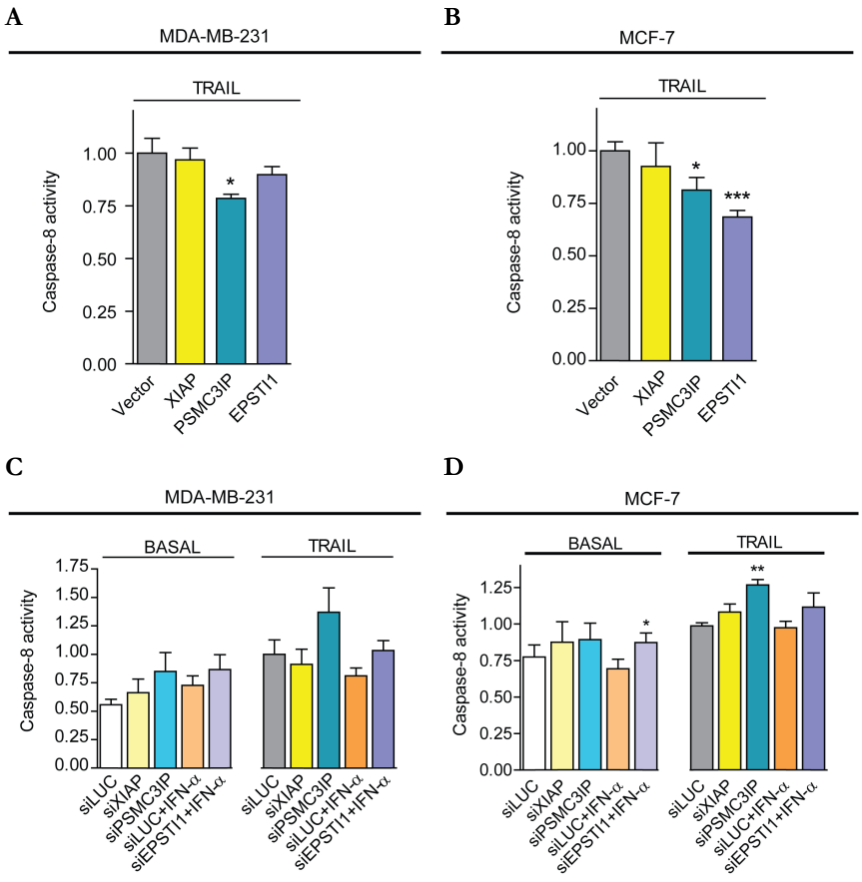

Figure 15. Caspase-8 activity modulation. Caspase-8 activity is quantified by measuring the chromophore levels released from caspase-8 cleaved substrates. Overexpression of PSMC3IP or EPSTI1 in TRAIL-treated MDA-MB-231 **(A)** and MCF-7 cells **(B)** Caspase-8 activity measured after gene silencing in MDA-MB-231 **(C)** and MCF-7 **(D)** cells, under basal or TRAIL-treated conditions. Genes are silenced using specific siRNAs targeting XIAP, PSMC3IP or EPSTI1 and siRNA against luciferase expression (siLUC) is used as a negative control. EPSTI1-depleted cells are previously treated with IFN-α at 1000 U/ml for 8h. MDA-MB-231 and MCF-7 cells are treated with TRAIL for 24h at 80 or 100ng/mL, respectively. XIAP is used as an anti-apoptotic reference in all experiments. Each bar represents the mean ±SD of three experiments performed in duplicate (*P <0.05, **P <0.01, ***P <0.001 vs MYC-tag vector in overexpression assays and vs siLUCIFERASE in silencing).

3.1.4 PSMC3IP and EPSTI1 expression modulates caspase-3 activity and PARP cleavage

It is well known that the activation of initiator caspases, like caspase-8, leads to the activation of executioner caspases, such as caspase-3 in MDA-MB-231 cells (Janicke et al., 1998). Therefore, we investigated whether PSMC3IP or EPSTI1 expression affects caspase-3 activity under basal or apoptotic conditions in MDA-MB-231 cells (**Figure 16**).

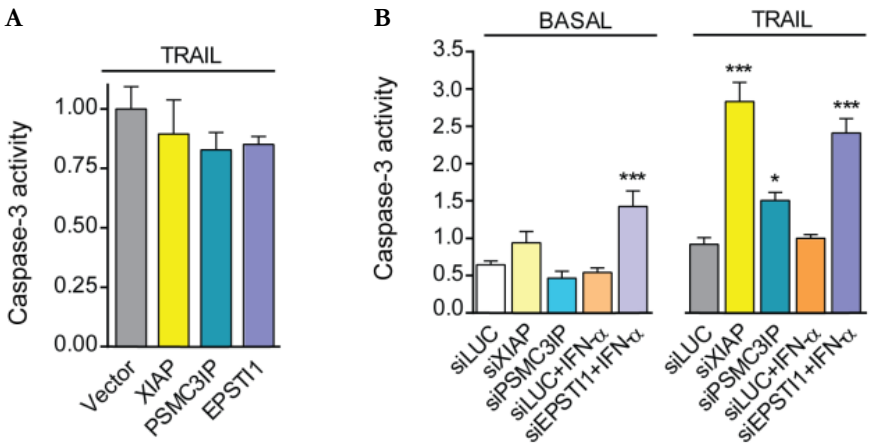

Figure 16. Caspase-3 activity modulation. (A) Caspase-3 activity is measured by colorimetric quantification of fluorescent products released from caspase-3 cleaved substrates in TRAIL-treated MDA-MB-231 cells overexpressing XIAP, PSMC3IP or EPSTI1. **(B)** Caspase-3 activity was also measured in MDA-MB-231 cells under basal or TRAIL-treated conditions after gene silencing using specific siRNA targeting XIAP, PSMC3IP or EPSTI1. Each bar represents the mean ±SD of three experiments performed in duplicate (*P <0.05, **P <0.01, ***P <0.001 vs MYC-tag vector in overexpression assays and vs siLUC in gene silencing assays).

We observed that overexpression of either gene did not alter caspase-3 activity levels (**Figure 16A**). Yet, EPSTI1 silencing resulted in an increased caspase-3 activity in both basal conditions (2.6-fold, P<0.001) and upon TRAIL treatment (2.4-fold, P<0.001), giving similar results as the silencing of the anti-apoptotic gene XIAP. On other hand, PSMC3IP silencing was

only able to increase caspase-3 activity under TRAIL treatment (1.5-fold, $P<0.05$) (**Figure 16B**). These results indicate that indeed EPSTI1 and PSMC3IP modulate caspase-3 activity in MDA-MB.231 cells, albeit at different levels.

Caspase-7 and caspase-3 coordinate the last phase of apoptosis by cleaving protein substrates such as PARP (Germain et al., 1999, Tewari et al., 1995), which has an essential role in repairing single-strand breaks (SSBs). PARP is inactivated by caspase cleavage, causing SSB repair inhibition that can result in lethal DNA damage (Lord et al., 2006). Interestingly, overexpressing PSMC3IP or EPSTI1 showed a significant decrease in PARP cleavage in MDA-MB-231 and MCF-7 cells (1.3-fold, $P<0.01$; 1.8-fold, $P<0.01$) (1.2-fold, $P<0.05$; 2.9-fold, $P<0.001$) (**Figure 17A-B**). Furthermore, in agreement with our caspase-3 activity results, there was an increase of cleaved PARP levels after PSMC3IP or EPSTI1 gene depletion in MDA-MB-231 cells upon TRAIL induction (PSMC3IP, 3.2-fold, $P<0.001$; EPSTI1, 1.5-fold, $P<0.05$) (**Figure 17C**). This effect was more pronounced in MCF-7 cells, where PARP cleavage was increased even in basal conditions (EPSTI1, 4.2-fold, $P<0.001$; PSMC3IP, 3.6-fold, $P<0.05$) (**Figure 17D**).

Taken together, although preclinical studies have shown that ER-negative breast cancer cell lines are more sensitive to PARP inhibitors compared to luminal cells (Hastak et al., 2010), our results indicate that PARP cleavage is similarly affected by the expression of putative extrinsic regulators such as PSMC3IP and EPSTI1 in both ER-negative (i.e. MDA-MB-231) and in luminal breast cancer cell lines (i.e. MCF-7). In addition, since EPSTI1 also interacts with AKT1, it could play an alternative role in modulating apoptosis through PI3K pathway, in line with preclinical data that demonstrate synergistic activity when PARP inhibitors are combined with PI3K inhibitors (Ibrahim et al., 2012).

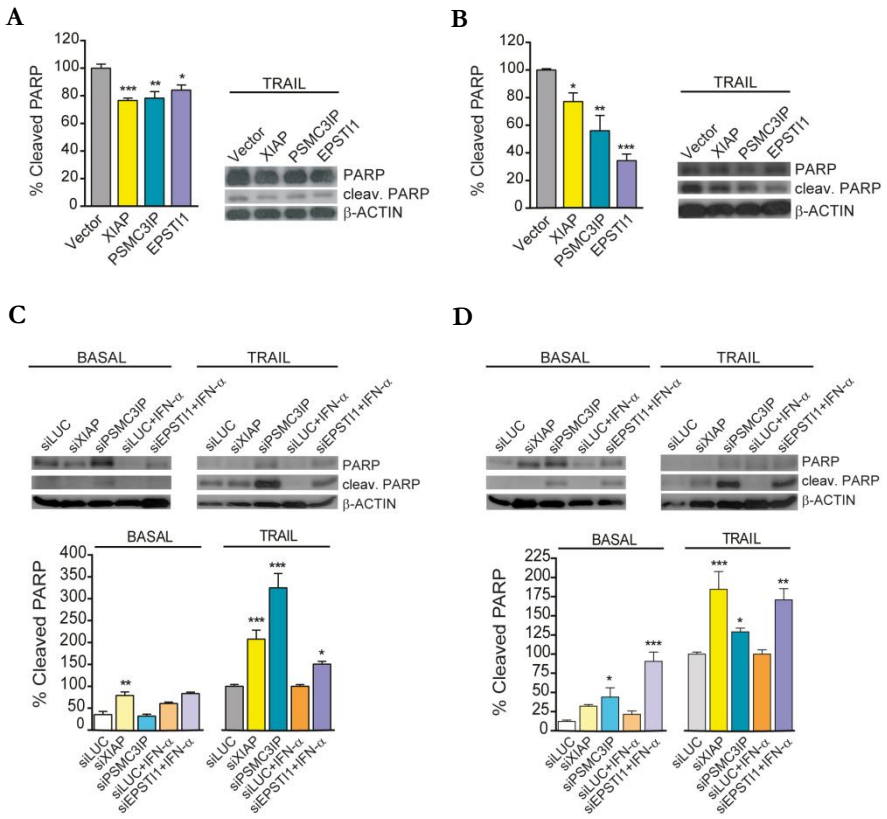

Figure 17. Analysis of cleaved PARP protein levels. (A) Immunoblot analysis of cleaved PARP protein levels in gene-overexpressing MDA-MB-231 cells under TRAIL conditions and in TRAIL-treated MCF-7 cells **(B)**. **(C)** Analysis of cleaved PARP protein levels after gene silencing in MDA-MB-231 cells. **(D)** The same analysis in MCF-7 cells. EPSTI1-depleted cells are previously treated with IFN-α at 1000 U/ml for 8h. In apoptosis-induced conditions, MDA-MB-231 and MCF-7 cells are treated with TRAIL for 24h at 80 or 100ng/mL, respectively. Each bar represents the mean ±SD of three experiments performed in duplicate (*P <0.05, **P <0.01, ***P <0.001 vs MYC-tag vector in overexpression assays and vs siLUC in gene silencing assays).

3.1.5 Increased DNA fragmentation and reduced cell viability are associated with PSMC3IP and EPSTI1 down-regulation

DNA fragmentation, resulting from apoptotic signalling cascades, is a hallmark of late-stage apoptosis (Collins et al., 1997). Hence, we wanted to examine whether EPSTI1 and PSMC3IP were able to alter the final apoptotic response beyond the modification of caspase activity. To this end, the number of apoptotic cells were quantified by flow cytometry (i.e. measurement of the sub-G_0/G_1 peak in the fluorescence histogram) and DNA fragmentation was further examined by TUNEL assay (**Figures 18 and 19**).

In MDA-MB-231 cells, an increased number of apoptotic cells was detected upon *PSMC3IP* silencing under TRAIL conditions (1.6-fold, $P<0.01$), while *EPSTI1* depletion had already a similar effect under basal conditions (1.7-fold, $P<0.05$) (**Figure 18A**). Yet, TUNEL-based fluorescent microscopy images did not show conclusive results (**Figure 18B**).

Interestingly, MCF-7 cells showed a clearer phenotype, where *PSMC3IP* depletion leaded to an increase in the number of apoptotic cells in basal conditions (4.3-fold, $P<0.01$) (**Figure 19A**) and *EPSTI1* silencing induced a high increase of apoptotic cells under both basal and TRAIL conditions (17.7-fold, $P<0.001$; 3.5-fold, $P<0.001$) (**Figure 19A**). These findings were in accordance with apoptotic positive cells observed in TUNEL assays (**Figure 19B**).

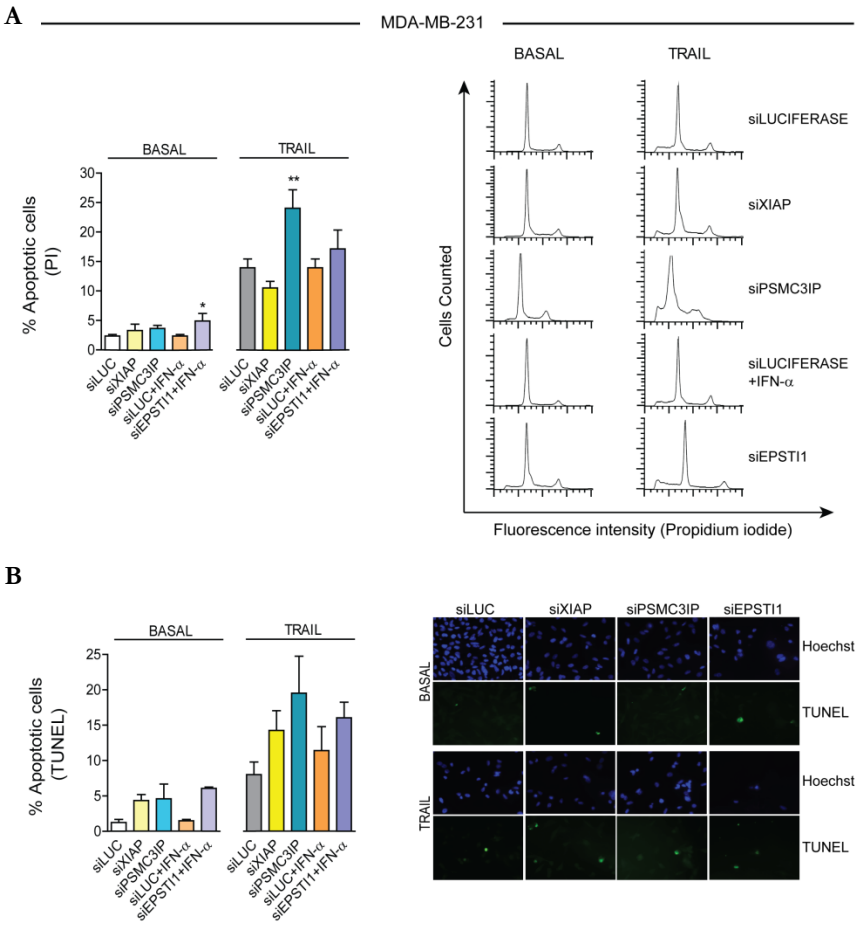

Figure 18. Detection of DNA fragmentation in MDA-MB-231 cells. **(A)** The number of apoptotic MDA-MB-231 cells is quantified by flow cytometry using propidium iodide DNA staining after gene depletion under basal or TRAIL-treated conditions. **(B)** Apoptosis is also evaluated in MDA-MB-231 by the inspection of DNA fragmentation by TUNEL assay. Cell nuclei is stained with Hoechst (blue fluorescence) to estimate the number of total cells. siLUC is used as a negative control. EPSTI1-depleted cells are previously treated with IFN-α at 1000 U/ml for 8h. In apoptosis-induced conditions, cells are treated with TRAIL for 24h, at 80 ng/mL. Each bar represents the mean ±SD of three experiments performed in duplicate (*P <0.05, **P <0.01, ***P <0.001 vs siLUC).

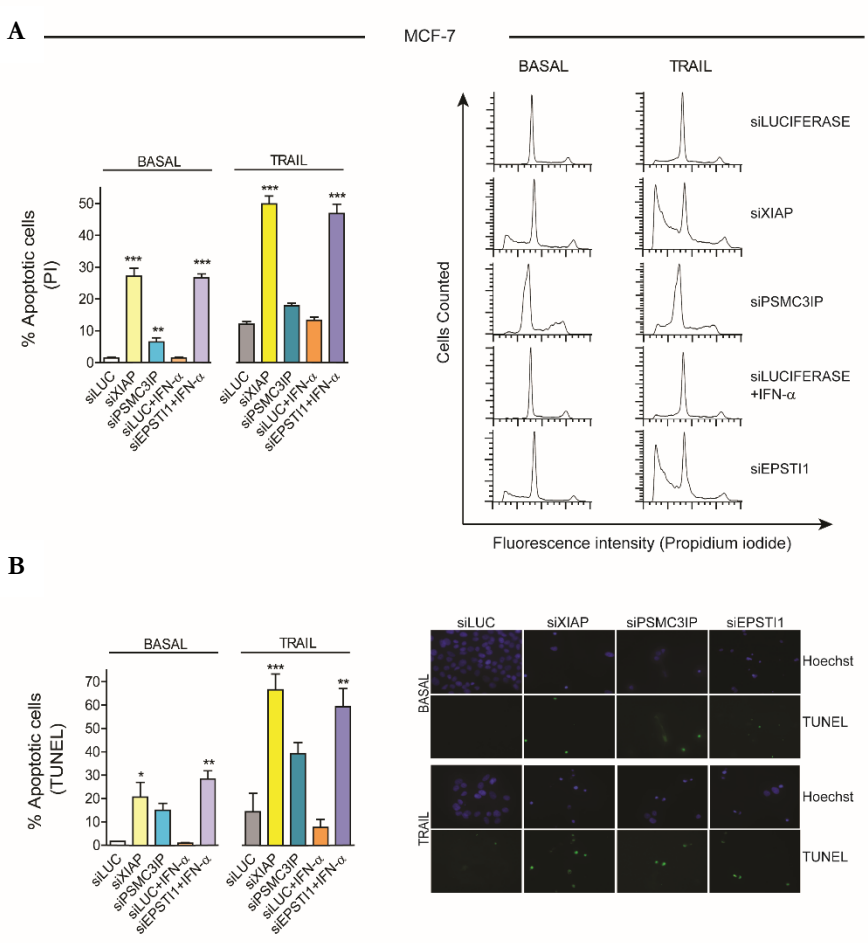

Figure 19. Detection of DNA fragmentation in MCF-7 cells. **(A)** The number of apoptotic MCF-7 cells is quantified by flow cytometry using propidium iodide DNA staining after gene depletion under basal or TRAIL-treated conditions **(B)** TUNEL positive nuclei are observed in MCF-7 cells. siLUC is used as a negative control. EPSTI1-depleted cells are previously treated with IFN-α at 1000 U/ml for 8h. In apoptosis-induced conditions, cells are treated with TRAIL for 24h, at 100ng/mL. Each bar represents the mean ±SD of three experiments performed in duplicate (*P <0.05, **P <0.01, ***P <0.001 vs siLUC).

Lastly, we sought to determine breast cancer cells viability after PSMC3IP or EPSTI1 expression modulation. As observed in **Figure 20**, up-regulation of either gene was not able to restore the viability of neither TRAIL-treated

MDA-MB-231 (**Figure 20A**) nor MCF-7 cells (**Figure 20B**). Conversely, *EPSTI1* down-regulation decreased the viability of MDA-MB-231 cells treated with TRAIL (1.9-fold, P<0.001) (**Figure 20C**). Intriguingly, *PSMC3IP* or *EPSTI1* silencing induced significant MCF-7 cell viability decrease only in basal conditions (1.3-fold, P<0.05 and 1.5-fold, P<0.01 respectively) (**Figure 20D**).

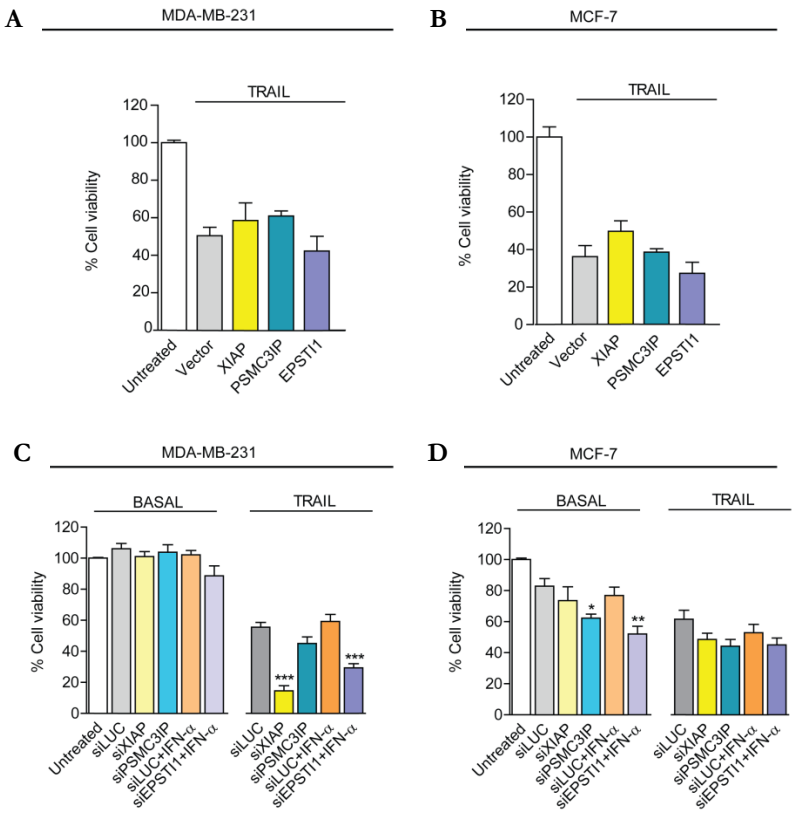

Figure 20. Cell viability and recovery. Cell viability is determined by MTT absorbance assays **(A)** Histograms showing the viability of PSMC3IP or EPSTI1-overexpressing MDA-MB-231 cells and **(B)** MCF-7 cells under TRAIL-induced conditions. **(C)** Viability measurement of gene-depleted in MDA-MB-231 and **(D)** MCF-7 cells**.** *EPSTI1*-depleted cells are previously treated with IFN-α at 1000 U/ml for 8h. In apoptosis-induced conditions, cells were treated with TRAIL for 24h, at 80 or 100ng/mL respectively. Each bar represents the mean ±SD of three experiments performed in duplicate (**P* <0.05, ***P* <0.01, ****P* <0.001 vs siLUC).

Collectively, our findings reveal that PSMC3IP and EPSTI1 have a strong anti-apoptotic role in breast cancer cells, particularly in estrogen receptor positive and triple negative, that could be explained by physical interaction with the apoptosis initiator caspase-8 (**Figure 21**).

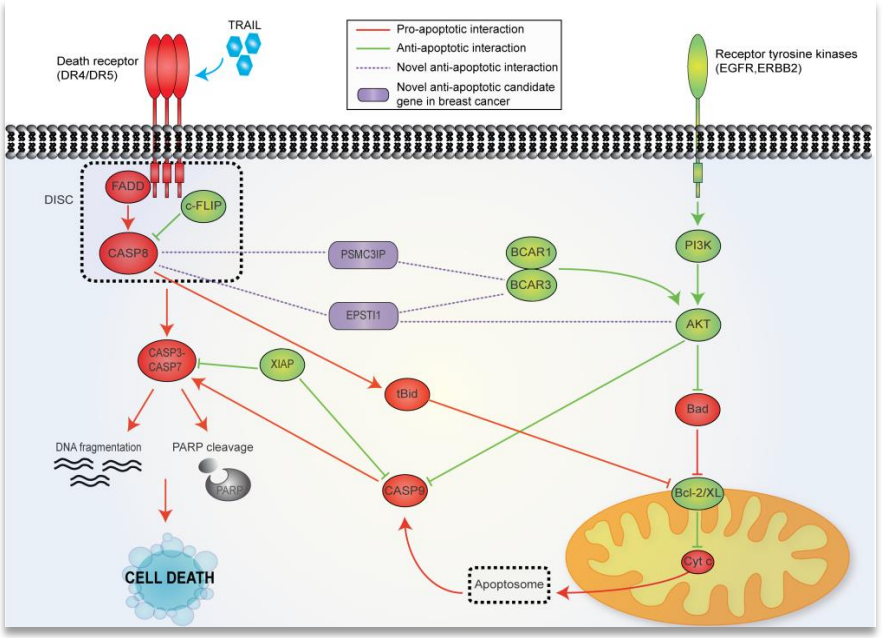

Figure 21. Mechanistic model of PSMC3IP and EPSTI1 as putative apoptotic factors. The extrinsic apoptosis pathway is initiated by the ligand binding to the death receptor, forming the DISC complex and leading to the activation of the caspase signalling cascade. Overexpression of EGFR and HER2 or activation of components of their downstream signalling pathways induces an anti-apoptotic signalling through PI3K-Akt pathway in endocrine resistant breast cancer cells. Based on our findings, we suggest that PSMC3IP and EPSTI1 may regulate the apoptotic pathway via the physical interaction mainly with the apoptosis initiator CASP8, but also with AKT1 and BCAR3. Pro-apoptotic proteins are displayed in red and anti-apoptotic in green. Passenger proteins are displayed in purple.

Interestingly, PSCM3IP or EPSTI1 depletion in breast cancer cells show increased DNA fragmentation and reduced cell viability even in the absence of apoptotic stimuli, indicating that they might also modulate the apoptotic

pathway trough alternative mechanisms, such as interaction with BCAR3 or AKT1, especially the in case of EPSTI1. Although further studies are required to gain deeper insight into the molecular mechanisms underlying the anti-apoptotic role of PSMC3IP and EPSTI1 in breast cancer, our findings highlight them beforehand as very interesting therapeutic targets, preeminently for their ability to apoptosis sensitization.

3.2 IDENTIFICATION OF NOVEL DRUG COMBINATIONS FOR BREAST CANCER THERAPY

Despite the therapeutic progress and the expanding repertoire of new anti-cancer agents, treatment failure remains a major challenge in the management of most advanced solid cancers such as breast cancer (Osborne and Schiff, 2011).

In order to address these problems, the second part of this thesis is divided in two different studies focused on the prediction and validation of novel synergistic therapies for breast cancer, which have the potential to better overcome the mechanisms of resistance and, in parallel, to reduce undesirable side effects. The aim of the first study is to find novel drug combinations by means of pathway crosstalk quantification, while the second study uses the network activity quantification to achieve the same goal.

3.2.1 DRUG COMBINATIONS PREDICTED BY PATHWAY CROSSTALK QUANTIFICATION

A critical aspect in improving cancer treatment is not only to inhibit primary oncogenic signalling pathways that induce abnormal cell proliferation but, at the same time, to prevent functional redundancies and pathway crosstalk that facilitate survival of cancer cell populations rendering tumours resistant to therapy (Kitano, 2004).

With this aim, a member of our group, Dr Samira Jaeger, developed a computational approach for inferring drug combinations regarding drug resistance by taking into account functional redundancy and pathway crosstalk. Our approach was based on quantifying crosstalk between pathways involved in breast cancer, based on which we then assessed the impact of combinatorial perturbation on pathway crosstalk (PCI). This measure was applied to a set of approved and experimental drugs to identify combinations which could potentially diminish efficiently the pathway crosstalk and thereby increase clinical efficacy. My contribution to this project was to experimentally validate a subset of 12 antineoplastic and 4 compassive drug combinations predicted as synergistic with significant crosstalk inhibition.

3.2.1.1 Drug combination selection

We analysed two different sets of drugs combinations (DCs):

- Approved or experimentally tested antineoplastic drugs combined with approved or experimental breast cancer drugs (named **antineoplastic combinations**).
- Approved drugs for any disease except cancer combined with approved or experimental breast cancer drugs (named **compassive combinations**).

We first collected a list of 64 drugs for breast cancer treatment which are either approved (National Cancer Institute) or have been experimentally tested (Zhu et al., 2012).

Secondly, we selected a set of 248 approved or experimentally studied antineoplastic drugs extracted from the Drugbank (Feuring et al., 2011, Gehlot et al., 2013) database according to their drug category annotations as well as the ATC code(s) (i.e. antineoplastic, antiangiogenics, anticancer,

anticarcinogenic). From these 248 drugs, we then obtained a final set of 191 antineoplastic drugs after excluding:

- Drugs belonging to the 64 breast cancer drug set mentioned above
- Target activators and agonists (since we are computing crosstalk inhibition)

In parallel, for the set of compassive drug combinations we selected 1,334 approved drugs from Drugbank, from which we selected a final set of 836 approved non-cancer drugs after excluding:

- Drugs having an indication for antineoplastic treatment according to their drug category annotations as well as the ATC code
- Target activators and agonists

Subsequently, all possible pair-wise combinations were generated between the set of breast cancer drugs and (i) the antineoplastic drugs (antineoplastic combinations) and (ii) the approved non-cancer drugs (compassive combinations). Given the two sets, we next computed the pathway crosstalk inhibition (PCI) between the involved drugs (as described in **Material and Methods**) for the 12,416 antineoplastic and 53,504 compassive drug combinations.

Figures 22 and 23 show the crosstalk inhibition values among all pairs of drugs in the antineoplastic and compassive groups respectively. In dark green are represented the combinations with high crosstalk inhibition values (PCI), while light green means lower PCI value.

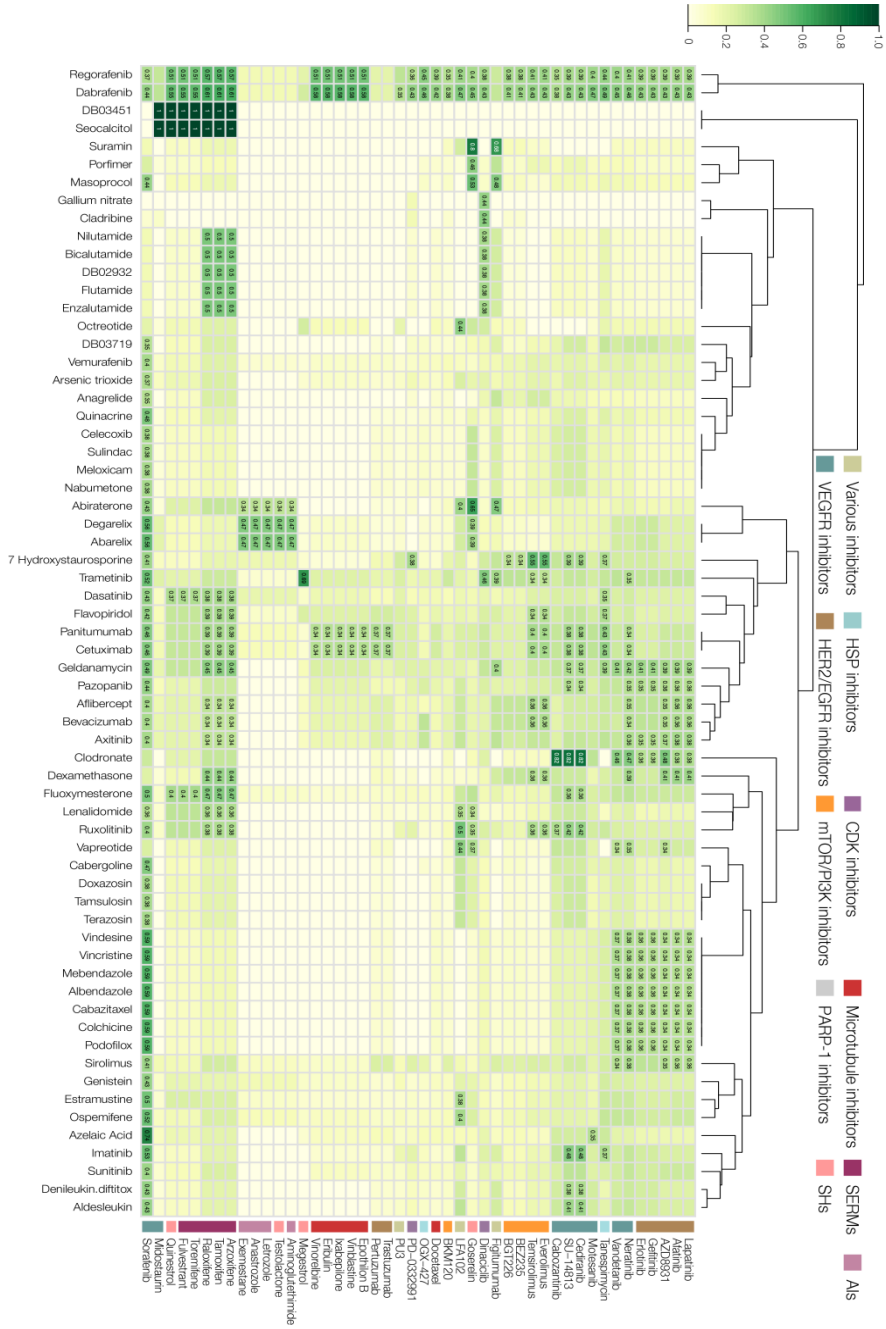

Figure 22. Crosstalk inhibition computed in the antineoplastic combinations. Crosstalk inhibition (PCI values) determined between breast cancer therapeutics (both approved and experimental) combined with antineoplastic drugs.

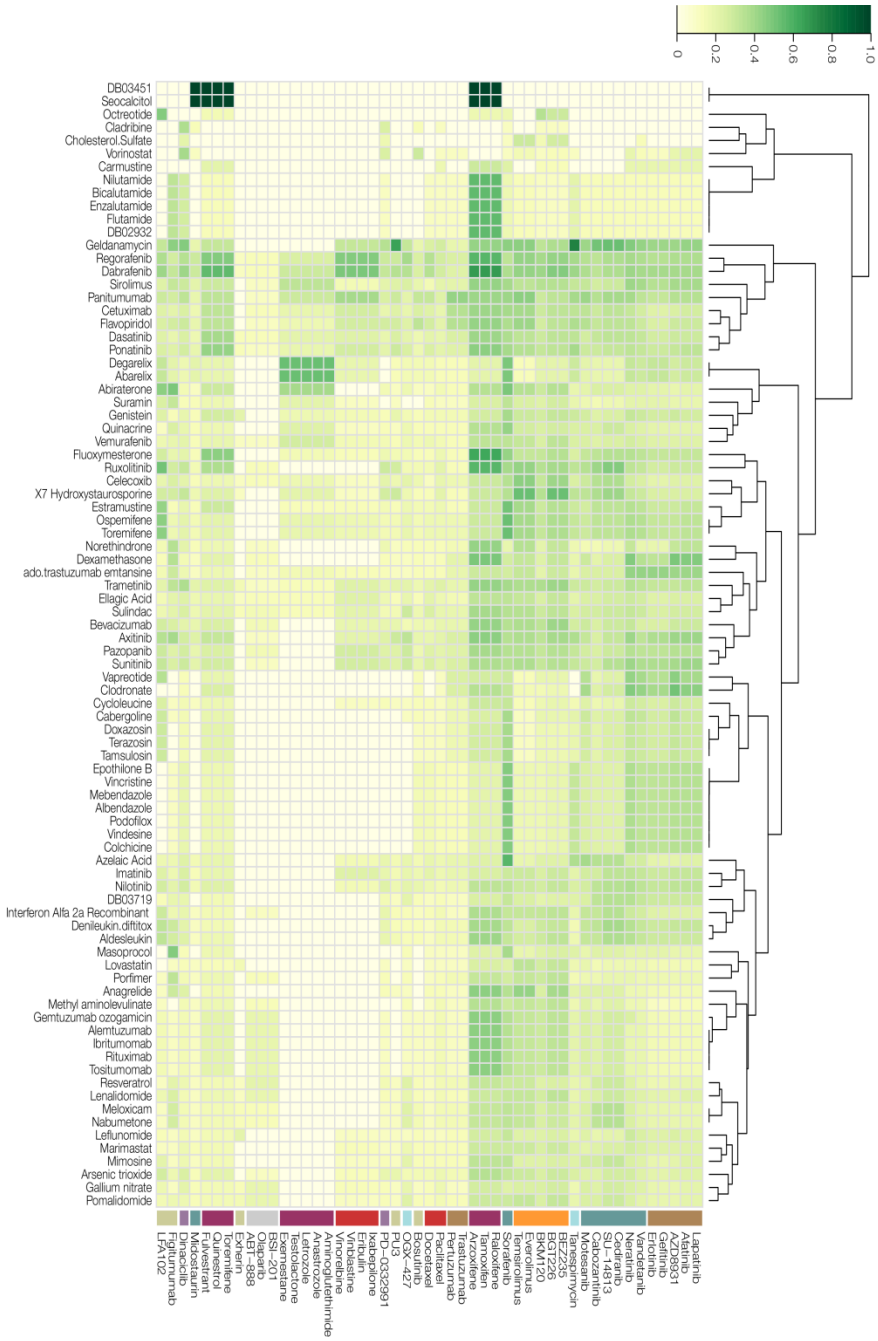

Figure 23. Crosstalk inhibition computed the in compassive combinations. Crosstalk inhibition determined between breast cancer therapeutics (both approved and experimental), combined with approved non-cancer drugs.

Drug combinations filtering

Since we obtained a huge number of possible drug combinations to test *in vitro*, we applied some filtering in order to highlight the most promising ones (**Figure 24**).

First, as we previously described (Jaeger S et al. submitted), combinations considered to be efficient (i.e. the ones documented by the ClinicalTrial.gov, the U.S. Food and Drug Administration (FDA) orange book, the NCI or the Drug Combination Database (DCDB)), have a significantly higher impact on pathway crosstalk than random combinations, with a mean pathway crosstalk inhibition of 0.34, compared to 0.25 in random combinations (P-value = 8.96×10^{-6}). Therefore, we set a threshold of 0.34 as an initial filter to select the most promising drug combinations.

Additionally, as a second level of filtering, we also excluded the combinations where the contribution of the non-breast cancer drug was negligible (PCI$\leq$ 0.1), combinations resembling drug subclasses of the currently approved or experimentally tested combinations and the ones involving cytotoxic drugs since we are interested on targeted therapies.

Finally, for the combinations targeting the same family of targets we selected the ones with higher PCI values and/or higher individual contributions.

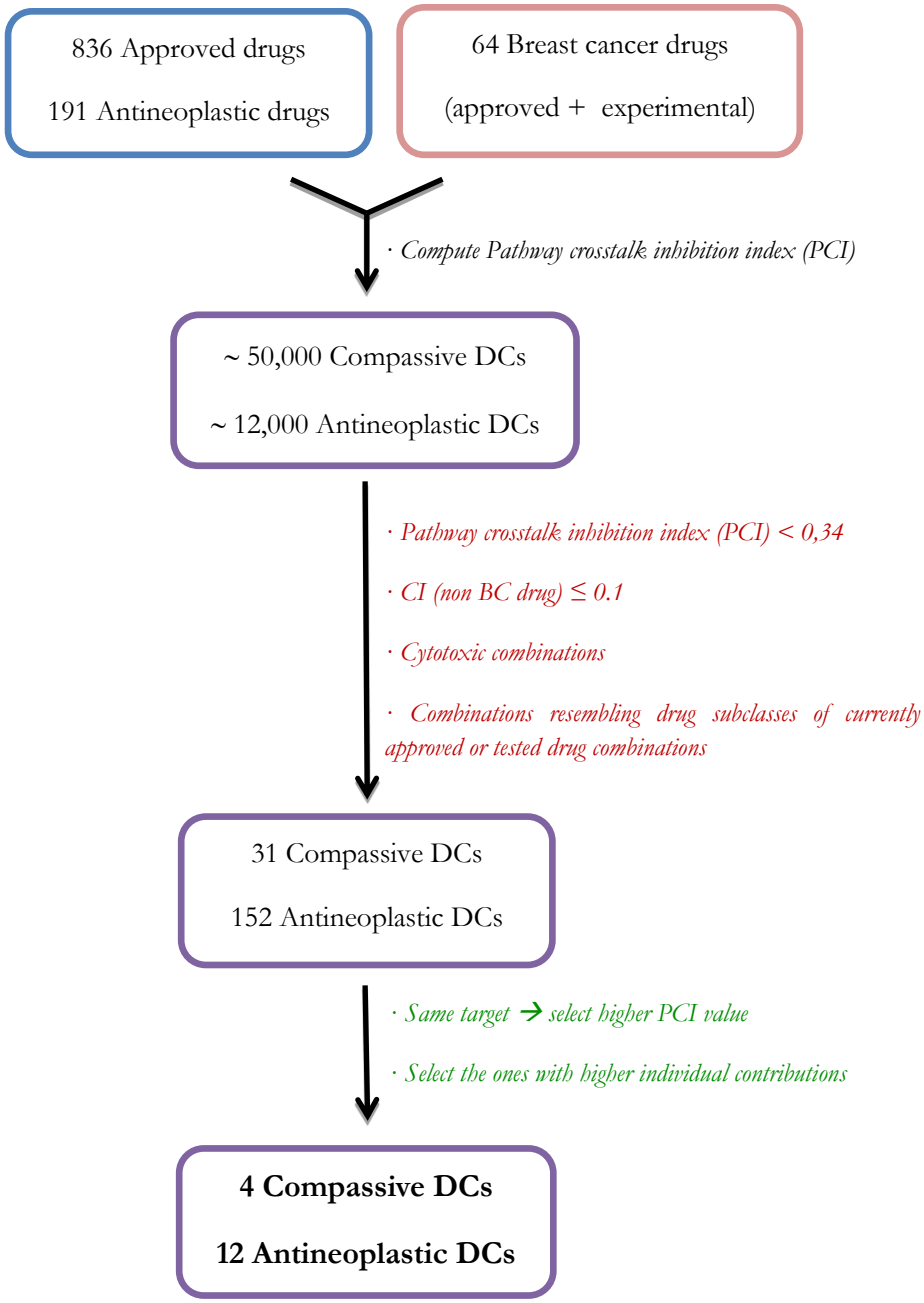

Figure 24. Schematic representation of drug combination filtering process. In red are described exclusion parameters and in green are represented inclusion criteria.

3.2.1.2 Experimental validation of novel combinations

After applying the filtering described in the previous section, we end up with 4 compassive and 12 antineoplastic drug combinations for the experimental validation in different breast cancer cell lines. **Tables 4 and 5** present an overview of the selected antineoplastic and compassive drug combinations respectively, showing the different pathway crosstalk inhibition values for each drug and drug combination, as well as the respective drug targets.

Id	BC drug (D1)	Non-cancer drug (D2)	PCI D1	PCI D2	PCI comb
DC13	**BEZ235** (PI3K/ mTOR inhibitor)	**Eplerenone** (NR3C2 inhibitor)	0.196	0.300	**0.456**
DC14	**Sorafenib** (VEGFR/PDGFR inhibitor)	**Eplerenone** (NR3C2 inhibitor)	0.196	0.280	**0.355**
DC15		**Dalteparin** (VEGFA, TFPI inhibitor)	0.131	0.320	**0.349**
DC16	**Bosutinib** (ABL1, Src inhibitor)	**Framycetin** (CXCR4 inhibitor)	0.396	0.009	**0.404**

Table 4. Overview of the selected compassive drug combinations. BC= breast cancer; D=drug and PCI=pathway crosstalk inhibition index.

Id	BC drug (D1)	Antineoplastic drug (D2)	PCI D1	PCI D2	PCI comb
DC01	**Raloxifene** (SERM)	**Dabrafenib** (BRAF, RAF1 inhibitor)	0.153	0.492	**0.615**
DC02		**Tanespimycin** (HSP inhibitor)	0.256	0.231	**0.452**
DC03		**Ruxolitinib** (JAK1/2 inhibitor)	0.134	0.261	**0.376**
DC04	**Tanespimycin** (HSP inhibitor)	**Dabrafenib** (BRAF, RAF1 inhibitor)	0.189	0.335	**0.485**
DC05	**Cediranib** (VEGFR/PDGFR inhibitor)	**Dabrafenib** (BRAF, RAF1 inhibitor)	0.177	0.371	**0.433**
DC06		**Ruxolitinib** (JAK1/2 inhibitor)	0.174	0.254	**0.425**
DC07	**Sorafenib** (VEGFR/PDGFR inhibitor)	**Trametinib** (MEK1/2 inhibitor)	0.318	0.229	**0.524**
DC08	**Everolimus** (mTOR inhibitor)	**Dabrafenib** (BRAF, RAF1 inhibitor)	0.160	0.276	**0.428**
DC09		**Ruxolitinib** (JAK1/2 inhibitor)	0.195	0.181	**0.361**
DC10	**Lapatinib** (HER2, EGFR inhibitor)	**Dabrafenib** (BRAF, RAF1 inhibitor)	0.129	0.336	**0.432**
DC11	**Erlotinib** (EGFR inhibitor)	**Tanespimycin** (HSP inhibitor)	0.214	0.206	**0.408**
DC12	**Dinaciclib** (CDK1/2/9 inhibitor)	**Dabrafenib** (BRAF, RAF1 inhibitor)	0.100	0.340	**0.430**

Table 5. Overview of the selected antineoplastic drug combinations. DC=drug combination; BC= breast cancer; D=drug; PCI=pathway crosstalk inhibition index and SERM=selective estrogen receptor modulator.

In vitro cytotoxicity assays (MTT)

We experimentally tested all the drug combinations described above by performing MTT assays (see **Material and Methods**). Our aim was to assess whether the selected drug combinations do have an impact on cell growth in breast cancer cell lines.

Each drug combination was tested in four different cell lines (**Table 6**) representing the main breast cancer subtypes regarding the hormone receptor status and the genetic aberrations representative of each subtype.

With the data obtained in the MTT assays, we modelled dose-response curves for each combination using sigmoidal fitting from which we then determined the half-maximal inhibitory concentration (IC_{50}), meaning the drug concentration that causes 50% inhibition of cell proliferation compared to non-treated cells.

	MDA-MB-231	MCF-7	SKBR-3	BT-474
Luminal	○	⊕	⊕	⊕
Basal	⊕	○	○	○
ER	○	⊕	○	⊕
PR	○	⊕	○	⊕
HER2	○	○	⊕	⊕
Other mutations	BRAF CDKN2A KRAS NF2 TP53	CDKN2A PI3KCA	TP53	PI3KCA TP53
Histology Subtype	Metastatic Adeno-carcinoma	Metastatic Adeno-carcinoma	Adeno-carcinoma	Invasive ductal carcinoma

Table 6. Breast cancer cell line features

Drug combination index (DCI) measurement

In order to determine whether the tested combinations were of synergistic, additive or antagonistic nature, we computed the Loewe additivity-based

drug combination index for each combination in each cell line (Chou, 2006) DCI_X compares the half-maximal effective concentrations for inhibiting X% of cell viability of single agents with the concentration derived for a combination, and is calculated as follows:

$$DCI_X = \frac{C_{D1,X}}{IC_{X,D1}} + \frac{C_{D2,X}}{IC_{X,D2}}$$

C_{D1} and C_{D2} represent the concentration of drug 1 and 2 used to achieve an effect X; $IC_{X,D}$ indicate the concentration of single agents that is required to induce the same effect X.

According to the Loewe additivity-based DCI we considered a DCI_X below 0.85 as synergistic, a DCI_X above 1.2 indicated antagonism while any value in-between depicted additivity ($0.85 > DCI_X \leq 1.2$).

In **Figure 25** is represented the DCI_{50} distribution in all cell lines. In two of them (DC10 in BT-474 and DC12 in SKBR-3), DCI_{50} values are not represented since the dose-response curve could be modelled.

Overall, taking into account antineoplastic and compassive combinations in all breast cancer cell lines, we obtain 29.7% synergistic combinations, while 25% are additive and 40.6% exhibit antagonistic effects. Given the heterogeneity of breast cancer, we do not expect that all combinations are synergistic in all cell lines, thus these values are quite encouraging, since previously reported high-throughput experimental synergy screens have found that synergistic drug pairs do only occur between 4 and 10% of the cases (Borisy et al., 2003, Zhang et al., 2007). Interestingly, in the antineoplastic combinations we observed that 75% were synergistic at least in one cell line, and 33.3% were synergistic at least in two different cell lines. However, for the compassive combinations we only found one clearly synergistic combination (DC13 in SKBR-3 cell line).

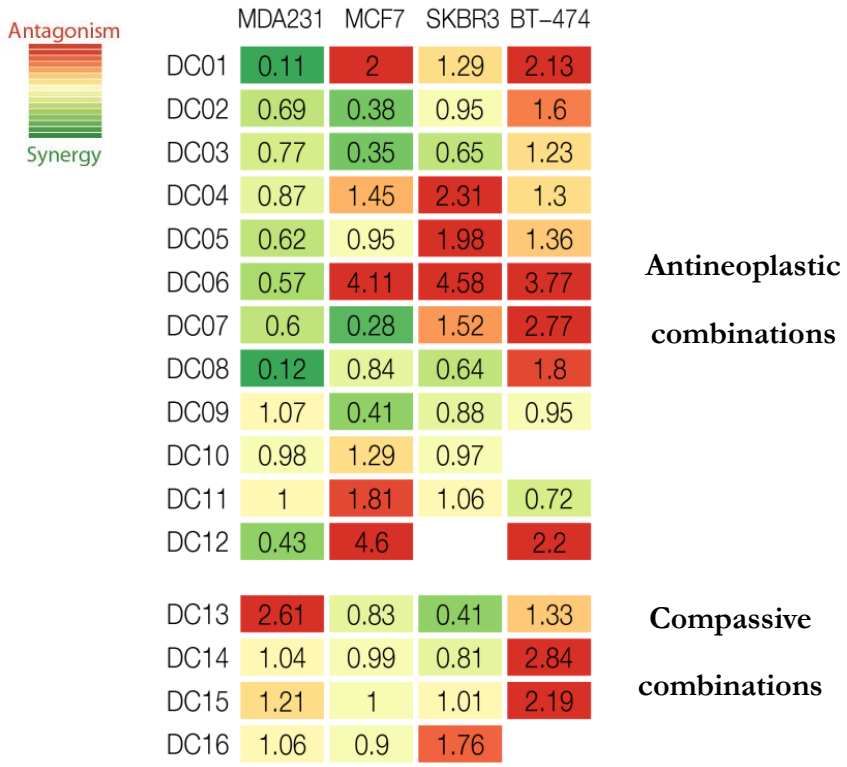

Figure 25. DCI_{50} values computed from the experimental validation. Blank cells indicate combinations for which DCI_{50} could not be determined. Synergistic values are depicted in green; yellow represents additivity and red antagonism.

Regarding the DCI distribution across the different cell lines (**Figure 26**), interestingly, almost 60% of the combinations appeared to be synergistic in the triple negative breast cancer (TNBC) cell line (MDA-MB-231), while in the triple positive (BT-474) 85% were antagonistic. It has been previously described that crosstalk between HER2 and ER receptors promote drug resistance (Bender and Nahta, 2008), thus this could be a plausible explanation for the high number of antagonistic combinations observed in BT-474 cell line expressing all, HER2, ER and PR receptors.

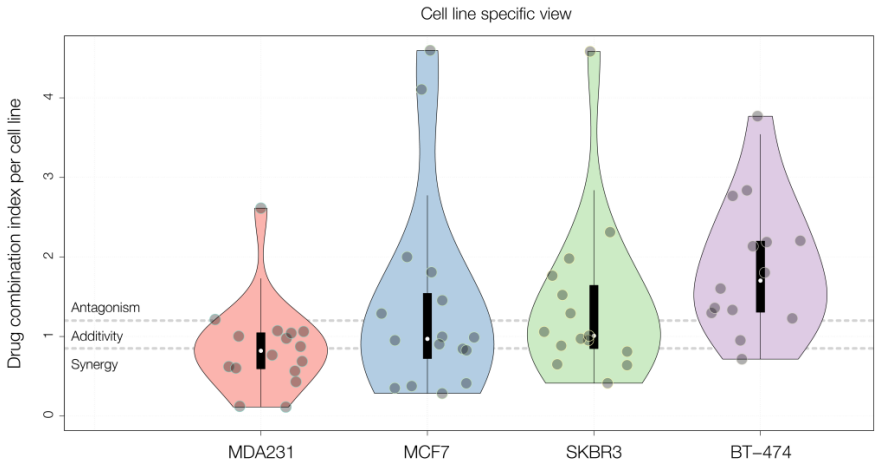

Figure 26. Cell line specific overview on the distribution of the DCI values across the different cell lines.

Taking into account all the data presented above, we can suggest that the pathway crosstalk inhibition approach depicted in this study is a promising and robust strategy to filter out synergistic drug combinations, allowing a significant enrichment compared to combinatorial studies without computational prioritization.

3.2.1.3 Effect of selected drug combinations on apoptosis and cell cycle

Since targeted cancer drugs are directly or indirectly modulating apoptosis and/or cell cycle (Ghobrial et al., 2005, Munagala et al., 2011), we next aimed to determine whether the synergistic effects induced by drug combinations in the previous MTT assays, are due to apoptosis induction or cell cycle arrest induction.

Drug combination selection and functional assays

In order to reveal the most promising antineoplastic combinations, we focused on MDA-MB-231 cell line (triple negative), since it showed a synergistic activity in the vast majority of the combinations tested. As mentioned before, triple negative breast cancer is characterized by a lack of expression of ER and PR, as well as non altered HER-2 status. Thus, to date,

chemotherapy remains the only possible therapeutic option.

We selected the two combinations with the lowest DCI values (DC01 and DC08) and the three combinations that were only synergistic in MDA-MB-231 (DC05, DC06 and DC12), suggesting that they could be specific treatment for the triple negative subtype. Additionally, in the compassive group, DC13 in SKBR-3 (HER2+) was selected as it is the only synergistic combination (see **Table 7** for detailed information).

Subsequently, we chose the concentrations corresponding to the IC_{50} for each drug in the combination treatment, and perform some functional apoptosis assays (determination of cleaved PARP levels combined with analysis of apoptotic cell population by flow cytometry) and cell cycle analysis (see **Material and Methods**).

Albeit all the selected combination presented promising results in the MTT assays, drug combinations involving mTOR inhibitors (DC06, DC12 and DC13) and raloxifene (DC01), did not show any effect either in apoptosis promotion or in cell cycle progression (data not shown). Additional techniques focused on autophagy detection would be needed in order to elucidate the mode of action of these combinations since both type of drugs lead to the induction of autophagy-dependent cell death (Albert et al., 2006, Kim et al., 2015). Thus, the following sections are focused on the antineoplastic combinations involving VEGFR inhibitors, cediranib and sorafenib, combined with the JAK1/2 inhibitor (ruxolitinib) or the MEK1/2 inhibitor (trametinib) respectively (i.e. DC05 and DC08).

Id	Drug 1 (D1)	Drug 2 (D2)	PCI D1	PCI D2	PCI comb	DCI_{50}
DC01	**Raloxifene** (SERM)	**Dabrafenib** (BRAF, RAF1 inhibitor)	0,153	0,492	**0,615**	**0,11**
DC05	**Cediranib** (VEGFR/PDGFR inhibitor)	**Ruxolitinib** (JAK1/2 inhibitor)	0,174	0,254	**0,425**	**0,62**
DC06	**Everolimus** (mTOR inhibitor)	**Dabrafenib** (BRAF, RAF1 inhibitor)	0,160	0,276	**0,428**	**0,43**
DC08	**Sorafenib** (VEGFR/PDGFR inhibitor)	**Trametinib** (MEK1/2 inhibitor)	0,318	0,229	**0,524**	**0,12**
DC12	**Everolimus** (mTOR inhibitor)	**Ruxolitinib** (JAK1/2 inhibitor)	0,195	0,181	**0,361**	**0,57**
DC13	**BEZ235** (PI3K/ mTOR inhibitor)	**Eplerone** (NR3C2 inhibitor)	0,196	0,300	**0,456**	**0,41**

Table 7. Overview of the selected antineoplastic (in light red) and compassive (in green) combinations. DC=drug combination; D=drug; PCI=pathway crosstalk inhibition index; DCI=drug combination index and SERM=selective estrogen receptor modulator.

Cediranib in combination with ruxolitinib (DC05) promote apoptosis and cell cycle arrest in TNBC cells

As described in the literature, none of the single agents induced apoptosis at the low concentrations used in our experiments (Liu et al., 2013, Yang et al., 2014) but, surprisingly, the combination significantly promoted apoptosis through PARP cleavage (**Figure 27A**).

The results obtained looking at PARP cleavage were confirmed by flow cytometry analysis, where the treatment with the drug combination resulted in a significant increase in the number of apoptotic cells as compared to single treatments (5.1 fold, $P<0.001$ and 1.7 fold, $P<0.05$ respectively) (**Figure 27B**), while drugs alone did not induce apoptosis, thus confirming the synergistic growth-inhibitory effects. Of note, clonogenic assays confirmed that the increase in apoptosis correlated with lower overall survival of the cancer cell population compared to single treatments (1.7 fold, $P<0.05$ and 1.8 fold $P<0.01$ respectively) (**Figure 27C**).

Additionally, to determine whether the synergistic effect observed in the MTT assays was also due to cytostatic effects, we sought to examine cell cycle phase distribution. As observed in **Figure 28**, none of the drugs alone were cytostatic at the low concentrations used in our experiments, but interestingly, the combination presented a cytostatic effect with a significant increase of cells in S phase (1.6 fold, $P<0.05$) accompanied by a significant reduction in the number of cells in G_1 phase as compared to cediranib alone (1.4 fold, $P<0.05$). The same differences were observed compared to ruxolitinib, although in this case they were not statistically significant.

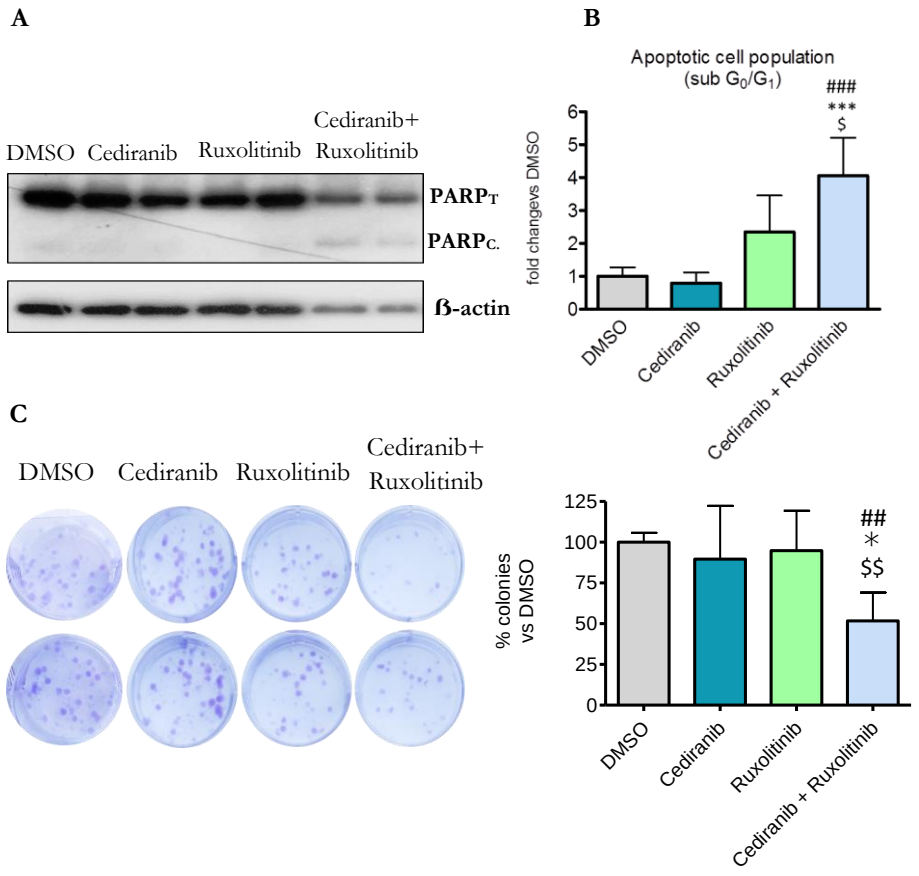

Figure 27. Cediranib in combination with ruxolitinib promotes cell apoptosis. **(A)** Immunoblot analysis of cleaved PARP protein levels in MDA-MB-231 cells treated with cediranib (6 μM), ruxolitinib (18 μM) and its combination for 72 hours **(B)** Flow cytometry analysis of sub G_0/G_1 peak in MDA-MB-231 cells treated with cediranib (6 μM), ruxolitinib (18 μM) and its combination during 72 hours with single drugs or the drug combination. **(C)** Clonogenic assay in MDA-MB-231 cells treated O/N with cediranib (6 μM), ruxolitinib (18 μM) and its combination. The vehicle (DMSO) is used as a negative control. (# P <0.05, ## P<0.001, ### P<0.0001 versus DMSO, * P<0.05, ** P<0.01, *** P<0.001 versus cediranib and $ P<0.5 versus ruxolitinib).

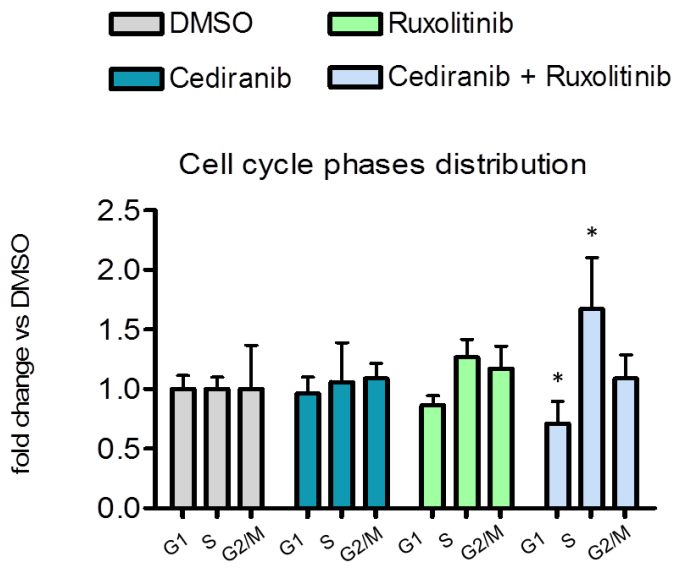

Figure 28. Cediranib in combination with ruxolitinib induces cell cycle arrest. Flow cytometry analysis in MDA-MB-231 cells treated with cediranib (6 μM), ruxolitinib (18 μM) and its combination. DMSO is used as a negative control. Cells are treated for 72 hours with single drugs or the drug combination. Each bar represents the mean ±SD of three experiments performed in duplicate. (# P <0.05, ## P<0.001, ### P<0.0001 versus DMSO, * P<0.05, ** P<0.01, *** P<0.001 versus cediranib).

The effects on cell cycle and apoptosis are in line with the current knowledge on the mechanisms of action of the two drugs. Cediranib, currently in phase III for solid tumours and in phase II in combination for metastatic breast cancer (http://www.clinicaltrials.gov), supresses VEGFR2 signalling, which crosstalks with SRC or PI3K/Akt, promoting VEGF-induced cytoskeletal reorganization, migration, proliferation and angiogenesis (Matsumoto et al., 2005). However, at low concentrations, cediranib is not able to promote apoptosis as observed in melanoma and glioblastoma cell lines (Friedman et al., 2015, Jones et al., 2015).

On the other hand, ruxolitinib, a potent and selective JAK1/JAK2 inhibitor

that significantly inhibits interleukin-6 signalling, is being investigated in clinic in patients with leukemia (Eghtedar et al., 2012, Pemmaraju et al., 2015) and pancreatic cancer (Hurwitz et al., 2015). It is described that ruxolitinib does not induce apoptosis nor cell cycle arrest when it is used as a single drug treatment in triple negative breast cancer cell lines (Yang et al., 2014).

Promisingly, our study confirms that the combination of these two drugs at low concentrations promotes a clear induction of apoptosis accompanied by a cell cycle arrest on S phase in triple negative breast cancer cells. Interestingly, the adverse effects could be reduced due to the lower concentrations needed for each drug. This is in agreement with a recent study suggesting that combined treatment with VEGF-neutralizing antibodies and VEGFR-2 or JAK/STAT inhibitors is a promising strategy to reduce breast and lung cancer stem cell (CSC) self-renewal (Zhao et al., 2015).

Sorafenib in combination with trametinib (DC08) promote apoptosis and cell cycle arrest in TNBC cells

In the same way as described for the previous combination, we aimed to analyse whether sorafenib in combination with trametinib was able to modulate the apoptotic response. As observed in **Figure 29A**, sorafenib alone did not induce PARP cleavage as previously described in the literature (Liu et al., 2013), nevertheless, treatment with trametinib resulted in apoptosis promotion compared to the negative control. Even more interesting, the combination of both drugs increased cleaved PARP levels as compared to single treatments. In agreement with these results, the number of apoptotic cells observed in the flow cytometry analysis (**Figure 29B**) revealed that trametinib alone promoted an apoptotic response as compared to the negative control (3.9 fold, $P<0.05$), and that its combination with sorafenib increased even more this response compared to the negative

control and sorafenib alone (5.6 fold, P<0.001 and 5.7 fold, P<0.001 respectively). Finally, clonogenic assays showed a general moderate decrease in cell survival of cancer cells treated with the drug combination, which was only statistically significant compared to sorafenib alone (1.3 fold, P<0.05) (**Figure 29C**).

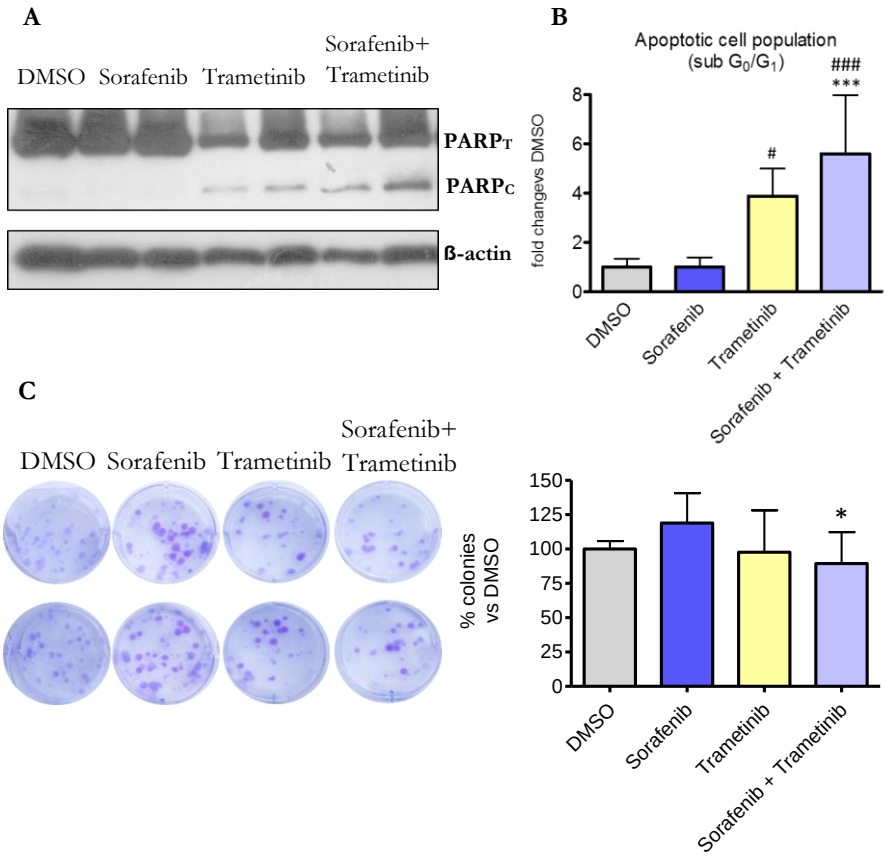

Figure 29. Sorafenib in combination with trametinib promotes cell apoptosis. **(A)** Immunoblot analysis of cleaved PARP protein levels in MDA-MB-231 cells treated with sorafenib (2 nM), trametinib (2 nM) and its combination **(B)** Flow cytometry analysis of sub G_0/G_1 peak in MDA-MB-231 cells treated with sorafenib (2 nM), trametinib (2 nM), and its combination. The vehicle (DMSO) is used as a negative control. Cells are treated for 72 hours with single drugs or the drug combination. (# P <0.05, ## P<0.001, ### P<0.0001 versus DMSO, * P<0.05, ** P<0.01, *** P<0.001 versus sorafenib).

Regarding to the cell cycle analysis (**Figure 30**), sorafenib alone was not able to induce a cytostatic effect in any phase, while trametinib treatment promoted a significant cell cycle arrest on G_1 phase (1.4 fold, P<0.001) coupled with a decrease in S (2.8 fold, P<0.0001) and G_2/M (1.9 fold, P<0.05) populations as compared to the negative control. In a similar way, trametinib in combination with sorafenib induced a cytostatic effect in G_1 (1.5 fold, P<0.0001), while in this case it was accompanied by a significant decrease in both, S (2.7 fold, P<0.0001) and G_2/M (6.0 fold, P<0.0001) phases versus the negative control, and similarly, to sorafenib alone.

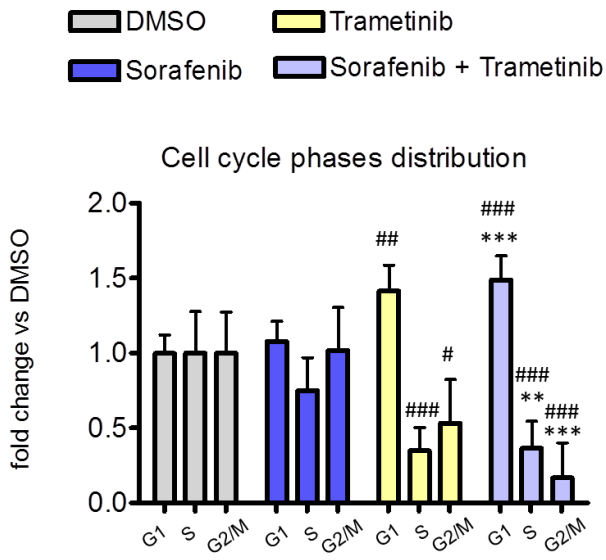

Figure 30. Sorafenib in combination with trametinib induces cell cycle arrest. Flow cytometry analysis in MDA-MB-231 cells treated with sorafenib (2 nM), trametinib (2 nM) and the combination. DMSO is used as a negative control. Cells are treated for 72 hours with single drugs or the drug combination. Each bar represents the mean ±SD of three experiments performed in duplicate. (# P <0.05, ## P<0.001, ### P<0.0001 versus DMSO, * P<0.05, ** P<0.01, *** P<0.001 versus sorafenib).

Trametinib, approved for melanoma and in phase I trial in combination for TNBC (http://www.clinicaltrials.gov), is able to induce apoptosis and cell

cycle arrest in G_1 phase, even at low concentrations, which is in line with other studies showing that MDA-MB-231 cells harbouring RAS and RAF mutations, present an active MAPK pathway signalling making them highly sensitive to MEK inhibitors, such as trametinib (Leung et al., 2014). Whilst sorafenib, a VEGFR inhibitor approved for renal carcinoma that is also in phase II in combination for breast cancer (http://www.clinicaltrials.gov) does not show any effect either in apoptosis or in cell cycle progression in TNBC cell line at low concentrations.

Interestingly, the combination of sorafenib and trametinib at low concentrations promotes synergistic effects basically through apoptosis induction. Although further studies are required, this is a promising treatment strategy, since the combination of MEK and VEGFR inhibitors has also been described to inhibit tumour angiogenesis, growth and metastasis in xenograft models in lung cancer (Takahashi et al., 2012).

Therefore, although further *in vivo* and clinical studies are required, our findings highlight both drug combinations as very promising therapeutic strategies for triple negative breast cancer subtype.

3.2.2 DRUG COMBINATIONS PREDICTED BY NETWORK ACTIVITY QUANTIFICATION

This work has been done in **collaboration** with **Dr. Miquel Angel Pujana**'s Group, Institut Català d'Oncologia, (ICO).

Since genes and proteins are functionally organized within complex networks (Barabasi and Oltvai, 2004) and that biological processes and signalling pathways are robust to perturbations in cancer cells (Breitkreutz et al., 2012, Serra-Musach et al., 2012, Shiraishi et al., 2010, Teschendorff and Severini, 2010, van Wieringen and van der Vaart, 2011, Zadran et al., 2013), this study

hypothesized that a measure of the cancer network activity (NA*)* could potentially predict sensitivity to a given therapy.

3.2.2.1 NA evidence can be used to predict synergism

This question was addressed by integrating the known human network of protein-protein-interactions with the basal gene expression measurements in hundreds of cancer cell lines whose sensitivity to several drugs was previously determined (Garnett et al., 2012). Taking into account all these data, a weighted path algorithm was computed for each cell line obtaining a NA value that potentially capture cancer-associated mechanisms and differences in the sensitivity to a given therapy (**Figure 31**).

Subsequently, in order to reflect the possible associations between NA and therapy sensitivity, Pearson correlation coefficients between the NA and IC_{50} were computed for each drug across all cell lines, or with respect to a cell line fulfilling a certain condition (i.e. driver mutations status). In this way, the correlation coefficients relative to various conditions such as genetic mutations, compound classes or biological processes were analysed demonstrating that certainly, NA profiles can distinguish types of drugs according to their characteristics and driver gene mutation status.

Taking into account all this information, it was hypothesized that NA measures could be useful to identify drugs that maximize the perturbation of the cancer network. In turn, since NA measures seem to capture the effect produced by biological processes, maximizing the perturbation may increase the likelihood of a synergistic effect between two drugs.

However, since drugs may overlap the effected cellular mechanisms, only those pairs of compounds with uncorrelated IC_{50} profiles were considered in order to affect different mechanisms through the cell lines, providing greater network perturbation, thus achieving higher synergistic effects.

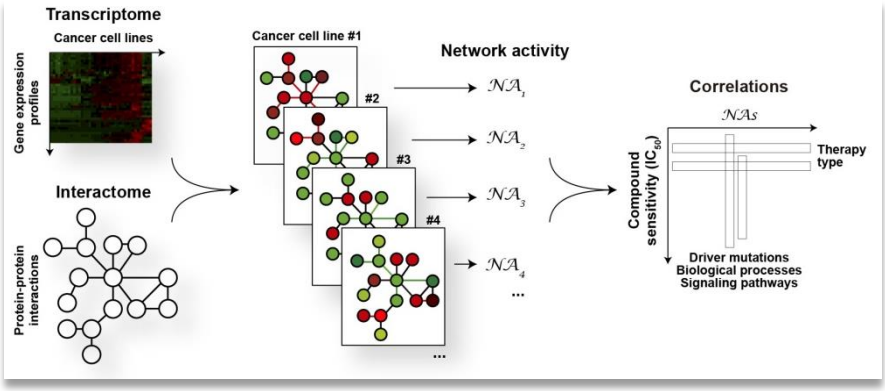

Figure 31. Study design. The basal gene expression of hundreds of cancer cell lines is integrated into the interactome network, and a *NA* score is then assigned to each cell line by computing a weighted path algorithm. Next, the *NA* profiles are examined for their potential correlations with types of compounds or therapies, known cancer driver mutations, biological processes and signalling pathways (*Serra-Musach J. et al, submitted*).

3.2.2.2 Validation of synergistic combinations by MTT assays

On the basis of the above hypotheses, the study was centered on PI3K/AKT signalling, as it plays a key role in carcinogenesis and therapy response, particularly in breast cancer (Lai et al., 2015). Thus, the following cancer cell lines were used to evaluate combinations of uncorrelated compounds in our laboratory: MCF-7 and BT-474 breast cancer cell lines, both harbouring an oncogenic *PIK3CA* mutation (She et al., 2008) and U2O2 osteosarcoma cell line in order to evaluate the strategy in other cancer types (see **Table 8** for additional information). In parallel, other breast cancer cell lines harbouring an oncogenic *PIK3CA* mutation (MDA-MB-453 and HCC1954) or molecular alterations linked to increased AKT activity (MDA-MB-231 and SKBR-3) were tested in Dr. Pujana's laboratory.

	MCF-7	BT-474	U2OS
Luminal	⊕	⊕	Osteosarcoma
Basal	○	○	
ER	⊕	⊕	
PR	⊕	⊕	
HER2	○	⊕	
Other mutations	CDKN2A PI3KCA	PI3KCA TP53	CDKN2A
Histology Subtype	Adeno-carcinoma	Invasive ductal carcinoma	Sarcoma of the tibia

Table 8. Overview of cancer cell lines used in our laboratory.

On the other hand, for the compounds targeting the PIK3CA/R1 status (identified by the correlation between the NA and IC_{50}), were considered the ones with uncorrelated IC_{50} through the cancer cell lines.

With these conditions, metformin in combination with AZD-8055, olaparib or SL-0101 were selected (see **Table 9**).

Id	Drug 1	Drug 2
DC01	**Metformin** (AMPK agonist)	**AZD-8055** (mTOR inhibitor)
DC02		**Olaparib** (PARP inhibitor)
DC03		**SL0101-1** (S6 kinase (RSK) inhibitor)

Table 9. Overview of selected drugs.

DCI index revealed significant synergism

Next, assessment of the inhibitory effect of each metformin combination was done by MTT assays, followed by the determination of synergistic activities (DCI < 0.85) as explained in **section 3.2.2.**

As depicted in **Figure 32**, six out of nine tests (66.6%) appeared to be synergistic in all cell lines. Drug combinations involving mTOR and PARP inhibitiors (DC01 and DC02) resulted in a synergistic effect in all the cell lines, while DC03 (involving S6 kinase inhibitor) promoted a clear synergistic effect only in the osteosarcoma cell line.

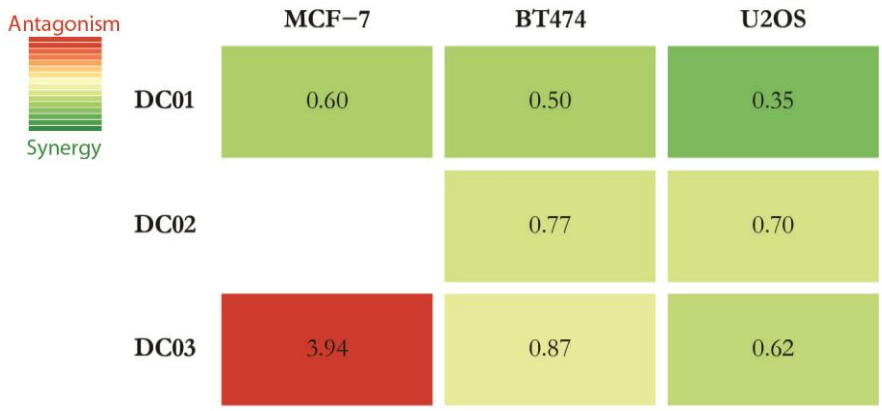

Figure 32. DCI_{50} values computed from the experimental validation. Blank cells indicate combinations for which DCI_{50} could not be determined. Synergistic values are depicted in green; yellow represents additivity and red antagonism.

Metformin is an approved anti-diabetic drug and is also being tested in clinical trials for breast cancer therapy, both as a single agent and in combination with other compounds (Bonanni et al., 2012, Grenader et al., 2009), although not in any of the combinations proposed here. The combination of metformin with AZD-8055 resulted in the highest synergistic effect, in agreement with recent studies showing promising results in *in vivo* and *in vitro* breast cancer models by using another mTOR inhibitor (everolimus) (Liu et al., 2012, Wang et al., 2015).

Taking into account our results and the ones obtained by our collaborators in other breast cancer cell lines (data not shown), we can suggest that cancer cell models relying on PI3K/AKT signalling can be specifically targeted with a combination of metformin and AZD-8055 or olaparib and possibly with other compounds targeting the same proteins. These results are coherent and expand on previous observations of the synergistic effect of combining PI3K and PARP inhibitors in the treatment of *BRCA1*-related breast cancer (Juvekar et al., 2012).

Collectively, our results demonstrate that the NA measure is useful to guide the identification of effective specific, synergistic compound combinations for cancer therapy.

4. CONCLUSIONS

In the present thesis network biology based approaches have been used to explore in detail the molecular mechanisms underlying breast cancer, which has led to the following conclusions:

• In the first part of this thesis we have provided new evidences on certain passenger genes related to breast cancer, EPSTI1 and PSMC3IP. We have revealed that both genes have a strong anti-apoptotic role in breast cancer cells by means of physical interaction with the apoptosis initiator caspase-8, highlighting them as potential therapeutic targets, preeminently for their ability to apoptosis sensitization.

• In the second part, two different network based approaches have allowed us to identify novel synergistic drug combinations with great potential for the treatment of breast cancer.

In particular, we have shown that drug combinations combining cediranib with ruxolitinib and sorafenib with trametinib, have a synergistic apoptotic effect in triple negative breast cancer cells, suggesting they could be considered as promising strategies for triple negative breast cancer treatment.

5. MATERIAL AND METHODS

5.1. EXPERIMENTAL METHODS

5.1.1 General basic instrumentation

Instrument	Model
Cell Incubator	Thermo Electron Corporation, Model 3121, Forma Series II, Water Jacketed CO_2 Incubator, HEPA class 100 filter
Laminar flow hood	Telstar, BIO II A Biological Safety Cabinet
Cell counter	Beckman Coulter, Z1 Coulter® Particle Counter
Centrifuges	Beckman Coulter Allegra™ 21 Centrifuge
	Eppendorf, Centrifuge 5415 R, centrifuge 5415 D
Thermomixer	Eppendorf, Thermomixer comfort
Microscopes	Nikon T1-SM
	Upright epifluorescence microscope**,** Nikon Eclipse E1000
Spectrophotometer	Thermo scientific, NanoDrop 2000, UV-VIS spectrophotometer

Table 10. General basic instrumentation

5.1.2 DNA protocols: Gateway Technology

General considerations

The manipulation of nucleic acids must be performed using sterile material devoided of DNAses, RNAses, and exogenous DNA contamination. Plasmid DNA can be kept at 2-8ºC for short term storage or in aliquots at -20ºC for long term storage.

Subcloning of human cDNAs into yeast two-hybrid (Y2H) plasmids

Human ORF clones AKT1, BCAR3, CDKN2A, CHEK2, EPSTI1, PARP1 and XIAP and derived from the human ORFeome v1.1 (Lamesch et al., 2007) and BAG4, CASP8, CDKN2C, IGF1R and PSMC3IP clones from Life Technologies Ultimate™ ORF Clones were obtained as a Gateway® cloning adapted plasmids and the corresponding sequences were verified.

Subcloning of cDNA into Y2H plasmids consists of three parts:

- Polymerase Chain Reaction (PCR)
- TOPO® Cloning

PCR amplification of cDNA clones was accomplished with primers specific for each gene containing additional nucleotides (CACC). Primers were designed with Clone Manager (Sci-Ed) and VectorNTI (Life Technologies) softwares. 50 µl reaction containing 1X PCR Buffer, 0.3 mM of each dNTP, 1 mM $MgSO_4$ 0.4 µM forward and reverse primers, 100 ng of template DNA, 1U of DNA polymerase, and autoclaved water to reach final volume, was prepared and amplified in a Mastercycler ep Gradient (Eppendorf) using the following parameters for touchdown PCR: initial denaturation at 95ºC for 2 minutes; 30 cycles of denaturation at 95ºC for 30 seconds, annealing for 40 seconds and extension at 72ºC (temperature of annealing and extension time were different in each reaction based on primers Tm and length of the fragment to amplify), final extension at 72ºC for 7 minutes.

TOPO® Cloning

Next, the cDNA were ligated into pENTR™/D-TOPO vector (pENTR Directional TOPO cloning kit (Life Technologies) and sequenced. TOPO® TA Cloning (Life Technologies) was performed to create Gateway® adapted Entry Clones. The following reactions were set up using the reagents in the order shown: 4 µl of fresh PCR product, 1 µl of salt solution and 1 µl of TOPO® Vector. The reaction was mixed gently, incubated for 5 minutes at room temperature and transformed into *Escherichia coli* cells (see below).

Gateway® Cloning

Finally, all ORFs were individually transferred into Y2H destination vectors by Gateway© recombinational cloning (ProQuest System, Life Technologies). Driver genes (*AKT1, BCAR3, CDKN2A, CHEK2, PARP1, BAG4, CASP8, CDKN2C, IGF1R*) were cloned into pDEST32 to generate bait plasmids, while passenger genes (*EPSTI1, PSMC3IP*) were cloned into pDEST22 to obtain prey plasmids.

Additionally, Gateway® cloning reaction was used to transfer our genes into a MYC-tagged destination vector (Gateway® pDEST™17 Vector-Myc), so that the encoded proteins contain an N-terminal MYC-tag (11KDa) that enables the use of a single anti-MYC antibody for protein detection by western blot analysis.

In order to perform the cloning, the following components were mixed at room temperature (RT): 150 ng of entry clone, 150 ng of destination vector and TE buffer (*p*H 8.0) to 8 µl. 2 µl of LR Clonase™ II enzyme were added to the reaction, the suspension was mixed by vortexing and incubated at 25ºC for 1 hour. After that, 1 µl of Proteinase K was added and incubated at 37ºC for 10 minutes to terminate the reaction. The reaction product was

transformed into competent DH5-α *Escherichia coli* cells (Invitrogen) as described in the following section.

Transformation in bacteria cells

5 µl from Gateway Cloning reaction were mixed in the reaction tube containing 25 µl of DH5-α competent cells, and incubated on ice for 20-30 minutes. After incubation, cells were heat-shocked for 45 seconds at 42ºC without shaking. Immediately after, tubes were cooled on ice for 2 minutes, then, 250 µl of pre-warmed S.O.C medium was added and the cells were incubated at 37ºC for 1 hour with shaking. The cells were spinned and all the supernatant except 100 µl was discarded. Pelleted cells were resuspended with the remaining supernatant and plated on pre-warmed selective LB plates and incubated overnight at 37ºC.

the appropriate antibiotic for the LB-agar (BD) plates was used:

- Ampicillin (amp), prepared at a concentration of 50 mg/mL in water, was used at final concentration of 100 µg/mL.
- Kanamycin (kan), prepared at a concentration of 25 mg/mL in water, was used at final concentration of 50 µg/mL.

After that, two colonies for each sample were selected from the LB-agar plates and grown in LB liquid medium with the selective antibiotic overnight at 37ºC with shaking. Ultimately, plasmids were purified from the bacterial culture suspensions using GENEJET Plasmid Miniprep Kit (Fermentas GMBH), following the manufacturer's instructions.

DNA sequencing

Commercial oligonucleotides (T7 or SP6) with adjacent complementary sequences to each end of the cloning site were used as primers for the sequencing of human cDNAs into Gateway® plasmids.

5.1.3 Yeast two-hybrid (Y2H) matrix screens

The Y2H technique allows detection of interacting proteins in living yeast (Fields and Song, 1989) Interaction between two proteins, called bait and prey, activates reporter genes that enable growth on specific media or participate in an enzymatic reaction producing a coloured product.

Bait and prey plasmids were co-transformed pair-wise into MaV203 yeast strain in 96-well arrays and plated onto selective SD2 agar media (lacking Leucine and Tryptophan amino acids) and incubated for 48 hours at 30ºC. Co-transformant arrays were then replica plated onto different selective media for interaction screening. To assay the activation of the HIS3 reporter gene, SD3 (lacking Leu,Trp,His) agar plates were supplemented with 12 to 100 mM of 3-aminotriazole (3AT, Sigma-Aldrich), 50 mM 3AT being the optimal concentration for positive HIS3 activation colonies. Similarly, we assayed the activation of the URA3 reporter gene by plating onto SD3 (lacking Leu, Trp, Uracil). Double reporter HIS3/URA3 activation was evaluated by SD4 (lacking Leu, Trp, His, Uracil) agar plates supplemented with 20 mM of 3AT and LacZ reporter gene expression was tested by the α-galactosidase assay on a nylon membrane placed onto a SD2 agar plate.

In order to minimize the number of false positives (at the cost of penalizing potential false negatives as well), we subsequently scored the positive interactions based on their ability to activate at least two reporter genes or being repeatedly observed in biological replica screens, which defined our high-confidence (HC) interaction set.

5.1.4 Mammalian cell culture

5.1.4.1 Cell lines

All the cells used in the present thesis were grown at 37ºC in a humidified atmosphere of 5% CO_2 to maintain the *p*H of the medium. Since these cells

show highly proliferating rates, the cultures have to be subcultured at least twice a week.

MCF-7 cells

The MCF-7 breast cancer cell line was derived from a pleural effusion taken from a 69-year-old Caucasian woman with metastatic breast cancer. These cells present the main features of the luminal A breast cancer subtype expressing both estrogen and progesterone receptors while they lack HER2 receptor, making it an ideal model to study the hormone response. Additionally, they present common mutations in CDKN2A /PIK3CA genes (http://www.atcc.org). This cells were grown in Dulbecco Modified Eagle's Medium (DMEM, Gibco, Invitrogen) with 10% Fetal Bovine Serum (FBS, Gibco), and 100 U/mL-100 μg/mL of penicillin-streptomycin solution (Gibco, Invitrogen).

MDA-MB-231 cells

MDA-MB-231 is one of the most used cell lines for *in vitro* experimental study of the hormone-independent breast cancer. These cells were isolated by Cailleau and colleagues in 1973, from a sample of pleural effusion of a 51-year-old Caucasian woman with breast cancer (Cailleau et al., 1974). They present abundant membrane receptors for epidermal growth factor (EGF) but, paradoxically they are not overstimulated by this factor (Martinez-Carpio et al., 1999). This cell line mimics the characteristics of the triple negative breast cancer subtype since they lack the expression of hormone receptors and the overexpression/amplification of HER2 receptor. These cells were grown in DMEM/F12 (Gibco, Invitrogen) with 10% FBS and 100 U/mL-100 μg/mL of penicillin-streptomycin solution.

SKBR-3 cells

SKBR-3 cell line was isolated by the Memorial Sloan–Kettering Cancer Center in 1970, and was derived from a pleural effusion due to an adenocarcinoma originated in the breast of a 43-year-old Caucasian female. These cells overexpress HER2 receptor but lack estrogen and progesterone receptors, which were the main characteristics observed in patients that belong to the HER2 breast cancer subtype. Additionally, SKBR-3 cells present mutations in the *TP53* gene (http://www.atcc.org). These cells were cultured in DMEM with 10% FBS, 100 U/mL-100 μg/mL of penicillin-streptomycin solution and 5% of glutamine (Sigma Aldrich).

BT-474 cells

BT-474 cell line was isolated by E. Lasfargues and W.G. Coutinho from a solid, invasive ductal carcinoma of the breast from a 60-year-old Caucasian female. It mimics the main characteristics of luminal B (or triple positive) breast cancer subtype by expressing estrogen and progesterone receptors, in addition to HER2 receptor amplification. Moreover, these cells present mutated *TP53* (http://www.atcc.org). According to these characteristics, this cell line presents the capability of responding to both hormone and trastuzumab treatments. Cell replication was maintained with DMEM/F12 with 10% FBS, 100 U/mL-100 μg/mL of penicillin-streptomycin solution and 5% of glutamine.

5.1.4.2 Maintenance and subculture

Maintenance cultures were normally plated in 75 cm^2 flask or 60 cm^2 plates at low confluences, with 20% being the minimal percentage recommended. Once cells reached a threshold confluence (80-90%), the culture was split into a new flask using trypsin-EDTA. First, cell culture media was removed and cells were washed using PBS in order to remove any traces of serum, calcium, and magnesium that would inhibit the action of the trypsin-EDTA

reagent. The wash solution was removed and trypsin-EDTA was added (1 mL per 60-75 cm^2, it must cover the entire cell layer). It was incubated at 37ºC for 3-5 minutes until cells detach. Subsequently, 9 mL of pre-warmed growth medium was added to the flask and transferred with the cells to a 15 mL conical tube and centrifuged at 200x g for 5 minutes at RT. The supernatant was discarded and the cell pellet was resuspended in pre-warmed complete growth medium. Cell suspension was then diluted to the desired seeding density (i.e. 1:3 or 1:6 dilution) in order to maintain cells growing.

Additionally, aliquots of cells could be cryopreserved in liquid nitrogen with complete medium in the presence of a cryoprotective agent, such as dimethylsulfoxide (DMSO) (5% v:v) (Sigma Aldrich), which reduces the freezing point of the medium and also allow a slower cooling rate, greatly reducing the risk of ice crystal formation, which can damage cells and cause cell death.

Freezing procedure

Cells were detached as described before and aliquots of 950 µl cell suspension with 50 µl DMSO were dispensed into sterile cryogenic storage vials, which should be kept on ice for toxic reasons. Quickly, cells should be frozen at -80ºC and after 24 hours they were immersed in the liquid nitrogen tank where they can be stored for several years.

Thawing procedure

Thawing procedure must be rapidly performed in order to minimize the risk of cell death due to DMSO exposure. Cell suspension was diluted slowly with 1mL of cold medium, and placed in a 15 mL conical tube containing 9 mL of cold fresh complete growth medium. Cell suspension was homogenized and centrifuged at 200x g for 5 minutes at RT. The supernatant was removed to eliminate DMSO and the cell pellet was resuspended in 10 mL of pre-warmed fresh complete growth medium and cells were plated in 75 cm^2 flask or 60 cm^2 plate.

Cell counting

In case a defined number of cells is needed to perform specific assays, 50 µL of cell suspension should be removed from the 1 mL cell suspension, and diluted in 10 mL of cell counter buffer (Beckman Coulter) in order to determine the number cells/mL in the cell counter machine according to the equipment instructions.

Different number of cells was plated depending on the cell line in order to achieve a final confluence of about 80-90% at the end of the experiment. In all the experiments, cells were plated 16-24 hours before starting drug treatments and/or transfections (**see Table 11**).

Assay	MCF-7	MDA-MB-231	SKBR-3	BT-474
MTT (96-well plate)	5,000	5,000	1,500	5,000
TUNEL (24-well plate)	50,000	50,000	-	-
Western Blot (12-well plate)	100,000	100,000	60,000	-
Caspase activity and Propidium iodide staining (6-well plate)	200,000	200,000	120,000	-

Table 11. Number of cells per well in each type of assay

5.1.4.3 Cell treatments

Transient cDNA transfection using MYC-tagged ORF clones

The overexpressed cDNA plasmid produced in competent DH5-α *Escherichia coli* cells (**described in section 5.1.2**) was extracted and purified via GENEJET Plasmid Miniprep Kit (Fermentas GMBH) following manufacturer's instructions.

Once purified cDNA was obtained, it was transfected to the cells by using X-tremeGene 9 reagent (Roche). X-tremeGene 9 reagent was diluted in OptiMEM medium (Gibco) and incubated for 5 minutes at RT. Then, cDNA was added, mixed without vortexing (reagent/cDNA ratio was 3:1 (v:v)) and incubated during 15-20 minutes at RT. Finally, the appropriate volume (described in manufacturer's instructions) was dispensed into each well and the cells were incubated for 48 hours at 37ºC.

RNA interference-mediated gene silencing

Small interfering RNA (siRNA) is a class of double-stranded RNA molecules of 20-25 base pairs in length highly effective in post-transcriptional regulation. The cellular incorporation of exogenous siRNA by transfection allows the total or partial inhibition of the targeted gene.

siRNA sequences were designed according to MitoCheck database (http://www.mitocheck.org). All siRNAs were purchased to Life Technologies (**see Table 12**) except for SignalSilence®XIAP siRNA II which was from Cell Signaling.

First, oligonucleotides were annealed by mixing 2 mmols of each oligonucleotide with 10 µl of Buffer 2 (10X) (New England Biolabs) and 50 µl of RNase-free water. The mixture was incubated at 95ºC during 5 minutes and let it cool down to RT. Lipofectamine® RNAiMAX transfection reagent (Life Technologies) and siRNA were diluted independently in OptiMEM

medium. Both tubes were combined and incubated for 20 minutes at RT. Finally, the cells were exposed to a final concentration of 50 nM of either specific or negative control (siLUCIFERASE) siRNA during 48 hours. Since *EPSTI1* is an interferon (IFN) response gene (Buess et al., 2007), EPSTI1 endogenous expression was induced by IFN-α (Chemicon, Millipore) treatment prior to gene silencing. IFN-α was added to a final concentration of 1000 U/mL 8 hours before harvesting the cells as previously described (de Neergaard et al., 2010).

Ultimately, in order to demonstrate a reduction/inhibition of the targeted gene, specific silencing was confirmed with the corresponding antibody and ß-actin as a loading control probe by means of western blot analysis.

siRNA	**Sequence (5' - 3')**
$EPSTI1_s$	GAGCAAUCUGGAGGCUGUUGGAAUA
$EPSTI1_{as}$	UAUUCCAACAGCCUCCAGAUUGCUC
$LUCIFERASE_s$	CGUACGCGGAAUACUUCGA
$LUCIFERASE_{as}$	UCGAAGUAUUCCGCGUACG
$PSMC3IP_s$	GCAGCUACCAAUCAUGUGA
$PSMC3IP_{as}$	UCACAUGAUUGGUAGCUGC

Table 12. siRNA specific sequences. s: sense; as: antisense

Apoptosis induction by TNF-related apoptosis-inducing ligand (TRAIL) treatment

Upon cDNA or siRNA transfection, the extrinsic apoptotic pathway was induced using TRAIL, a death receptor agonist, in order to enhance the apoptotic response. Recombinant Human TRAIL/Apo2 Ligand (PeproTech) aliquots were prepared as described by manufacturer's

instructions and breast cancer cells were treated during 24 hours at different concentrations depending on the cell line as previously described in the literature (Rahman et al., 2009, Xu et al., 2010):

- MCF-7: 100 ng/mL TRAIL
- MDA-MB-231: 80 ng/mL TRAIL

Chemical compounds

Cultured cells were exposed to different treatments with antineoplastic and non-cancer drugs to evaluate their diverse responses. All the compounds were purchased to Selleckchem except Dalteparin and Framycetin which are from Sigma-Aldrich. Stock solutions were prepared as indicated by the provider using either DMSO or water as solvent. Additionally, a final DMSO percentage without showing toxic effects on the cells was previously established. **Table 13** shows the specific details for each compound tested as well as the experimental conditions and the references used to determine drug concentrations.

Name	Concentration range	References
Raloxifene	0.2 / 1 / 5 / 25 / 50 µM	(Fryar et al., 2006, Liu et al., 2003)
Dinaciclib (SCH727965)	0.01 / 0.1 / 1 / 10 / 100 nM	(Bates et al., 2011, Nagaria et al., 2013)
Erlotinib	0.04 / 0.2 / 1 / 5 / 25 µM	(Aguilar et al., 2014, Nagaria et al., 2013)
Everolimus (RAD001)	0.01 / 0.1 / 1 / 10 / 50 µM	(Chen et al., 2013, Treeck et al., 2006)
Dabrafenib (GSK2118436)	0.4 / 2 / 10 / 50 / 250 µM	(Hirschi et al., 2014)

Ruxolitinib (INCB018424)	0.2 / 1 / 5 /25 / 125 µM	(Yang et al., 2014)
Cediranib (AZD2171)	0.01 / 0.1 / 1 / 10 / 100 µM	(Tao et al., 2009)
Sorafenib Tosylate	0.01 / 0.1 / 1 / 10 / 100 µM	(Nagaria et al., 2013)
Tanespimycin (17-AAG)	0.5 / 5 / 50 / 500 / 5000 nM	(Stecklein et al., 2012)
Bosutinib (SKI-606)	0.01 / 0.1 / 1 / 10 / 100 µM	(Tarpley et al., 2014)
BEZ235 (Dactolisib)	10^{-4} / 10^{-3} / 0.01 / 0.1 / 1 µM	(Chen et al., 2013)
Lapatinib (GW-572016)	0.2 / 1 / 5 /25 / 125 µM	(Nagaria et al., 2013)
Trametinib (GSK1120212)	0.01 / 0.1 / 1 / 10 / 100 µM	(Leung et al., 2014)
Eplerone	0.01 / 0.1 / 1 / 10 / 100 µM	(Dovio et al., 2009, Fujii et al., 2012)
Dalteparin sodium	0.1 / 1 / 10 / 100 /1000 µg/mL	(Feuring et al., 2011)
Framycetin sulphate	0.01 / 0.1 / 1 / 10 / 100 µM	(Perigolo de Oliveira et al., 2013)

Table 13. Detailed description of tested compounds.

Drug combination experiments

After culturing cells overnight in a 96 well plate, the corresponding drug was added at five different concentrations surrounding, or at least reaching the corresponding IC_{50}. In combined treatment, both drugs were added

simultaneously and the cells were exposed continuously to the drugs during 72 hours. At that time, cell viability was measured as described in **section 5.1.7**.

5.1.5 Protein protocols

5.1.5.1 Cell lysis

Procedure for functional apoptosis assays

After cell transfection or treatment, floating and adherent cells were combined. The cell medium was collected and centrifuged at 400x g for 5 minutes at 4ºC and the supernatant was discarded. At that point, the attached cells were scraped with PBS 1X and collected with the previously obtained pellet. The cell suspension was centrifuged at 800x g for 5 minutes at 4ºC, the supernatant was removed and the pellet was resuspended in 100 µl of ice-cold commercial cell lysis buffer ((capsase-3 (MBL), caspase-8 (Biovision)). The cell suspension was incubated on ice during 10 minutes, cell lysates were centrifuged at 10,000x g for 5min at 4ºC, the supernatant (cell extract) was transferred to a new microcentrifuge tube and placed on ice until protein quantification.

Procedure for non-apoptotic assays

First, cells were collected as described above. The cell suspension was centrifuged at 1,200x g for 10 minutes at 4ºC and the supernatant was removed. The pellet was resuspended in 100 µl of ice-cold cell lysis buffer (its composition is described below) and the cell suspension was incubated on ice for 30 minutes. Cell lysates were sonicated at 4ºC during 15 minutes and centrifuged at 16,000x g for 20min at 4ºC. The supernatant was transferred to a new microcentrifuge tube and placed on ice in order to proceed to protein concentration determination.

Lysis buffer for Western blot assays
Tris-HCl 500 mM
Triton X-100 5% (v:v)
NaCl (1.5M)
Ethylenediaminetetraacetate-Disodium (EDTA) (Sigma Aldrich) (10mM)
$MgCl_2$ (100mM)
Glycerol (Merck) 85% (v:v)
1 tablet of Protease inhibitor cocktail, EDTA-free (Roche)

Table 14. Composition of lysis buffer used in non-apoptotic assays.

5.1.5.2 Protein quantification

The colorimetric *DC* Protein Assay (Bio-Rad), was used for protein quantification following the manufacturer's indications. Firstly, working reagent (containing 20 µl reagent S /1 mL reagent A) and protein standard dilutions (from 0.25 mg/mL to 4 mg/mL of BSA) were prepared. Afterward, 5 µl of standards or samples were pipetted into a 96-well plate. Next, 25 µl of working reagent and 200 µl of reagent B were added into each well and incubated 15 minutes at RT before determining the absorbance at 750 nm.

5.1.5.3 Protein detection and analysis by western blot

Protein detection and analysis was done by western blot assay, which is an analytical technique used to detect specific proteins in a given sample. First, denatured proteins are separated by length by means of sodium dodecyl sulphate polyacrylamide gel electrophoresis (SDS-PAGE) and

subsequently, the proteins are transferred to a membrane in order to detect target proteins with specific antibodies.

One dimension electrophoresis gel (SDS-PAGE)

It was performed according to the method of Laemmli (1970) using a Miniprotean BioRad TM II system with 1.5mm spacers. Depending on the protein size, 12% or 10% (v:v) acrylamide gels were made. Protein extracts were resuspended in 5X SDS loading buffer (final concentration 1X) and boiled at 100ºC during 5 minutes in the presence of D1-Dithiothreitol (DTT) (Sigma Aldrich) before loading the electrophoresis gel. Electrophoresis was done at 120 V for 100 minutes in electrophoresis buffer. The composition of the gel, the loading and electrophoresis buffers is detailed in the following tables:

Resolving gel			**Stacking gel**	
	10%	**12%**		
bis-Acrilamide 30% Solution 29:1 (Sigma Aldrich)	6 mL	6.8 mL	bis-Acrilamide 30% Solution 29:1	0.6 mL
Buffer A[a]	4.8 mL	4.5 mL	Buffer B[b]	1.25 mL
H_2O	7.0 mL	5.6 mL	H_2O	3.0 mL
APS 10% (w:v)	150 µl	150 µl	APS 10%	50 µl
TEMED (Sigma Aldrich)	10 µl	10 µl	TEMED	5 µl

Table 15. One dimension electrophoresis gel composition. [a]Buffer A: Tris-HCl 1.5 M (*p*H 8.8) and SDS 0.4% (w:v) , [b]Buffer B: Tris-HCl 500 mM (*p*H 6.8) and SDS 0.4% (w:v)

5X SDS loading buffer	Electrophoresis buffer (*p*H 8.3)
Tris-HCl (Sigma Aldrich) 0.5M (*p*H 6.8)	Tris-HCl 25 mM
Glycerol (Merck) 10% (v:v)	Glycine (Sigma Aldrich) 0.2 M
SDS (Sigma Aldrich) 2% (w:v)	SDS 0.1% (w:v)
Bromophenol blue (Sigma Aldrich) 0.05% (w:v)	-
DTT 5% (v:v)	-

Table 16. Loading and electrophoresis buffers composition.

Western blot analysis and immunodetection

Western-blot analysis of the proteins separated by SDS-PAGE gel is performed by incubating specific antibodies with the proteins previously transferred to PVDF membranes (Immobilon-P, Millipore). The transfer process was done in transfer buffer (see composition in **Table 17**), during 90 minutes at 300 mA at 4ºC.

Transfer buffer	TBS-Tween 1X (TBST) (*p*H 7.6)
Tris-HCl 25 mM	Tris-HCl 20 mM
Glycine (Sigma Aldrich) 0.2 M	NaCl 0.14 M
Methanol 0.2% (v:v)	Tween-20 (Biorad) 0.1% (v:v)

Table 17. Transfer buffer and TBS-Tween composition.

Once the transfer process is over, the PVDF membranes were stained with Ponceau S (Sigma Aldrich) 0.1% (w:v) in 0,1% (v:v) acetic acid (Sigma Aldrich) in order to visualize the loading of the proteins and locate molecular

weight markers. The Ponceau S was then eliminated by washing in Tris-Buffered Saline (TBS)-Tween 1X (see composition in **Table 17**) for 10 minutes at RT. PVDF membranes were blocked in TBS-Tween with 5% (w:v) milk powder, 1 hour at RT. At that time, the membranes were washed 3 times during 5 minutes each with TBS-Tween at RT and incubated with primary antibody (see **Table 18** for description) in TBS-Tween with 5% (w:v) milk powder overnight at 4ºC. The next day, the membranes were washed as previously described and incubated with secondary antibody (anti-rabbit or anti-mouse conjugated to peroxidase dilution 1:5,000) in TBS-Tween with 5% (w:v) milk powder for 1 hour at RT. Finally, the membranes were washed in TBS-Tween as previously described and protein detection was performed by chemiluminescence using Enhanced Chemiluminescence (ECL) (GE Healthcare) system following the instructions of the supplier, and exposing the membranes to a hypersensitive film (Fuji Medical X-Ray Film Super RX) for variable times.

Primary Antibodies			
Antigen	**Brand and reference**	**Source**	**Dilution**
c-Myc	Life Technologies, 13-2500	Mouse	1:5,000
EPSTI1	Sigma Aldrich, SAB2100696	Rabbit	1:2,000
PARP	Cell Signaling , 9542	Rabbit	1:1,000
PSMC3IP	Sigma Aldrich, HPA044439	Rabbit	1:1,000
XIAP(3B6)	Cell Signaling, 2045	Rabbit	1:1,000
ß-actin (HRP conjugate)	Abcam, ab20272	Mouse	1:20,000

Table 18. List of primary antibodies used for protein detection.

Secondary Antibodies			
Antigen	**Brand and reference**	**Source**	**Dilution**
Mouse IgG-HRP conjugate	Life Technologies, G-21040	Goat	1:5,000
Rabbit IgG-HRP conjugate	Life Technologies, G-21234	Goat	1:5,000

Table 19. List of secondary antibodies used for protein detection.

5.1.6 Apoptosis assays

Cell death induced by drug treatment or gene expression modulation was evaluated through a variety of functional apoptotic assays.

5.1.6.1 Caspase activity assays

Caspases are members of the cysteine aspartic acid-specific protease family, which may be activated by a variety of signals including death receptor ligation, DNA damage, serum starvation, stress, and many more. The cleavage of several structural proteins by caspases leads to chromatin condensation, nucleus fragmentation and loss of cytoplasmic integrity contributing to the unique apoptotic cell morphology. Detection of caspase activity is a standard method to measure apoptosis activity, and is commonly done via fluorometric or colorimetric detection of caspase-specific substrates cleavage (www.mblintl.com).

Caspase-3 and Caspase-8 activity assay

Active caspase-3 or caspase-8 recognize four amino acid residues (DEVD or IETD sequence respectively) in a substrate molecule and specifically cleaves immediately after the second aspartate residue. This propriety is useful for

detecting caspase activity by using synthetic substrates. In this method, DEVD or IETD sequences are labelled with *p*NA (*p*-nitroanilide) at the C-terminal side. Free *p*NA is released from the labelled synthetic substrate upon cleavage by active caspase, and monitored by a 96 well microplate reader at 405 nm wavelength. Since the amount of free *p*NA is proportional to the amount of caspase activity present in the sample, caspase activity can be calculated by monitoring the optical density of free *p*NA.

Caspase-3 activity was detected by using APOPCYTO Caspase-3 Colorimetric Assay Kit (MBL Medical & Biological Laboratories Co.), while the FLICE/Caspase-8 Colorimetric Assay kit (BioVision) was used for assaying the activity of caspase-8. The assays were performed as described in the manufacturer's indications:

Floating and adherent cells were combined and cell lysates were prepared as described in **section 5.1.5.1**. Protein content was quantified as previously described and adjusted to 100-200μg protein/50μl cell lysis buffer. 100 mM *p*NA stock was diluted to 5 mM *p*NA in cell lysis buffer in order to prepare the standard curve as described in the manufacturer's instructions. Then, 100μl of *p*NA standards were transferred in duplicates into a 96-well microplate. The following components were added subsequently into the empty wells:

- 50 μl 2X Reaction Buffer containing 10 mM DTT
- 50 μl cell lysate
- 5 μl caspase-3/8 substrate

Lastly, the plate was covered with plate sealer in order to protect the substrates from the light and was incubated at 37ºC overnight. The next day, absorbance was measured at 405 nm and the Specific Activity (SA) of caspase present in each sample was calculated as described in the manufacturer's instructions.

5.1.6.2 Propidium iodide staining and flow cytometry analysis

The propidium iodide (PI) flow cytometry assay has been widely used to distinguish cells in different phases of the cell cycle by means of DNA content analysis. Since PI is capable of binding DNA, the fluorescence intensity of the stained cells will therefore correlate with the amount of DNA they contain. As the DNA content of cells duplicates during the S phase of the cell cycle, the relative amount of cells in G_0/G_1 phase, S phase and in G_2-M phase can be determined. Additionally, apoptotic cells which contain less DNA due to its fragmentation by endonucleases are represented in the so-called "sub-G_0/G_1" peak in the fluorescence histogram.

Fixation step

First, the supernatants were collected and each well was washed with 1 mL cold PBS 1X. 400 µl of trypsin was then added into each well and the plate was incubated at 37ºC for 2-3 minutes. The cells were collected and pooled with the corresponding supernatants and cell suspensions were centrifuged for 3 minutes at 1,200x g, 4ºC. The supernatants were discarded and the pellets were washed with 3ml of cold PBS 1X. Finally, the pellets were resuspended in 100 µl of cold PBS 1X by vortexing and mixed with 900 µl of cold ethanol 70% (Panreac). The cell suspensions were incubated for at least 30min at 4ºC before proceeding with the next step.

Labelling step

The cell suspensions were centrifuged during 3-5 minutes at 1,200x g, 4ºC. Then, the pellets were washed with 3 mL of cold PBS 1X and resuspended in 250 µl of cold PBS 1X by vortexing. 250 µl of extracting solution (see **Table 20**) was added and the cells were incubated for 10 minutes at 37ºC. The cell suspensions were centrifuged 3 minutes at 1,200x g, 4ºC and 300µl of PI/RNase solution (see **Table 20**) was added to each pellet. The samples were incubated for 30 minutes at 37ºC and protected from the light before being analysed by the flow cytometer.

Finally, the number of cells presents in each phase of the cell cycle and the apoptotic cell population were determined using the software FlowJo (http://www.flowjo.com/).

Solutions	
Extracting solution (pH 7.8)	Na_2HPO_4 (0.2M)
	Citric acid (4 mM) (Sigma Aldrich)
	RNase A (100 µg/mL) (Fermentas GmbH)
PI/RNase solution	PI (40 µg/mL) (Sigma Aldrich)
	Filtered PBS 1X (Sigma Aldrich)

Table 20. Description of solutions used in propidium iodide staining.

5.1.6.3 Terminal deoxynucleotidyl transferase dUTP nick end labelling (TUNEL)

TUNEL assay is another technique used for detecting DNA fragmentation that results from apoptotic signalling cascades, which works by labelling the terminal end of nucleic acids. The assay relies on the presence of nicks in the DNA which can be identified by terminal deoxynucleotidyl transferase (or TdT). This enzyme catalyses the addition of dUTPs at free 3'-OH termini, which are secondarily labelled with a green marker (i.e. fluorescein). This kind of assay allows the identification of apoptosis at a molecular level (DNA-strand breaks) and identification of cells at the very early stages of apoptosis.

By using *In Situ* Cell Death Detection Kit, Fluorescein (Roche), DNA fragmentation was quantified by means of fluorescent microscopy, where fragmented DNA was identified by the detection of fluorescein (green fluorescence), which labels the incorporated nucleotides. Furthermore,

Hoechst 33342 (Life Technologies), which binds to DNA, was used as a nuclear dye (blue fluorescence). Combining Hoechst 33342 and TUNEL staining allows the comparison of TUNEL-positive nuclei with surrounding normal nuclei and the observation of changes in nuclear size and morphology. The assay is composed of three different steps:

- Cell fixation
- Cell permeabilization
- Labelling

First of all, sterile coverslips were placed in 24-well plates and the cells were seeded. After treatment, growth medium was removed, the coverslips were washed 3 times with PBS 1X, 900 µl of 4% paraformaldehyde (PFA) was added to completely cover the coverslips and the cells were fixed during 1 hour at RT. The slides were rinsed with PBS 1X and incubated with 900 µl of permeabilization solution (see **Table 21**) during 2 minutes on ice. Additionally, as described in the manufacturer's protocol, the positive control cells were incubated with DNase I recombinant solution (see **Table 21**) for 10 minutes at RT to induce DNA strand breaks, prior to labelling procedure. In the last step, 50 µl of Enzyme Solution was added to 450 µl of Label Solution to obtain 500 µl of TUNEL reaction mixture. The slides were rinsed twice with PBS 1X and 50 µl of TUNEL reaction mixture were added to each sample. To ensure a homogeneous spread of TUNEL reaction and to avoid evaporative loss, the samples were covered with parafilm or coverslip during incubation. For negative controls, 50 µl of Label Solution were added to each sample instead of TUNEL reaction mixture. The chamber was covered with aluminium foil to protect from direct light and incubated for 1 hour at 37ºC in a humidified atmosphere in the dark.

Solutions	
Washing buffer	Phosphate buffered saline (PBS1X)
Fixation solution	4% Paraformaldehyde (PFA) (Sigma Aldrich) in PBS, *p*H 7.4 freshly prepared
Permeabilization solution	0.1% Triton-X-100 (Sigma Aldrich) in 0.1% sodium citrate, freshly prepared
DNase I recombinant (Roche) solution	DNase I (2U/mL in 10 mM Tris-HCl, *p*H 7.5 containing 1mM $MgCl_2$ and 1mg/mL BSA)

Table 21. Description of solutions used in TUNEL assay.

In order to stain the cell nuclei, 100 µl Hoechst (1:15,000 in PBS) were added to each sample and incubated for 5 minutes at RT protected from light. Subsequently, the cells were washed with PBS 1X and assembled as follows:

- 5 µl of antifade were added in the object holder
- The coverslips were washed with water and the object cover was placed in the object holder, upsetting it down
- The samples were incubated at RT overnight, protected from light

Lastly, the cells were visualized in an upright epifluorescence microscope and images were analysed by ImageJ software.

5.1.7 Cell viability assays

5.1.7.1 MTT assay

MTT (methyl 3-[4,5-dimethylthiazol-2-il]-2,5-diphenyltetrazolium bromide) (Sigma-Aldrich) assay was used to measure drug sensitivity. MTT is a colorimetric assay which reflects the mitochondrial activity of living cells

based on their ability to reduce a soluble tetrazolium salt to formazan, a purple compound insoluble in aqueous medium (van Meerloo et al., 2011). The concentration of solubilised formazan can be determined by measuring the optical density at 570 nm using a plate reader. Since the mitochondrial activity is typically constant in viable cell, an increase or decrease in the activity correlates linearly with the number of viable cells. Results were expressed as percentage of cell survival, calculated as the absorbance 100 x (treated/untreated).

Prior to the experiments, the optimal cell density was assessed to ensure exponential growth of the cells at 72 hours in 96-well plates. The cells were seeded in 96-well plates and cultured overnight, after which the corresponding treatment was applied and incubated at 37ºC in a humidified atmosphere with 5% CO_2 during 72 hours. Once finished the treatment, 20 µl of MTT (5 mg/mL in PBS) were added into each well, and the plates were incubated at 37ºC during 30 minutes for SKBR-3 cells and 2 hours for the other cell lines. Finally, the growth medium containing the MTT solution was aspirated, 100 µl of DMSO were transferred into each well and the absorbance was measured at 570 nm wavelength.

5.1.7.2 Clonogenic assay

This is a cell survival assay based on the ability of single cells to grow into colonies. It is used to determine cell death after treatment with cytotoxic agents.

MDA-MB-231 breast cancer cells were incubated 24 hours with single drug and the corresponding drug combinations. Then, 50 cells were plated per well in 6-well plates and allowed to grow until visible colonies were formed (about two weeks) when the cells were washed with PBS and fixed for 20 minutes with 4% PFA. After that, cells were rinsed with H_2O and stained for 15 min with 0.05% crystal violet. Finally, colonies were washed with H_2O,

drained and photographed for colony counting (colonies can be counted several months after staining).

5.2 COMPUTATIONAL METHODS

The computational methods of the present thesis were performed by Dr Samira Jaeger from our group.

5.2.1 Correlation in gene expression profiles

In order to analyse the correlation between driver and passenger BC genes expression profiles, the microarray data from (Su et al., 2004), a compendium of gene expression profiles from 73 normal tissue and cell types, and the protein data from the Human Protein Atlas (Uhlen et al., 2010) was compiled. Next, a mixture model was applied in order to obtain robust correlation coefficients under the presence of noise. Finally, the model was fitted using the Expectation-Maximization (EM) algorithm (Dempster, 1977) and two genes were defined as co-expressed if their EM correlation coefficient was greater than 0.5 and the probability of noise less than 0.5.

5.2.2 Therapeutic signalling networks and pathway crosstalk inhibition

To chart the therapeutic networks associated with each drug, all KEGG pathways (excluding disease pathways) that include any of the primary targets of the drug were compiled. On average each drug affects 6.5 KEGG pathways (median = 3, sd ± 8.3). Pathways have been retrieved from KEGG using the REST-style KEGG API. Subsequently, given the XML representation of a pathway, a directed network including proteins and their interactions was created. The type of an interaction, such as activation or inhibition, was used to determine the directionality of an edge in the network.

Based on the therapeutic signalling networks, a crosstalk inhibition measure was developed in order to estimate the amount of crosstalk signalling that

could be prevented between pathways by inhibiting specific proteins simultaneously. The concept of pathway crosstalk refers to protein interactions shared between distinct pathways. Since these interactions might also influence the downstream signalling within a pathway, the concept also comprises proteins and interactions downstream of the respective crosstalking interactions (i.e. indirect crosstalk).

Given two therapeutic signalling networks, the potential crosstalk between them was determined by identifying interactions directly and indirectly involved in the crosstalk, and representing them as a directed crosstalk network. Then, using this crosstalk representation, a topology-based measure namely network efficiency (Csermely et al., 2005) was applied, to determine the information flow within the network. Network efficiency (NE) is defined as the sum of the inverse length of the shortest path between all network elements and can be computed as follows:

$$\mathrm{NE} = \frac{\sum_{i \neq j} \frac{1}{d(i,j)}}{N(N-1)}$$

N representing the number of network elements and *d* denoting the shortest distance between two elements i, j Є N. The network efficiency ranges between 0 and 1, where 1 indicates that all proteins communicate directly with each other.

Using the network efficiency determined for crosstalking pathways, as described above, the inhibition of specific protein target(s) was simulated to then measure the amount of signalling that persists (NE_X) when removing protein interactions affected by a pharmacological intervention. The relative reduction of network efficiency, i.e., the pathway crosstalk inhibition (PCI), was determined as follows:

$$PCI = 1 - \frac{NE_X}{NE}$$

The final PCI for a given pair of drugs is the average of the crosstalk inhibitions between each pair of crosstalking pathways forming the respective therapeutic networks.

5.2.3 Drug combination index

Given the MTT cell viability measurements, we assessed whether a drug combination induces additive, synergistic or antagonistic effects in cultured cells. To this end, the drug combination index (DCI) was determined using the Loewe additivity as a reference model, assuming that a drug cannot interact with itself (Chou, 2006, Chou and Talalay, 1984). This means that if two drugs are the same or very similar, we expect their combined effect at equal concentrations to be comparable to the one observed when administering one drug alone at double concentration.

The DCI of a combination was computed based on the half-maximal effective concentration that is needed to inhibit cell viability by X% with X commonly corresponding to an inhibition level of 50%, that is, the IC_{50}. Formally, the DCI_X is defined as follows:

$$DCI_X = \frac{C_{D1,X}}{IC_{X,D_1}} + \frac{C_{D2,X}}{IC_{X,D_2}}$$

$C_{D1,X}$ and $C_{D2,X}$ represent the concentration of drug D_1 and drug D_2 used in combination to induce an effect X while $IC_{X,D1}$ and $IC_{X,D2}$ indicate the corresponding concentrations of the single agents required to produce the same effect. Using the refined measure proposed by Chou (Chou, 2006), combinations with a DCI below 0.85 were defined as synergistic, combinations with a DCI above 1.2 as antagonistic and the remaining ones as additive.

IC_X values can be determined from dose-response curves for any inhibition level X using the *drc* R package to generate sigmoid-fitted dose-response curves from which the IC_X for single drugs and combinations were then estimated (Ritz, 2005). In some cases the single agents do not reach the pre-defined inhibition level while in others the estimated IC_X corresponds to a value beyond the tested concentration range. In the latter one, we exploited the relative standard error (RSE) associated with each fit to decide whether to consider an IC_X. If this error is below 0.15, we assumed that the estimated value is reliable. Otherwise, we presumed that the required inhibition level has not been reached and that the contribution of the respective agent to the combination is marginal, i.e., $C_{D1,X} = 0$ or $C_{D2,X} = 0$ (Miller et al., 2013).

6. BIBLIOGRAPHY

1. Aguilar, H., Urruticoechea, A., Halonen, P., Kiyotani, K., Mushiroda, T., Barril, X., . . . Pujana, M.A. (2014) VAV3 mediates resistance to breast cancer endocrine therapy. *Breast Cancer Res* 16, R53.

2. Al-Bazz, Y.O., Brown, B.L., Underwood, J.C., Stewart, R.L., and Dobson, P.R. (2009) Immuno-analysis of phospho-Akt in primary human breast cancers. *Int J Oncol* 35, 1159-1167.

3. Albert, J.M., Kim, K.W., Cao, C., and Lu, B. (2006) Targeting the Akt/mammalian target of rapamycin pathway for radiosensitization of breast cancer. *Mol Cancer Ther* 5, 1183-1189.

4. Altomare, D.A. and Testa, J.R. (2005) Perturbations of the AKT signaling pathway in human cancer. *Oncogene* 24, 7455-7464.

5. Allred, D.C., Mohsin, S.K., and Fuqua, S.A. (2001) Histological and biological evolution of human premalignant breast disease. *Endocr Relat Cancer* 8, 47-61.

6. Arroyo, R., Sune, G., Zanzoni, A., Duran-Frigola, M., Alcalde, V., Stracker, T.H., . . . Aloy, P. (2015) Systematic identification of molecular links between core and candidate genes in breast cancer. *J Mol Biol* 427, 1436-1450.

7. Ashkenazi, A. (2002) Targeting death and decoy receptors of the tumour-necrosis factor superfamily. *Nat Rev Cancer* 2, 420-430.

8. Ashkenazi, A., Holland, P., and Eckhardt, S.G. (2008) Ligand-based targeting of apoptosis in cancer: the potential of recombinant human apoptosis ligand 2/Tumor necrosis factor-related apoptosis-inducing ligand (rhApo2L/TRAIL). *J Clin Oncol* 26, 3621-3630.

9. Bai, L. (2006) p53: structure, function and therapeutic applications. *J Cancer Mol.* 2, 141-153.

10. Baker, A.T., Zlobin, A., and Osipo, C. (2014) Notch-EGFR/HER2 Bidirectional Crosstalk in Breast Cancer. *Front Oncol* 4, 360.

11. Banerjee, K. and Resat, H. (2015) Constitutive activation of STAT3 in breast cancer cells: A review. *Int J Cancer.*

12. Barabasi, A.L., Gulbahce, N., and Loscalzo, J. (2011) Network medicine: a network-based approach to human disease. *Nat Rev Genet* 12, 56-68.

13. Barabasi, A.L. and Oltvai, Z.N. (2004) Network biology: understanding the cell's functional organization. *Nat Rev Genet* 5, 101-113.

14. Baselga, J., Campone, M., Piccart, M., Burris, H.A., 3rd, Rugo, H.S., Sahmoud, T., . . . Hortobagyi, G.N. (2012) Everolimus in postmenopausal hormone-receptor-positive advanced breast cancer. *N Engl J Med* 366, 520-529.

15. Bates, D.J., Salerni, B.L., Lowrey, C.H., and Eastman, A. (2011) Vinblastine sensitizes leukemia cells to cyclin-dependent kinase inhibitors, inducing acute cell cycle phase-independent apoptosis. *Cancer Biol Ther* 12, 314-325.

16. Bauer, J.H. and Helfand, S.L. (2006) New tricks of an old molecule: lifespan regulation by p53. *Aging Cell* 5, 437-440.

17. Beatson, G. (1896) On the treatment of inoperable cases of carcinoma of the mamma: suggestions for a new method of treatment, with illustrative cases. *Lancet* 2.

18. Bender, L.M. and Nahta, R. (2008) Her2 cross talk and therapeutic resistance in breast cancer. *Front Biosci* 13, 3906-3912.

19. Berger, S.I. and Iyengar, R. (2009) Network analyses in systems pharmacology. *Bioinformatics* 25, 2466-2472.

20. Blackwell, K.L., Pegram, M.D., Tan-Chiu, E., Schwartzberg, L.S., Arbushites, M.C., Maltzman, J.D., . . . Burstein, H.J. (2009) Single-agent lapatinib for HER2-overexpressing advanced or metastatic breast cancer that progressed on first- or second-line trastuzumab-containing regimens. *Ann Oncol* 20, 1026-1031.

21. Bonanni, B., Puntoni, M., Cazzaniga, M., Pruneri, G., Serrano, D., Guerrieri-Gonzaga, A., . . . Decensi, A. (2012) Dual effect of metformin on breast cancer proliferation in a randomized presurgical trial. *J Clin Oncol* 30, 2593-2600.

22. Borisy, A.A., Elliott, P.J., Hurst, N.W., Lee, M.S., Lehar, J., Price, E.R., . . . Keith, C.T. (2003) Systematic discovery of multicomponent therapeutics. *Proc Natl Acad Sci U S A* 100, 7977-7982.

23. Breitkreutz, D., Hlatky, L., Rietman, E., and Tuszynski, J.A. (2012) Molecular signaling network complexity is correlated with cancer patient survivability. *Proc Natl Acad Sci U S A* 109, 9209-9212.

24. Buess, M., Nuyten, D.S., Hastie, T., Nielsen, T., Pesich, R., and Brown, P.O. (2007) Characterization of heterotypic interaction effects in vitro to deconvolute global gene expression profiles in cancer. *Genome Biol* 8, R191.

25. Burstein, H.J., Griggs, J.J., Prestrud, A.A., and Temin, S. (2010) American society of clinical oncology clinical practice guideline update on adjuvant endocrine therapy for women with hormone receptor-positive breast cancer. *J Oncol Pract* 6, 243-246.

26. Burstein, H.J., Polyak, K., Wong, J.S., Lester, S.C., and Kaelin, C.M. (2004) Ductal carcinoma in situ of the breast. *N Engl J Med* 350, 1430-1441.

27. Cailleau, R., Young, R., Olive, M., and Reeves, W.J., Jr. (1974) Breast tumor cell lines from pleural effusions. *J Natl Cancer Inst* 53, 661-674.

28. Cancer Genome Atlas, N. (2012) Comprehensive molecular portraits of human breast tumours. *Nature* 490, 61-70.

29. Cande, C., Cecconi, F., Dessen, P., and Kroemer, G. (2002) Apoptosis-inducing factor (AIF): key to the conserved caspase-independent pathways of cell death? *J Cell Sci* 115, 4727-4734.

30. Cardone, M.H., Roy, N., Stennicke, H.R., Salvesen, G.S., Franke, T.F., Stanbridge, E., . . . Reed, J.C. (1998) Regulation of cell death protease caspase-9 by phosphorylation. *Science* 282, 1318-1321.

31. Carninci, P., Kasukawa, T., Katayama, S., Gough, J., Frith, M.C., Maeda, N., . . . Genome Science, G. (2005) The transcriptional landscape of the mammalian genome. *Science* 309, 1559-1563.

32. Cichon, M.A., Degnim, A.C., Visscher, D.W., and Radisky, D.C. (2010) Microenvironmental influences that drive progression from benign breast disease to invasive breast cancer. *J Mammary Gland Biol Neoplasia* 15, 389-397.

33. Collins, J.A., Schandi, C.A., Young, K.K., Vesely, J., and Willingham, M.C. (1997) Major DNA fragmentation is a late event in apoptosis. *J Histochem Cytochem* 45, 923-934.

34. Csermely, P., Agoston, V., and Pongor, S. (2005) The efficiency of multi-target drugs: the network approach might help drug design. *Trends Pharmacol Sci* 26, 178-182.

35. Cusick, M.E., Klitgord, N., Vidal, M., and Hill, D.E. (2005) Interactome: gateway into systems biology. *Hum Mol Genet* 14 Spec No. 2, R171-181.

36. Chan, T.O. and Tsichlis, P.N. (2001) PDK2: a complex tail in one Akt. *Sci STKE* 2001, pe1.

37. Chen, X., Zhao, M., Hao, M., Sun, X., Wang, J., Mao, Y., . . . Shen, K. (2013) Dual inhibition of PI3K and mTOR mitigates compensatory AKT activation and improves tamoxifen response in breast cancer. *Mol Cancer Res* 11, 1269-1278.

38. Chou, T.C. (2006) Theoretical basis, experimental design, and computerized simulation of synergism and antagonism in drug combination studies. *Pharmacol Rev* 58, 621-681.

39. Chou, T.C. and Talalay, P. (1984) Quantitative analysis of dose-effect relationships: the combined effects of multiple drugs or enzyme inhibitors. *Adv Enzyme Regul* 22, 27-55.

40. Chung, A.S., Lee, J., and Ferrara, N. (2010) Targeting the tumour vasculature: insights from physiological angiogenesis. *Nat Rev Cancer* 10, 505-514.

41. Darnell, J.E., Jr. (1997) STATs and gene regulation. *Science* 277, 1630-1635.

42. Datta, S.R., Dudek, H., Tao, X., Masters, S., Fu, H., Gotoh, Y., and Greenberg, M.E. (1997) Akt phosphorylation of BAD couples survival signals to the cell-intrinsic death machinery. *Cell* 91, 231-241.

43. De Las Rivas, J. and Fontanillo, C. (2010) Protein-protein interactions essentials: key concepts to building and analyzing interactome networks. *PLoS Comput Biol* 6, e1000807.

44. de Neergaard, M., Kim, J., Villadsen, R., Fridriksdottir, A.J., Rank, F., Timmermans-Wielenga, V., . . . Ronnov-Jessen, L. (2010) Epithelial-stromal interaction 1 (EPSTI1) substitutes for peritumoral fibroblasts in the tumor microenvironment. *Am J Pathol* 176, 1229-1240.

45. Dearth, R.K., Cui, X., Kim, H.J., Kuiatse, I., Lawrence, N.A., Zhang, X., . . . Lee, A.V. (2006) Mammary tumorigenesis and metastasis caused by overexpression of insulin receptor substrate 1 (IRS-1) or IRS-2. *Mol Cell Biol* 26, 9302-9314.

46. Decaudin, D., Marzo, I., Brenner, C., and Kroemer, G. (1998) Mitochondria in chemotherapy-induced apoptosis: a prospective novel target of cancer therapy (review). *Int J Oncol* 12, 141-152.

47. Dempster, A., Laird, N., and Rubin, D. (1977) Likelihood from Incomplete Data via the EM Algorithm. *Journal of the Royal Statistical Society. Series B (Methodological)* 39, 1-38.

48. Derijard, B., Raingeaud, J., Barrett, T., Wu, I.H., Han, J., Ulevitch, R.J., and Davis, R.J. (1995) Independent human MAP-kinase signal transduction pathways defined by MEK and MKK isoforms. *Science* 267, 682-685.

49. Devarajan, E., Sahin, A.A., Chen, J.S., Krishnamurthy, R.R., Aggarwal, N., Brun, A.M, Mehta, K (2002) Down-regulation of caspase 3 in breast cancer: a possible mechanism for chemoresistance. *Oncogene* 21, 8843-8851.

50. Deveraux, Q.L., Roy, N., Stennicke, H.R., Van Arsdale, T., Zhou, Q., Srinivasula, S.M., . . . Reed, J.C. (1998) IAPs block apoptotic events induced by caspase-8 and cytochrome c by direct inhibition of distinct caspases. *EMBO J* 17, 2215-2223.

51. Deveraux, Q.L., Takahashi, R., Salvesen, G.S., and Reed, J.C. (1997) X-linked IAP is a direct inhibitor of cell-death proteases. *Nature* 388, 300-304.

52. Dittrich, M.T., Klau, G.W., Rosenwald, A., Dandekar, T., and Muller, T. (2008) Identifying functional modules in protein-protein interaction networks: an integrated exact approach. *Bioinformatics* 24, i223-231.

53. Dovio, A., Sartori, M.L., De Francia, S., Mussino, S., Perotti, P., Saba, L., . . . Angeli, A. (2009) Differential expression of determinants of glucocorticoid sensitivity in androgen-dependent and androgen-independent human prostate cancer cell lines. *J Steroid Biochem Mol Biol* 116, 29-36.

54. Dreze, M., Monachello, D., Lurin, C., Cusick, M.E., Hill, D.E., Vidal, M., and Braun, P. (2010) High-quality binary interactome mapping. *Methods Enzymol* 470, 281-315.

55. Duarte, N.C., Becker, S.A., Jamshidi, N., Thiele, I., Mo, M.L., Vo, T.D., . . . Palsson, B.O. (2007) Global reconstruction of the human metabolic network based on genomic and bibliomic data. *Proc Natl Acad Sci U S A* 104, 1777-1782.

56. Eghtedar, A., Verstovsek, S., Estrov, Z., Burger, J., Cortes, J., Bivins, C., . . . Ravandi, F. (2012) Phase 2 study of the JAK kinase inhibitor ruxolitinib in patients with refractory leukemias, including postmyeloproliferative neoplasm acute myeloid leukemia. *Blood* 119, 4614-4618.

57. Eichhorn, P.J., Gili, M., Scaltriti, M., Serra, V., Guzman, M., Nijkamp, W., . . . Baselga, J. (2008) Phosphatidylinositol 3-kinase hyperactivation results in lapatinib resistance that is reversed by the

mTOR/phosphatidylinositol 3-kinase inhibitor NVP-BEZ235. *Cancer Res* 68, 9221-9230.

58. Feuring, M., Wehling, M., and Schultz, A. (2011) Dalteparin dose-dependently increases ROTEM((R)) thrombelastography parameters only at supratherapeutic anti-factor Xa levels: an in vitro study. *Clin Exp Pharmacol Physiol* 38, 783-786.

59. Fields, S. and Song, O. (1989) A novel genetic system to detect protein-protein interactions. *Nature* 340, 245-246.

60. Friedman, A.A., Amzallag, A., Pruteanu-Malinici, I., Baniya, S., Cooper, Z.A., Piris, A., . . . Fisher, D.E. (2015) Landscape of Targeted Anti-Cancer Drug Synergies in Melanoma Identifies a Novel BRAF-VEGFR/PDGFR Combination Treatment. *PLoS One* 10, e0140310.

61. Fryar, E.B., Das, J.R., Davis, J.H., Desoto, J.A., Laniyan, I., Southerland, W.M., and Bowen, D. (2006) Raloxifene attenuation of 5-FU/methotrexate cytotoxicity in human breast cancer cells: the importance of sequence in combination chemotherapy. *Anticancer Res* 26, 1861-1867.

62. Fu, X., Osborne, C.K., and Schiff, R. (2013) Biology and therapeutic potential of PI3K signaling in ER+/HER2-negative breast cancer. *Breast* 22 Suppl 2, S12-18.

63. Fujii, M., Inoki, I., Saga, M., Morikawa, N., Arakawa, K., Inaba, S., . . . Miyamori, I. (2012) Aldosterone inhibits endothelial morphogenesis and angiogenesis through the downregulation of vascular endothelial growth factor receptor-2 expression subsequent to peroxisome proliferator-activated receptor gamma. *J Steroid Biochem Mol Biol* 129, 145-152.

64. Gage, M., Wattendorf, D., and Henry, L.R. (2012) Translational advances regarding hereditary breast cancer syndromes. *J Surg Oncol* 105, 444-451.

65. Gandhi, T.K., Zhong, J., Mathivanan, S., Karthick, L., Chandrika, K.N., Mohan, S.S., . . . Pandey, A. (2006) Analysis of the human protein interactome and comparison with yeast, worm and fly interaction datasets. *Nat Genet* 38, 285-293.

66. Garnett, M.J., Edelman, E.J., Heidorn, S.J., Greenman, C.D., Dastur, A., Lau, K.W., . . . Benes, C.H. (2012) Systematic identification of genomic markers of drug sensitivity in cancer cells. *Nature* 483, 570-575.

67. Gehlot, H.S., Tak, N., Kaushik, M., Mitra, S., Chen, W.M., Poweleit, N., . . . Gyaneshwar, P. (2013) An invasive Mimosa in India does not adopt the symbionts of its native relatives. *Ann Bot* 112, 179-196.

68. Germain, M., Affar, E.B., D'Amours, D., Dixit, V.M., Salvesen, G.S., and Poirier, G.G. (1999) Cleavage of automodified poly(ADP-ribose) polymerase during apoptosis. Evidence for involvement of caspase-7. *J Biol Chem* 274, 28379-28384.

69. Geyer, F.C., Weigelt, B., Natrajan, R., Lambros, M.B., de Biase, D., Vatcheva, R., . . . Reis-Filho, J.S. (2010) Molecular analysis reveals a genetic basis for the phenotypic diversity of metaplastic breast carcinomas. *J Pathol* 220, 562-573.

70. Ghobrial, I.M., Witzig, T.E., and Adjei, A.A. (2005) Targeting apoptosis pathways in cancer therapy. *CA Cancer J Clin* 55, 178-194.

71. Gianni, L., Pienkowski, T., Im, Y.H., Roman, L., Tseng, L.M., Liu, M.C., . . . Valagussa, P. (2012) Efficacy and safety of neoadjuvant pertuzumab and trastuzumab in women with locally advanced, inflammatory, or early HER2-positive breast cancer (NeoSphere): a

randomised multicentre, open-label, phase 2 trial. *Lancet Oncol* 13, 25-32.

72. Giltnane, J.M. and Balko, J.M. (2014) Rationale for targeting the Ras/MAPK pathway in triple-negative breast cancer. *Discov Med* 17, 275-283.

73. Goh, K.I., Cusick, M.E., Valle, D., Childs, B., Vidal, M., and Barabasi, A.L. (2007) The human disease network. *Proc Natl Acad Sci U S A* 104, 8685-8690.

74. Goldstein, D.B. (2009) Common genetic variation and human traits. *N Engl J Med* 360, 1696-1698.

75. Gray, J. and Druker, B. (2012) Genomics: the breast cancer landscape. *Nature* 486, 328-329.

76. Green, D.R. and Kroemer, G. (2004) The pathophysiology of mitochondrial cell death. *Science* 305, 626-629.

77. Grenader, T., Goldberg, A., and Shavit, L. (2009) Metformin as an addition to conventional chemotherapy in breast cancer. *J Clin Oncol* 27, e259; author reply e260.

78. Gross, A., McDonnell, J.M., and Korsmeyer, S.J. (1999) BCL-2 family members and the mitochondria in apoptosis. *Genes Dev* 13, 1899-1911.

79. Gudjonsson, T., Ronnov-Jessen, L., Villadsen, R., Bissell, M.J., and Petersen, O.W. (2003) To create the correct microenvironment: three-dimensional heterotypic collagen assays for human breast epithelial morphogenesis and neoplasia. *Methods* 30, 247-255.

80. Guo, S., Colbert, L.S., Fuller, M., Zhang, Y., and Gonzalez-Perez, R.R. (2010) Vascular endothelial growth factor receptor-2 in breast cancer. *Biochim Biophys Acta* 1806, 108-121.

81. Hanahan, D. and Weinberg, R.A. (2000) The hallmarks of cancer. *Cell* 100, 57-70.

82. Hanahan, D. and Weinberg, R.A. (2011) Hallmarks of cancer: the next generation. *Cell* 144, 646-674.

83. Hastak, K., Alli, E., and Ford, J.M. (2010) Synergistic chemosensitivity of triple-negative breast cancer cell lines to poly(ADP-Ribose) polymerase inhibition, gemcitabine, and cisplatin. *Cancer Res* 70, 7970-7980.

84. Hengartner, M.O. (2001) Apoptosis: corralling the corpses. *Cell* 104, 325-328.

85. Higgins, M.J. and Baselga, J. (2011) Targeted therapies for breast cancer. *J Clin Invest* 121, 3797-3803.

86. Hirschi, B., Gallmeier, E., Ziesch, A., Marschall, M., and Kolligs, F.T. (2014) Genetic targeting of B-RafV600E affects survival and proliferation and identifies selective agents against BRAF-mutant colorectal cancer cells. *Mol Cancer* 13, 122.

87. Holohan, C., Van Schaeybroeck, S., Longley, D.B., and Johnston, P.G. (2013) Cancer drug resistance: an evolving paradigm. *Nat Rev Cancer* 13, 714-726.

88. Hopkins, A.L. (2008) Network pharmacology: the next paradigm in drug discovery. *Nat Chem Biol* 4, 682-690.

89. Howell, A., Cuzick, J., Baum, M., Buzdar, A., Dowsett, M., Forbes, J.F., . . . Group, A.T. (2005) Results of the ATAC (Arimidex, Tamoxifen, Alone or in Combination) trial after completion of 5 years' adjuvant treatment for breast cancer. *Lancet* 365, 60-62.

90. http://www.atcc.org.

91. http://www.cancer.gov.

92. http://www.clinicaltrials.gov.

93. http://www.genenames.org.

94. Huang, D.C. and Strasser, A. (2000) BH3-Only proteins-essential initiators of apoptotic cell death. *Cell* 103, 839-842.

95. Hurwitz, H.I., Uppal, N., Wagner, S.A., Bendell, J.C., Beck, J.T., Wade, S.M., 3rd, . . . Levy, R.S. (2015) Randomized, Double-Blind, Phase II Study of Ruxolitinib or Placebo in Combination With Capecitabine in Patients With Metastatic Pancreatic Cancer for Whom Therapy With Gemcitabine Has Failed. *J Clin Oncol* 33, 4039-4047.

96. Ibrahim, Y.H., Garcia-Garcia, C., Serra, V., He, L., Torres-Lockhart, K., Prat, A., . . . Baselga, J. (2012) PI3K inhibition impairs BRCA1/2 expression and sensitizes BRCA-proficient triple-negative breast cancer to PARP inhibition. *Cancer Discov* 2, 1036-1047.

97. Ideker, T. and Sharan, R. (2008) Protein networks in disease. *Genome Res* 18, 644-652.

98. Isakoff, S.J., Engelman, J.A., Irie, H.Y., Luo, J., Brachmann, S.M., Pearline, R.V., . . . Brugge, J.S. (2005) Breast cancer-associated PIK3CA mutations are oncogenic in mammary epithelial cells. *Cancer Res* 65, 10992-11000.

99. Jaeger, S. and Aloy, P. (2012) From protein interaction networks to novel therapeutic strategies. *IUBMB Life* 64, 529-537.

100. Janicke, R.U., Sprengart, M.L., Wati, M.R., and Porter, A.G. (1998) Caspase-3 is required for DNA fragmentation and morphological changes associated with apoptosis. *J Biol Chem* 273, 9357-9360.

101. Jeong, H., Tombor, B., Albert, R., Oltvai, Z.N., and Barabasi, A.L. (2000) The large-scale organization of metabolic networks. *Nature* 407, 651-654.

102. Jia, J., Zhu, F., Ma, X., Cao, Z., Li, Y., and Chen, Y.Z. (2009) Mechanisms of drug combinations: interaction and network perspectives. *Nat Rev Drug Discov* 8, 111-128.

103. Jiang, X. and Wang, X. (2000) Cytochrome c promotes caspase-9 activation by inducing nucleotide binding to Apaf-1. *J Biol Chem* 275, 31199-31203.

104. Jones, K.A., Gilder, A.S., Lam, M.S., Du, N., Banki, M.A., Merati, A., . . . Gonias, S.L. (2015) Selective coexpression of VEGF receptor 2 in EGFRvIII-positive glioblastoma cells prevents cellular senescence and contributes to their aggressive nature. *Neuro Oncol*.

105. Jonsson, P.F. and Bates, P.A. (2006) Global topological features of cancer proteins in the human interactome. *Bioinformatics* 22, 2291-2297.

106. Juo, P., Kuo, C.J., Yuan, J., and Blenis, J. (1998) Essential requirement for caspase-8/FLICE in the initiation of the Fas-induced apoptotic cascade. *Curr Biol* 8, 1001-1008.

107. Juvekar, A., Burga, L.N., Hu, H., Lunsford, E.P., Ibrahim, Y.H., Balmana, J., . . . Wulf, G.M. (2012) Combining a PI3K inhibitor with a PARP inhibitor provides an effective therapy for BRCA1-related breast cancer. *Cancer Discov* 2, 1048-1063.

108. Karkkainen, M.J. and Petrova, T.V. (2000) Vascular endothelial growth factor receptors in the regulation of angiogenesis and lymphangiogenesis. *Oncogene* 19, 5598-5605.

109. Kennecke, H., Yerushalmi, R., Woods, R., Cheang, M.C., Voduc, D., Speers, C.H., . . . Gelmon, K. (2010) Metastatic behavior of breast cancer subtypes. *J Clin Oncol* 28, 3271-3277.

110. Kerr JF, H.B. (1991) Apoptosis: the molecular basis of cell death.

111. Kim, D.E., Kim, Y., Cho, D.H., Jeong, S.Y., Kim, S.B., Suh, N., . . . Kim, C.S. (2015) Raloxifene induces autophagy-dependent cell death in breast cancer cells via the activation of AMP-activated protein kinase. *Mol Cells* 38, 138-144.

112. Kischkel, F.C., Hellbardt, S., Behrmann, I., Germer, M., Pawlita, M., Krammer, P.H., and Peter, M.E. (1995) Cytotoxicity-dependent APO-1 (Fas/CD95)-associated proteins form a death-inducing signaling complex (DISC) with the receptor. *EMBO J* 14, 5579-5588.

113. Kitano, H. (2002) Computational systems biology. *Nature* 420, 206-210.

114. Kitano, H. (2004) Biological robustness. *Nat Rev Genet* 5, 826-837.

115. Kroemer, G., El-Deiry, W.S., Golstein, P., Peter, M.E., Vaux, D., Vandenabeele, P., . . . Nomenclature Committee on Cell, D. (2005) Classification of cell death: recommendations of the Nomenclature Committee on Cell Death. *Cell Death Differ* 12 Suppl 2, 1463-1467.

116. Kumar V, F.N., Aster JC (2010) Pathologic basis of disease. *Robbins and Cotran*.

117. Kushner, P.J., Agard, D.A., Greene, G.L., Scanlan, T.S., Shiau, A.K., Uht, R.M., and Webb, P. (2000) Estrogen receptor pathways to AP-1. *J Steroid Biochem Mol Biol* 74, 311-317.

118. Lai, K., Killingsworth, M.C., and Lee, C.S. (2015) Gene of the month: PIK3CA. *J Clin Pathol* 68, 253-257.

119. Lamesch, P., Li, N., Milstein, S., Fan, C., Hao, T., Szabo, G., . . . Vidal, M. (2007) hORFeome v3.1: a resource of human open reading frames representing over 10,000 human genes. *Genomics* 89, 307-315.

120. Lavrik, I.N., Golks, A., and Krammer, P.H. (2005) Caspases: pharmacological manipulation of cell death. *J Clin Invest* 115, 2665-2672.

121. Lawrence, M.S., Stojanov, P., Mermel, C.H., Robinson, J.T., Garraway, L.A., Golub, T.R., . . . Getz, G. (2014) Discovery and saturation analysis of cancer genes across 21 tumour types. *Nature* 505, 495-501.

122. Lawrence, M.S., Stojanov, P., Polak, P., Kryukov, G.V., Cibulskis, K., Sivachenko, A., . . . Getz, G. (2013) Mutational heterogeneity in cancer and the search for new cancer-associated genes. *Nature* 499, 214-218.

123. Lehar, J., Krueger, A.S., Avery, W., Heilbut, A.M., Johansen, L.M., Price, E.R., . . . Borisy, A.A. (2009) Synergistic drug combinations tend to improve therapeutically relevant selectivity. *Nat Biotechnol* 27, 659-666.

124. Lenferink, A.E., Busse, D., Flanagan, W.M., Yakes, F.M., and Arteaga, C.L. (2001) ErbB2/neu kinase modulates cellular p27(Kip1) and cyclin D1 through multiple signaling pathways. *Cancer Res* 61, 6583-6591.

125. Leung, E.Y., Kim, J.E., Askarian-Amiri, M., Rewcastle, G.W., Finlay, G.J., and Baguley, B.C. (2014) Relationships between signaling pathway usage and sensitivity to a pathway inhibitor: examination of trametinib responses in cultured breast cancer lines. *PLoS One* 9, e105792.

126. Levy, D.E. and Darnell, J.E., Jr. (2002) Stats: transcriptional control and biological impact. *Nat Rev Mol Cell Biol* 3, 651-662.

127. Lewis, B.P., Burge, C.B., and Bartel, D.P. (2005) Conserved seed pairing, often flanked by adenosines, indicates that thousands of human genes are microRNA targets. *Cell* 120, 15-20.

128. Li, H., Zhu, H., Xu, C.J., and Yuan, J. (1998) Cleavage of BID by caspase 8 mediates the mitochondrial damage in the Fas pathway of apoptosis. *Cell* 94, 491-501.

129. Li, P., Nijhawan, D., Budihardjo, I., Srinivasula, S.M., Ahmad, M., Alnemri, E.S., and Wang, X. (1997) Cytochrome c and dATP-dependent formation of Apaf-1/caspase-9 complex initiates an apoptotic protease cascade. *Cell* 91, 479-489.

130. Li, T., Lu, H., Shen, C., Lahiri, S.K., Wason, M.S., Mukherjee, D., . . . Zhao, J. (2014) Identification of epithelial stromal interaction 1 as a novel effector downstream of Kruppel-like factor 8 in breast cancer invasion and metastasis. *Oncogene* 33, 4746-4755.

131. Lichtenberger, B.M., Tan, P.K., Niederleithner, H., Ferrara, N., Petzelbauer, P., and Sibilia, M. (2010) Autocrine VEGF signaling synergizes with EGFR in tumor cells to promote epithelial cancer development. *Cell* 140, 268-279.

132. Lin, A., Minden, A., Martinetto, H., Claret, F.X., Lange-Carter, C., Mercurio, F., . . . Karin, M. (1995) Identification of a dual specificity kinase that activates the Jun kinases and p38-Mpk2. *Science* 268, 286-290.

133. Linding, R., Jensen, L.J., Pasculescu, A., Olhovsky, M., Colwill, K., Bork, P., . . . Pawson, T. (2008) NetworKIN: a resource for exploring cellular phosphorylation networks. *Nucleic Acids Res* 36, D695-699.

134. Liu, C.Y., Tseng, L.M., Su, J.C., Chang, K.C., Chu, P.Y., Tai, W.T., . . . Chen, K.F. (2013) Novel sorafenib analogues induce apoptosis through SHP-1 dependent STAT3 inactivation in human breast cancer cells. *Breast Cancer Res* 15, R63.

135. Liu, H., Lee, E.S., Gajdos, C., Pearce, S.T., Chen, B., Osipo, C., . . . Jordan, V.C. (2003) Apoptotic action of 17beta-estradiol in raloxifene-resistant MCF-7 cells in vitro and in vivo. *J Natl Cancer Inst* 95, 1586-1597.

136. Liu, H., Scholz, C., Zang, C., Schefe, J.H., Habbel, P., Regierer, A.C., . . . Eucker, J. (2012) Metformin and the mTOR inhibitor everolimus (RAD001) sensitize breast cancer cells to the cytotoxic effect of chemotherapeutic drugs in vitro. *Anticancer Res* 32, 1627-1637.

137. Lobenhofer, E.K., Huper, G., Iglehart, J.D., and Marks, J.R. (2000) Inhibition of mitogen-activated protein kinase and phosphatidylinositol 3-kinase activity in MCF-7 cells prevents estrogen-induced mitogenesis. *Cell Growth Differ* 11, 99-110.

138. Lord, C.J., Garrett, M.D., and Ashworth, A. (2006) Targeting the double-strand DNA break repair pathway as a therapeutic strategy. *Clin Cancer Res* 12, 4463-4468.

139. Luo, X., Budihardjo, I., Zou, H., Slaughter, C., and Wang, X. (1998) Bid, a Bcl2 interacting protein, mediates cytochrome c release from mitochondria in response to activation of cell surface death receptors. *Cell* 94, 481-490.

140. Martinez-Carpio, P.A., Mur, C., Rosel, P., and Navarro, M.A. (1999) Constitutive and regulated secretion of epidermal growth factor and transforming growth factor-beta1 in MDA-MB-231 breast cancer cell line in 11-day cultures. *Cell Signal* 11, 753-757.

141. Matsumoto, T., Bohman, S., Dixelius, J., Berge, T., Dimberg, A., Magnusson, P., . . . Claesson-Welsh, L. (2005) VEGF receptor-2 Y951 signaling and a role for the adapter molecule TSAd in tumor angiogenesis. *EMBO J* 24, 2342-2353.

142. McCarthy, N.J. and Evan, G.I. (1998) Methods for detecting and quantifying apoptosis. *Curr Top Dev Biol* 36, 259-278.

143. McKusick, V.A. (2007) Mendelian Inheritance in Man and its online version, OMIM. *Am J Hum Genet* 80, 588-604.

144. Miller, M.L., Molinelli, E.J., Nair, J.S., Sheikh, T., Samy, R., Jing, X., . . . Sander, C. (2013) Drug synergy screen and network modeling in dedifferentiated liposarcoma identifies CDK4 and IGF1R as synergistic drug targets. *Sci Signal* 6, ra85.

145. Minn, A.J., Velez, P., Schendel, S.L., Liang, H., Muchmore, S.W., Fesik, S.W., . . . Thompson, C.B. (1997) Bcl-x(L) forms an ion channel in synthetic lipid membranes. *Nature* 385, 353-357.

146. Montagut, C. and Settleman, J. (2009) Targeting the RAF-MEK-ERK pathway in cancer therapy. *Cancer Lett* 283, 125-134.

147. Munagala, R., Aqil, F., and Gupta, R.C. (2011) Promising molecular targeted therapies in breast cancer. *Indian J Pharmacol* 43, 236-245.

148. Musgrove, E.A. and Sutherland, R.L. (2009) Biological determinants of endocrine resistance in breast cancer. *Nat Rev Cancer* 9, 631-643.

149. Myers, M.G., Jr., Sun, X.J., Cheatham, B., Jachna, B.R., Glasheen, E.M., Backer, J.M., and White, M.F. (1993) IRS-1 is a common element in insulin and insulin-like growth factor-I signaling to the phosphatidylinositol 3'-kinase. *Endocrinology* 132, 1421-1430.

150. Nagaria, T.S., Williams, J.L., Leduc, C., Squire, J.A., Greer, P.A., and Sangrar, W. (2013) Flavopiridol synergizes with sorafenib to induce

cytotoxicity and potentiate antitumorigenic activity in EGFR/HER-2 and mutant RAS/RAF breast cancer model systems. *Neoplasia* 15, 939-951.

151. Nahta, R. and Esteva, F.J. (2006) HER2 therapy: molecular mechanisms of trastuzumab resistance. *Breast Cancer Res* 8, 215.

152. National Cancer Institute, N.

153. Nielsen, H.L., Ronnov-Jessen, L., Villadsen, R., and Petersen, O.W. (2002) Identification of EPSTI1, a novel gene induced by epithelial-stromal interaction in human breast cancer. *Genomics* 79, 703-710.

154. Nielsen, T.O., Hsu, F.D., Jensen, K., Cheang, M., Karaca, G., Hu, Z., . . . Perou, C.M. (2004) Immunohistochemical and clinical characterization of the basal-like subtype of invasive breast carcinoma. *Clin Cancer Res* 10, 5367-5374.

155. Nugoli, M., Chuchana, P., Vendrell, J., Orsetti, B., Ursule, L., Nguyen, C., . . . Theillet, C. (2003) Genetic variability in MCF-7 sublines: evidence of rapid genomic and RNA expression profile modifications. *BMC Cancer* 3, 13.

156. Olsson, A.K., Dimberg, A., Kreuger, J., and Claesson-Welsh, L. (2006) VEGF receptor signalling - in control of vascular function. *Nat Rev Mol Cell Biol* 7, 359-371.

157. Osaki, M., Oshimura, M., and Ito, H. (2004) PI3K-Akt pathway: its functions and alterations in human cancer. *Apoptosis* 9, 667-676.

158. Osborne, C.K. and Schiff, R. (2011) Mechanisms of endocrine resistance in breast cancer. *Annu Rev Med* 62, 233-247.

159. Oti, M. and Brunner, H.G. (2007) The modular nature of genetic diseases. *Clin Genet* 71, 1-11.

160. Pasche, B. (2010) Cancer genetics. Introduction. *Cancer Treat Res*

161. Pemmaraju, N., Kantarjian, H., Kadia, T., Cortes, J., Borthakur, G., Newberry, K., . . . Verstovsek, S. (2015) A phase I/II study of the Janus kinase (JAK)1 and 2 inhibitor ruxolitinib in patients with relapsed or refractory acute myeloid leukemia. *Clin Lymphoma Myeloma Leuk* 15, 171-176.

162. Perigolo de Oliveira, M., Constant, J.F., Peuchmaur, M., Pitta, I., and Decout, J.L. (2013) Antibiotic drugs aminoglycosides cleave DNA at abasic sites: shedding new light on their toxicity? *Chem Res Toxicol* 26, 1710-1719.

163. Perou, C.M., Sorlie, T., Eisen, M.B., van de Rijn, M., Jeffrey, S.S., Rees, C.A., . . . Botstein, D. (2000) Molecular portraits of human breast tumours. *Nature* 406, 747-752.

164. Peruzzi, F., Prisco, M., Dews, M., Salomoni, P., Grassilli, E., Romano, G., . . . Baserga, R. (1999) Multiple signaling pathways of the insulin-like growth factor 1 receptor in protection from apoptosis. *Mol Cell Biol* 19, 7203-7215.

165. Peter, M.E. and Krammer, P.H. (2003) The CD95(APO-1/Fas) DISC and beyond. *Cell Death Differ* 10, 26-35.

166. Polyak, K. (2007) Breast cancer: origins and evolution. *J Clin Invest* 117, 3155-3163.

167. Polyak, K. (2011) Heterogeneity in breast cancer. *J Clin Invest* 121, 3786-3788.

168. Polyak, K. and Metzger Filho, O. (2012) SnapShot: breast cancer. *Cancer Cell* 22, 562-562 e561.

169. Prat, A., Parker, J.S., Fan, C., and Perou, C.M. (2012) PAM50 assay and the three-gene model for identifying the major and clinically relevant molecular subtypes of breast cancer. *Breast Cancer Res Treat* 135, 301-306.

170. Prat, A., Parker, J.S., Karginova, O., Fan, C., Livasy, C., Herschkowitz, J.I., . . . Perou, C.M. (2010) Phenotypic and molecular characterization of the claudin-low intrinsic subtype of breast cancer. *Breast Cancer Res* 12, R68.

171. Prat, A. and Perou, C.M. (2011) Deconstructing the molecular portraits of breast cancer. *Mol Oncol* 5, 5-23.

172. Prenzel, N., Fischer, O.M., Streit, S., Hart, S., and Ullrich, A. (2001) The epidermal growth factor receptor family as a central element for cellular signal transduction and diversification. *Endocr Relat Cancer* 8, 11-31.

173. Pujol, A., Mosca, R., Farres, J., and Aloy, P. (2010) Unveiling the role of network and systems biology in drug discovery. *Trends Pharmacol Sci* 31, 115-123.

174. Rahman, M., Davis, S.R., Pumphrey, J.G., Bao, J., Nau, M.M., Meltzer, P.S., and Lipkowitz, S. (2009) TRAIL induces apoptosis in triple-negative breast cancer cells with a mesenchymal phenotype. *Breast Cancer Res Treat* 113, 217-230.

175. Reed, J.C., Jurgensmeier, J.M., and Matsuyama, S. (1998) Bcl-2 family proteins and mitochondria. *Biochim Biophys Acta* 1366, 127-137.

176. Reynolds, A., Leake, D., Boese, Q., Scaringe, S., Marshall, W.S., and Khvorova, A. (2004) Rational siRNA design for RNA interference. *Nat Biotechnol* 22, 326-330.

177. Ritz, C.S., J.C. (2005) Bioassay analysis using R. *Journal of Statistical Software* 12.

178. Rodriguez, J. and Lazebnik, Y. (1999) Caspase-9 and APAF-1 form an active holoenzyme. *Genes Dev* 13, 3179-3184.

179. Rommens, J.M., Durocher, F., McArthur, J., Tonin, P., LeBlanc, J.F., Allen, T., . . . et al. (1995) Generation of a transcription map at the HSD17B locus centromeric to BRCA1 at 17q21. *Genomics* 28, 530-542.

180. Rouzier, R., Perou, C.M., Symmans, W.F., Ibrahim, N., Cristofanilli, M., Anderson, K., . . . Pusztai, L. (2005) Breast cancer molecular subtypes respond differently to preoperative chemotherapy. *Clin Cancer Res* 11, 5678-5685.

181. Rual, J.F., Venkatesan, K., Hao, T., Hirozane-Kishikawa, T., Dricot, A., Li, N., . . . Vidal, M. (2005) Towards a proteome-scale map of the human protein-protein interaction network. *Nature* 437, 1173-1178.

182. Saelens, X., Festjens, N., Vande Walle, L., van Gurp, M., van Loo, G., and Vandenabeele, P. (2004) Toxic proteins released from mitochondria in cell death. *Oncogene* 23, 2861-2874.

183. Safe, S. (2001) Transcriptional activation of genes by 17 beta-estradiol through estrogen receptor-Sp1 interactions. *Vitam Horm* 62, 231-252.

184. Saji, S. and Kimura-Tsuchiya, R. (2015) Combination of molecular-targeted drugs with endocrine therapy for hormone-resistant breast cancer. *Int J Clin Oncol* 20, 268-272.

185. Saleh, A., Srinivasula, S.M., Acharya, S., Fishel, R., and Alnemri, E.S. (1999) Cytochrome c and dATP-mediated oligomerization of Apaf-1 is a prerequisite for procaspase-9 activation. *J Biol Chem* 274, 17941-17945.

186. Samuels, Y., Diaz, L.A., Jr., Schmidt-Kittler, O., Cummins, J.M., Delong, L., Cheong, I., . . . Velculescu, V.E. (2005) Mutant PIK3CA

promotes cell growth and invasion of human cancer cells. *Cancer Cell* 7, 561-573.

187. Schadt, E.E. (2009) Molecular networks as sensors and drivers of common human diseases. *Nature* 461, 218-223.

188. Senkus, E., Kyriakides, S., Penault-Llorca, F., Poortmans, P., Thompson, A., Zackrisson, S., . . . Group, E.G.W. (2013) Primary breast cancer: ESMO Clinical Practice Guidelines for diagnosis, treatment and follow-up. *Ann Oncol* 24 Suppl 6, vi7-23.

189. Serra-Musach, J., Aguilar, H., Iorio, F., Comellas, F., Berenguer, A., Brunet, J., . . . Pujana, M.A. (2012) Cancer develops, progresses and responds to therapies through restricted perturbation of the protein-protein interaction network. *Integr Biol (Camb)* 4, 1038-1048.

190. Sharan, R., Ulitsky, I., and Shamir, R. (2007) Network-based prediction of protein function. *Mol Syst Biol* 3, 88.

191. She, Q.B., Chandarlapaty, S., Ye, Q., Lobo, J., Haskell, K.M., Leander, K.R., . . . Rosen, N. (2008) Breast tumor cells with PI3K mutation or HER2 amplification are selectively addicted to Akt signaling. *PLoS One* 3, e3065.

192. Shi, Y. (2002) Mechanisms of caspase activation and inhibition during apoptosis. *Mol Cell* 9, 459-470.

193. Shiraishi, T., Matsuyama, S., and Kitano, H. (2010) Large-scale analysis of network bistability for human cancers. *PLoS Comput Biol* 6, e1000851.

194. Sircoulomb, F., Bekhouche, I., Finetti, P., Adelaide, J., Ben Hamida, A., Bonansea, J., . . . Chaffanet, M. (2010) Genome profiling of ERBB2-amplified breast cancers. *BMC Cancer* 10, 539.

195. Skrabanek, L. and Campagne, F. (2001) TissueInfo: high-throughput identification of tissue expression profiles and specificity. *Nucleic Acids Res* 29, E102-102.

196. Soler-Lopez, M., Zanzoni, A., Lluis, R., Stelzl, U., and Aloy, P. (2011) Interactome mapping suggests new mechanistic details underlying Alzheimer's disease. *Genome Res* 21, 364-376.

197. Song, M.S., Salmena, L., and Pandolfi, P.P. (2012) The functions and regulation of the PTEN tumour suppressor. *Nat Rev Mol Cell Biol* 13, 283-296.

198. Song, R.X., Barnes, C.J., Zhang, Z., Bao, Y., Kumar, R., and Santen, R.J. (2004) The role of Shc and insulin-like growth factor 1 receptor in mediating the translocation of estrogen receptor alpha to the plasma membrane. *Proc Natl Acad Sci U S A* 101, 2076-2081.

199. Sorlie, T., Perou, C.M., Tibshirani, R., Aas, T., Geisler, S., Johnsen, H., . . . Borresen-Dale, A.L. (2001) Gene expression patterns of breast carcinomas distinguish tumor subclasses with clinical implications. *Proc Natl Acad Sci U S A* 98, 10869-10874.

200. Spirin, V. and Mirny, L.A. (2003) Protein complexes and functional modules in molecular networks. *Proc Natl Acad Sci U S A* 100, 12123-12128.

201. Stecklein, S.R., Kumaraswamy, E., Behbod, F., Wang, W., Chaguturu, V., Harlan-Williams, L.M., and Jensen, R.A. (2012) BRCA1 and HSP90 cooperate in homologous and non-homologous DNA double-strand-break repair and G2/M checkpoint activation. *Proc Natl Acad Sci U S A* 109, 13650-13655.

202. Stelzl, U., Worm, U., Lalowski, M., Haenig, C., Brembeck, F.H., Goehler, H., . . . Wanker, E.E. (2005) A human protein-protein

interaction network: a resource for annotating the proteome. *Cell* 122, 957-968.

203. Stumpf, M.P., Kelly, W.P., Thorne, T., and Wiuf, C. (2007) Evolution at the system level: the natural history of protein interaction networks. *Trends Ecol Evol* 22, 366-373.

204. Su, A.I., Wiltshire, T., Batalov, S., Lapp, H., Ching, K.A., Block, D., . . . Hogenesch, J.B. (2004) A gene atlas of the mouse and human protein-encoding transcriptomes. *Proc Natl Acad Sci U S A* 101, 6062-6067.

205. Su, G.H., Hilgers, W., Shekher, M.C., Tang, D.J., Yeo, C.J., Hruban, R.H., and Kern, S.E. (1998) Alterations in pancreatic, biliary, and breast carcinomas support MKK4 as a genetically targeted tumor suppressor gene. *Cancer Res* 58, 2339-2342.

206. Takahashi, O., Komaki, R., Smith, P.D., Jurgensmeier, J.M., Ryan, A., Bekele, B.N., . . . O'Reilly, M.S. (2012) Combined MEK and VEGFR inhibition in orthotopic human lung cancer models results in enhanced inhibition of tumor angiogenesis, growth, and metastasis. *Clin Cancer Res* 18, 1641-1654.

207. Tao, L.Y., Liang, Y.J., Wang, F., Chen, L.M., Yan, Y.Y., Dai, C.L., and Fu, L.W. (2009) Cediranib (recentin, AZD2171) reverses ABCB1- and ABCC1-mediated multidrug resistance by inhibition of their transport function. *Cancer Chemother Pharmacol* 64, 961-969.

208. Tarpley, M., Abdissa, T.T., Johnson, G.L., and Scott, J.E. (2014) Bosutinib reduces the efficacy of Dasatinib in triple-negative breast cancer cell lines. *Anticancer Res* 34, 1629-1635.

209. Teschendorff, A.E. and Severini, S. (2010) Increased entropy of signal transduction in the cancer metastasis phenotype. *BMC Syst Biol* 4, 104.

210. Tewari, M., Quan, L.T., O'Rourke, K., Desnoyers, S., Zeng, Z., Beidler, D.R., . . . Dixit, V.M. (1995) Yama/CPP32 beta, a mammalian homolog of CED-3, is a CrmA-inhibitable protease that cleaves the death substrate poly(ADP-ribose) polymerase. *Cell* 81, 801-809.

211. Thomas, R.J., Guise, T.A., Yin, J.J., Elliott, J., Horwood, N.J., Martin, T.J., and Gillespie, M.T. (1999) Breast cancer cells interact with osteoblasts to support osteoclast formation. *Endocrinology* 140, 4451-4458.

212. Torre, L.A., Bray, F., Siegel, R.L., Ferlay, J., Lortet-Tieulent, J., and Jemal, A. (2015) Global cancer statistics, 2012. *CA Cancer J Clin* 65, 87-108.

213. Tortora, G. (2011) Mechanisms of resistance to HER2 target therapy. *J Natl Cancer Inst Monogr* 2011, 95-98.

214. Toss, A. and Cristofanilli, M. (2015) Molecular characterization and targeted therapeutic approaches in breast cancer. *Breast Cancer Res* 17, 60.

215. Treeck, O., Wackwitz, B., Haus, U., and Ortmann, O. (2006) Effects of a combined treatment with mTOR inhibitor RAD001 and tamoxifen in vitro on growth and apoptosis of human cancer cells. *Gynecol Oncol* 102, 292-299.

216. Tsai, E.M., Wang, S.C., Lee, J.N., and Hung, M.C. (2001) Akt activation by estrogen in estrogen receptor-negative breast cancer cells. *Cancer Res* 61, 8390-8392.

217. Tsang, R.Y. and Finn, R.S. (2012) Beyond trastuzumab: novel therapeutic strategies in HER2-positive metastatic breast cancer. *Br J Cancer* 106, 6-13.

218. Uhlen, M., Oksvold, P., Fagerberg, L., Lundberg, E., Jonasson, K., Forsberg, M., . . . Ponten, F. (2010) Towards a knowledge-based Human Protein Atlas. *Nat Biotechnol* 28, 1248-1250.

219. van Agthoven, T., van Agthoven, T.L., Dekker, A., van der Spek, P.J., Vreede, L., and Dorssers, L.C. (1998) Identification of BCAR3 by a random search for genes involved in antiestrogen resistance of human breast cancer cells. *EMBO J* 17, 2799-2808.

220. van Meerloo, J., Kaspers, G.J., and Cloos, J. (2011) Cell sensitivity assays: the MTT assay. *Methods Mol Biol* 731, 237-245.

221. van Wieringen, W.N. and van der Vaart, A.W. (2011) Statistical analysis of the cancer cell's molecular entropy using high-throughput data. *Bioinformatics* 27, 556-563.

222. Varfolomeev, E.E., Schuchmann, M., Luria, V., Chiannilkulchai, N., Beckmann, J.S., Mett, I.L., . . . Wallach, D. (1998) Targeted disruption of the mouse Caspase 8 gene ablates cell death induction by the TNF receptors, Fas/Apo1, and DR3 and is lethal prenatally. *Immunity* 9, 267-276.

223. Vaux, D.L. and Silke, J. (2003) Mammalian mitochondrial IAP binding proteins. *Biochem Biophys Res Commun* 304, 499-504.

224. Vogel, C.L., Cobleigh, M.A., Tripathy, D., Gutheil, J.C., Harris, L.N., Fehrenbacher, L., . . . Press, M. (2002) Efficacy and safety of trastuzumab as a single agent in first-line treatment of HER2-overexpressing metastatic breast cancer. *J Clin Oncol* 20, 719-726.

225. Vogelstein, B. and Kinzler, K.W. (2004) Cancer genes and the pathways they control. *Nat Med* 10, 789-799.

226. Vogelstein, B., Papadopoulos, N., Velculescu, V.E., Zhou, S., Diaz, L.A., Jr., and Kinzler, K.W. (2013) Cancer genome landscapes. *Science* 339, 1546-1558.

227. Wang, Y., Wei, J., Li, L., Fan, C., and Sun, Y. (2015) Combined Use of Metformin and Everolimus Is Synergistic in the Treatment of Breast Cancer Cells. *Oncol Res* 22, 193-201.

228. Wei, M.C., Zong, W.X., Cheng, E.H., Lindsten, T., Panoutsakopoulou, V., Ross, A.J., . . . Korsmeyer, S.J. (2001) Proapoptotic BAX and BAK: a requisite gateway to mitochondrial dysfunction and death. *Science* 292, 727-730.

229. Wei, Y., Fan, T., and Yu, M (2008) Inhibitor of apoptosis proteins and apoptosis. *Acta Biochim Biophys Sin (Shanghai)* 40, 278-288.

230. Wong, R.S. (2011) Apoptosis in cancer: from pathogenesis to treatment. *J Exp Clin Cancer Res* 30, 87.

231. Xu, J. and Li, Y. (2006) Discovering disease-genes by topological features in human protein-protein interaction network. *Bioinformatics* 22, 2800-2805.

232. Xu, J., Zhou, J.Y., Tainsky, M.A., and Wu, G.S. (2007) Evidence that tumor necrosis factor-related apoptosis-inducing ligand induction by 5-Aza-2'-deoxycytidine sensitizes human breast cancer cells to adriamycin. *Cancer Res* 67, 1203-1211.

233. Xu, J., Zhou, J.Y., Wei, W.Z., and Wu, G.S. (2010) Activation of the Akt survival pathway contributes to TRAIL resistance in cancer cells. *PLoS One* 5, e10226.

234. Xue, G. and Hemmings, B.A. (2013) PKB/Akt-dependent regulation of cell motility. *J Natl Cancer Inst* 105, 393-404.

235. Yang, H., Lawrence, H.R., Kazi, A., Gevariya, H., Patel, R., Luo, Y., . . . Sebti, S.M. (2014) Dual Aurora A and JAK2 kinase blockade effectively suppresses malignant transformation. *Oncotarget* 5, 2947-2961.

236. Yang, H.Y., Shao, R., Hung, M.C., and Lee, M.H. (2001) p27 Kip1 inhibits HER2/neu-mediated cell growth and tumorigenesis. *Oncogene* 20, 3695-3702.

237. Yardley, D.A., Ismail-Khan, R.R., Melichar, B., Lichinitser, M., Munster, P.N., Klein, P.M., . . . Trepel, J.B. (2013) Randomized phase II, double-blind, placebo-controlled study of exemestane with or without entinostat in postmenopausal women with locally recurrent or metastatic estrogen receptor-positive breast cancer progressing on treatment with a nonsteroidal aromatase inhibitor. *J Clin Oncol* 31, 2128-2135.

238. Yerushalmi, R., Gelmon, K.A., Leung, S., Gao, D., Cheang, M., Pollak, M., . . . Kennecke, H. (2012) Insulin-like growth factor receptor (IGF-1R) in breast cancer subtypes. *Breast Cancer Res Treat* 132, 131-142.

239. Yook, S.H., Oltvai, Z.N., and Barabasi, A.L. (2004) Functional and topological characterization of protein interaction networks. *Proteomics* 4, 928-942.

240. Yu, H., Braun, P., Yildirim, M.A., Lemmens, I., Venkatesan, K., Sahalie, J., . . . Vidal, M. (2008) High-quality binary protein interaction map of the yeast interactome network. *Science* 322, 104-110.

241. Yue, P. and Turkson, J. (2009) Targeting STAT3 in cancer: how successful are we? *Expert Opin Investig Drugs* 18, 45-56.

242. Zack, T.I., Schumacher, S.E., Carter, S.L., Cherniack, A.D., Saksena, G., Tabak, B., . . . Beroukhim, R. (2013) Pan-cancer patterns of somatic copy number alteration. *Nat Genet* 45, 1134-1140.

243. Zadran, S., Remacle, F., and Levine, R.D. (2013) miRNA and mRNA cancer signatures determined by analysis of expression levels

in large cohorts of patients. *Proc Natl Acad Sci U S A* 110, 19160-19165.

244. Zhang, L., Yan, K., Zhang, Y., Huang, R., Bian, J., Zheng, C., . . . Chen, X. (2007) High-throughput synergy screening identifies microbial metabolites as combination agents for the treatment of fungal infections. *Proc Natl Acad Sci U S A* 104, 4606-4611.

245. Zhang, Q., Fan, H., Shen, J., Hoffman, R.M., and Xing, H.R. (2010) Human breast cancer cell lines co-express neuronal, epithelial, and melanocytic differentiation markers in vitro and in vivo. *PLoS One* 5, e9712.

246. Zhao, D., Pan, C., Sun, J., Gilbert, C., Drews-Elger, K., Azzam, D.J., . . . Slingerland, J.M. (2015) VEGF drives cancer-initiating stem cells through VEGFR-2/Stat3 signaling to upregulate Myc and Sox2. *Oncogene* 34, 3107-3119.

247. Zhu, F., Shi, Z., Qin, C., Tao, L., Liu, X., Xu, F., . . . Chen, Y. (2012) Therapeutic target database update 2012: a resource for facilitating target-oriented drug discovery. *Nucleic Acids Res* 40, D1128-1136.

248. Zou, H., Li, Y., Liu, X., and Wang, X. (1999) An APAF-1.cytochrome c multimeric complex is a functional apoptosome that activates procaspase-9. *J Biol Chem* 274, 11549-11556.

7. RESUM DE LA TESIS

El càncer de mama és una malaltia molt heterogènia pel que fa a les alteracions moleculars subjacents, la composició cel·lular dels tumors, i els diferents resultats clínics (Polyak, 2011). El mal pronòstic del càncer de mama és en gran part a causa de la seva resistència a les teràpies actuals, on l'equilibri entre la proliferació cel·lular i l'apoptosi juga un paper clau en la determinació del creixement global o la regressió del tumor en resposta als tractaments (Wong, 2011). Per tant, la identificació de tractaments contra la resistència a l'apoptosi desenvolupada per les cèl·lules tumorals té una importància essencial per tal de trobar noves estratègies terapèutiques.

S'han descrit dues vies principals d'apoptosi: la via intrínseca que es dóna a través de la mitocondria i la via extrínseca que és activada pels receptors de mort. La via apoptòtica intrínseca es caracteritza per la permeabilització de les membranes mitocondrials, un cop s'ha trencat la membrana mitocondrial externa, s'alliberen al citoplasma un conjunt de proteïnes, entre elles el citocrom c, el qual forma un complex multi-proteic anomenat apoptosoma que inicia l'activació de la cascada de caspases a través de la caspasa iniciadora (caspasa-9) (Li et al., 1997). D'altra banda, la via apoptòtica extrínseca s'inicia degut a la unió de lligands com ara el TNF-α o el lligand inductor d'apoptosi relacionat amb TNF (TRAIL) als receptors de mort (Ashkenazi et al., 2008). Una vegada s'han activat els receptors, aquests oligomeritzen i formen complexos que recluten i activen la caspasa iniciadora, caspasa-8. La caspasa-8 activa posteriorment les caspases efectores, com la caspasa-3 i caspasa-7, fet del qual en resulta l'activació o inactivació (així com també la translocació), de diversos substrats com ara la poli ADP ribosa polimerasa (PARP), amb la conseqüent inducció de la mort cel·lular (Juo et al., 1998, Varfolomeev et al., 1998).

En comptades ocasions l'heterogeneïtat del càncer és deguda a anormalitats en gens individuals, sinó que més aviat reflecteix la interrupció de complexos processos intercel·lulars (Barabasi et al., 2011). Per tant, una manera útil de descriure i analitzar l'heterogeneïtat del càncer és l'ús de la biologia de sistemes. Aquest enfocament es basa en l'estudi de les interaccions entre els elements d'un sistema determinat, per tal de comprendre'n les seves propietats. En particular, l'ús de les xarxes d'interacció proteïna-proteïna dóna una perspectiva més àmplia de l'entorn de la proteïna sense perdre els detalls moleculars, proporcionant així una comprensió més profunda dels mecanismes moleculars subjacents als processos patològics complexos.

Per tant, l'aplicació de la biologia de xarxes pot ajudar significativament a l'elucidació de noves dianes terapèutiques i en el desenvolupament de teràpies més eficaces.

7.2. Objectius

El propòsit d'aquesta tesis es pot dividir en dos objectius principals, el primer està dirigit a la identificació i validació de nous gens de càncer de mama relacionats amb l'apoptosi, i el segon es centra en la validació de noves combinacions de fàrmacs pel tractament d'aquesta malaltia.

Objectiu I: Els mecanismes moleculars que relacionen els canvis en l'expressió de la majoria de gens passatgers, amb l'inici i progressió del càncer de mama són en gran part desconeguts. Per aquest motiu, el primer objectiu d'aquesta tesis és identificar el paper de certes proteïnes en l'apoptosi del càncer de mama, la funció de les quals en la malaltia és desconeguda.

Objectiu II: Actualment les teràpies combinatòries aprovades són el resultat de l'experiència clínica empírica, això implica que aquest enfocament, encara que de vegades eficaç, no analitza en detall els mecanismes moleculars subjacents, la qual cosa dificulta el disseny de teràpies combinatòries eficaces. Per aquesta raó, el nostre segon objectiu és aplicar un enfocament basat en la

biologia de xarxes per tal de predir i validar noves combinacions de fàrmacs pel tractament del càncer de mama, les quals assoleixin una major eficàcia clínica i minimitzin els efectes secundaris.

7.3. Resultats i discussió

7.3.1. Nous gens relacionats amb l'apoptosi en el càncer de mama

Ha estat prèviament descrit que PSMC3IP i EPSTI1 presenten rellevants aberracions transcriptòmiques i genòmiques en el càncer de mama (de Neergaard et al., 2010, Gudjonsson et al., 2003, Nielsen et al., 2002), malgrat que els mecanismes moleculars de la seva implicació en aquesta malaltia encara es desconeixen.

Ja que la proliferació cel·lular i l'apoptosi són elements clau pel desenvolupament de la tumorigènesi en el càncer mama, hem explorat la possible implicació de PSMC3IP i EPSTI1 en la regulació d'aquests processos.

Amb aquest objectiu es va induir o inhibir l'expressió dels nostres gens candidats en dues línies cel·lulars de càncer de mama humanes (MDA-MB-231 i MCF-7) per mitjà de la sobreexpressió (transfecció d'ADNc) o del silenciament gènic (transfecció de ARNsi). A més, es va activar la via extrínseca d'apoptosi amb TRAIL, un agonista dels receptors de mort, per tal d'obtenir diferències significatives en la resposta apoptòtica. Posteriorment, es van dur a terme assajos de viabilitat cel·lular (assaig MTT) i assajos específics d'apoptosi (assajos d'activatat caspasa-3/8, d'escissió de PARP, de fragmentació d'ADN (TUNEL) i anàlisi per citometria de flux) per tal d'avaluar el paper d'aquests gens en l'apoptosi del càncer de mama.

PSMC3IP i EPSTI1 interactuen amb proteïnes clau en l'apoptosi

Primer vam explotar l'alta interconnectivitat observada entre els gens d'una determinada malaltia (Oti and Brunner, 2007) per revelar noves relacions entre els gens descrits com a apoptòtics en càncer de mama i PSMC3IP/EPSTI1, fet que podria donar una explicació molecular per a la implicació d'aquests gens en la malaltia.

Amb aquest objectiu, es va fer una cerca bibliogràfica per tal de seleccionar els gens més rellevants implicats en l'apoptosi o proliferació cel·lular en el càncer de mama: AKT1, BAG4, BCAR3, CASP8, CDKN2A, CDKN2C, CHEK2, IGF1R i PARP1. A continuació es van realitzar assajos de yeast-two hibrid (Y2H) per identificar noves interaccions entre aquests gens i PSMC3IP/EPSTI1.

Entre les set interaccions que van ser identificades, aquelles de PSMC3IP i EPSTI1 amb proteïnes centrals de la via extrínseca d'apoptosi (és a dir, amb caspasa-8) van aparèixer com les més prometedores. Curiosament, tant PSMC3IP com EPSTI1 també van mostrar un fort perfil de co-expressió amb la caspasa-8 en teixits de mama normals i en altres tipus de càncer. A més, es va observar que PSMC3IP i EPSTI1 interactuaven amb la proteïna BCAR3, coneguda per regular la proliferació i induir la resistència a estrògens en les línies cel·lulars de càncer de mama ZR75-1 i MCF-7 (van Agthoven et al., 1998). Finalment, observàrem que EPSTI1 interactuava amb AKT1, una proteïna antiapoptòtica que fosforila i inactiva certs components de la maquinària apoptòtica, com ara Bcl2, l'antagonista de mort cel·lular (BAD) i la caspasa-9 (Cardone et al., 1998, Datta et al., 1997). En conjunt, aquests resultats suggereixen que PSMC3IP i EPSTI1 podrien tenir un paper en la regulació de la resposta apoptòtica.

PSMC3IP i EPSTI1 regulen l'activitat de la caspasa-8

Donat que PSMC3IP i EPSTI1 interactuen directament amb la caspasa-8, primer vam examinar la influència d'aquestes interaccions en l'activitat d'aquesta caspasa iniciadora. En aquest sentit, només es va observar una disminució significativa en l'activitat de la caspasa-8 al sobreexpressar PSMC3IP en les cèl·lules MDA-MB-231. Però curiosament, els dos candidats van disminuir l'activitat caspasa-8 en les cèl·lules MCF-7. D'acord amb els resultats de sobreexpressió, l'activitat de la caspasa-8 va augmentar al silenciar l'expressió de PSMC3IP o EPSTI1 en les dues línies cel·lulars, encara que preeminentment en les MCF-7 tractades amb TRAIL després del silenciament de PSMC3IP, i en condicions basals al silenciar EPSTI1.

L'expressió de PSMC3IP i EPSTI1 modula l'activitat caspasa-3 i l'escissió de PARP

Està àmpliament descrit que l'activació de les caspases iniciadores, condueix a l'activació de les caspases efectores, com ara la caspasa-3 en cèl·lules MDA-MB-231 (Janicke et al., 1998). Per tant, vam investigar si la modulació de l'expressió de PSMC3IP o EPSTI1 era capaç d'afectar l'activitat de la caspasa-3 sota condicions basals o d'apoptosi en les cèl·lules MDA-MB-231. Per una banda, la sobreexpressió de qualsevol dels gens no va alterar els nivells d'activitat de la caspasa-3. No obstant això, el silenciament de EPSTI1 va resultar en un augment de l'activitat de caspasa-3 en ambdues condicions, basal i després del tractament amb TRAIL. Mentre que el silenciament de PSMC3IP només va ser capaç d'incrementar l'activitat caspasa-3 en les cèl·lules tractades amb TRAIL. Aquests resultats indiquen que, efectivament, EPSTI1 i PSMC3IP modulen l'activitat de la caspasa-3 en les cèl·lules MDA-MB-231, encara que a diferents graus d'estimulació d'apoptosi.

La caspasa-7 i la caspasa-3 coordinen l'última fase de l'apoptosi mitjançant l'escissió de substrats proteics, com ara PARP (Germain et al., 1999, Tewari et al., 1995), que té un paper essencial en la reparació dels trencaments de ADN d'una sola cadena. Curiosament, la sobreexpressió de PSMC3IP o

EPSTI1 van mostrar una disminució significativa en l'escissió de PARP en ambdues línies cel·lulars. A més, d'acord amb els nostres resultats d'activitat caspasa-3, es va produir un augment dels nivells de PARP escindit al silenciar PSMC3IP o EPSTI1 en les cèl·lules MDA-MB-231 després de la inducció d'apoptosi amb TRAIL. Aquest efecte va ser més pronunciat en les cèl·lules MCF-7, on l'escissió de PARP es va veure incrementada fins i tot en condicions basals.

Tot i que estudis preclínics han demostrat que les cèl·lules de càncer de mama ER-negatives són més sensibles als inhibidors de PARP en comparació amb les cèl·lules luminals (Hastak et al., 2010), els nostres resultats indiquen que l'escissió de PARP és afectada de forma similar per l'expressió de reguladors extrínsecs com PSMC3IP i EPSTI1 tant en ER-negatives (MDA-MB-231) com en línies luminals de càncer de mama (MCF-7). A més, degut a que EPSTI1 també interactua amb AKT1, aquest podria tenir un paper alternatiu en la modulació de l'apoptosi a través de la via PI3K, fet que estaria en línia amb dades preclíniques que demostren una activitat sinèrgica quan es combinen inhibidors de PARP amb inhibidors de PI3K (Ibrahim et al., 2012).

L'augment de la fragmentació de l'ADN i la reducció de la viabilitat cel·lular s'associen amb el silenciament de PSMC3IP i EPSTI1

La fragmentació de l'ADN resultant de les cascades de senyalització d'apoptosi, és un segell distintiu de l'última fase de l'apoptosi (Collins et al., 1997). Per tant, vam examinar si EPSTI1 i PSMC3IP són capaços d'alterar la resposta apoptòtica final més enllà de la modificació de l'activitat caspasa. Amb aquesta finalitat, es van quantificar el nombre de cèl·lules apoptòtiques per citometria de flux i en paral·lel es va analitzar també la fragmentació d'ADN mitjançant l'assaig TUNEL.

En la línia cel·lular MDA-MB-231 vam detectar un augment en el nombre de cèl·lules apoptòtiques al silenciar PSMC3IP sota el tractament amb TRAIL,

mentre que en el silenciament d'EPSTI1 ja s'observava un efecte similar en condicions basals. No obstant això, les imatges de microscòpia de fluorescència de TUNEL no van mostrar resultats concloents. Curiosament, en MCF-7 es va observar un fenotip més clar, on el silenciament de PSMC3IP va ser capaç d'augmentar el nombre de cèl·lules apoptòtiques en condicions basals i el de EPSTI1 va induir un gran augment de cèl·lules apoptòtiques en ambdues condicions. Aquests resultats van concordar amb les cèl·lules apoptòtiques positives observades en els assajos de TUNEL.

Finalment, vam determinar la viabilitat de les cèl·lules de càncer de mama després de la modulació de l'expressió de PSMC3IP o EPSTI1. En aquest cas vam observar que la sobreexpressió de cap dels dos gens va recapitular la viabilitat cel·lular ni en MDA-MB-231 ni en MCF-7 tractades amb TRAIL. En canvi, el silenciament de EPSTI1 va disminuir la viabilitat cel·lular de la línia MDA-MB-231 tractada amb TRAIL. Curiosament, en la línia MCF-7 el silenciament de PSMC3IP o EPSTI1 només va induir una disminució significativa de la viabilitat cel·lular en condicions basals.

En conclusió, els nostres resultats revelen que PSMC3IP i EPSTI1 tenen una funció anti-apoptòtica en les cèl·lules de càncer de mama positives per receptors d'estrogen i en les triple negatives. Tot i que es necessiten estudis addicionals per obtenir una visió més profunda dels mecanismes moleculars subjacents de la funció anti-apoptòtica de PSMC3IP i EPSTI1, les nostres troballes ressalten aquestes dues proteïnes com a prometedores dianes terapèutiques, preeminentment per la seva capacitat de sensibilització respecte l'apoptosi.

7.3.2. Noves combinacions de fàrmacs pel tractament del càncer de mama

Els tumors de mama típicament alberguen poques mutacions consistents i funcionalment caracteritzades, combinades amb nombroses aberracions (no

patògenes) que són sovint úniques per a cada tumor (Gray and Druker, 2012). Aquesta diversitat genètica intrínseca es tradueix en una diversitat fenotípica, la qual dificulta el disseny d'estratègies eficaces pel seu tractament (Geyer et al., 2010). Per tant, malgrat el progrés terapèutic i un repertori en expansió de nous fàrmacs contra el càncer, el fracàs en el seu tractament segueix sent un repte important en la majoria de càncers sòlids avançats, com ara el càncer de mama (Osborne and Schiff, 2011).

Per fer front a aquestes limitacions, la segona part de la present tesi es divideix en dos estudis diferents centrats en la predicció i validació de noves teràpies sinèrgiques pel càncer de mama, dissenyades per tal de superar els mecanismes de resistència i, en paral·lel, reduir els efectes secundaris.

La primera part està dirigida a la recerca de noves combinacions de fàrmacs a través de la quantificació del solapament entre vies de senyalització, mentre que la segona part fa referència a la quantificació de l'activitat de la xarxa.

7.3.2.1. Combinacions de fàrmacs predites a través de la quantificació del solapament entre vies de senyalització

Un aspecte crític en la millora del tractament contra el càncer no és només inhibir les rutes de senyalització oncogèniques primàries que indueixen la proliferació cel·lular anormal, sinó també les redundàncies funcionals i solapaments entre vies que faciliten la supervivència de les cèl·lules canceroses, promovent així la resistència a les teràpies (Kitano, 2004).

Amb aquest objectiu, hem proposat un mètode basat en la biologia de xarxes per tal de quantificar el solapament entre rutes de senyalització implicades en el càncer de mama, en base al qual després hem avaluat l'impacte de la pertorbació combinatòria sobre el solapament de vies. Aquesta mesura ha estat aplicada a un conjunt de fàrmacs aprovats i experimentals per tal d'identificar noves combinacions amb l'objectiu de disminuir de manera

eficient el solapament entre vies i d'aquesta manera augmentar la seva eficàcia clínica.

Selecció de combinacions de fàrmacs

Es van analitzar dos conjunts diferents de combinacions de fàrmacs:

• Fàrmacs aprovats o en fase experimental pel tractament del càncer, en combinació amb medicaments contra el càncer de mama aprovats o experimentals (combinacions antineoplàstiques).

• Fàrmacs aprovats per qualsevol malaltia excepte el càncer, combinats amb medicaments contra el càncer de mama aprovats o en fase experimental (combinacions compassives).

D'entre tots els fàrmacs es van excloure els agonistes o activadors, ja que el nostre objectiu és calcular la inhibició del solapament entre vies de senyalització. Addicionalment, durant el procés de selecció, només es van considerar combinacions de medicaments realment innovadores, per tant, es van ometre combinacions similars a les que estan actualment aprovades o en fase clínica. I a continuació, amb les combinacions prèviament seleccionades es van calcular els diferents valors d'inhibició de solapament entre vies de senyalització (PCI).

Tenint en compte que ha estat prèviament descrit (Jaeger S et al, dipositat) que les combinacions considerades efectives tenen un impacte superior en la inhibició del solapament entre vies (mitjana de PCI=0.34) comparat amb combinacions a l'atzar (mitjana de PCI=0.25), vam establir un llindar de PCI≥0.34 com a filtre inicial per seleccionar les combinacions de fàrmacs més prometedores. Addicionalment, es van excloure les combinacions on la contribució del fàrmac no descrit pel càncer de mama fos negligible (PCI<0.1), així com també les combinacions amb fàrmacs citotòxics ja que el nostre objectiu és treballar amb teràpies dirigides. Finalment, per a les combinacions dirigides contra la mateixa família de dianes terapèutiques es

van seleccionar les que presentaven valors de PCI més elevats i/o majors contribucions individuals.

Validació experimental de les noves combinacions de fàrmacs

Un cop seleccionades les combinacions més prometedores (12 antineoplàstiques i 4 compassives) es procedí a la seva validació experimental per tal de confirmar l'efecte sinèrgic entre els dos fàrmacs.

Amb aquest objectiu, es van realitzar assajos de MTT per tal de quantificar l'efecte citotòxic induït pels fàrmacs individualment i en combinació, en quatre línies cel·lulars de càncer de mama humanes les quals representen els diferents subtipus de càncer de mama: triple negatiu (MDA-MB-231), positiu per receptors hormonals (MCF-7), amb sobreexpressió de HER2 (SKBR-3) i triple positiu (BT-474).

Per tal de determinar si les combinacions provades eren sinèrgiques, additives o de naturalesa antagònica, un cop realitzats els assajos MTT es va calcular l'índex de combinació de fàrmacs basat en l'additivitat de Loewe (DCI) per a cada combinació en cada línia cel·lular (Chou, 2006). L'índex de la combinació de fàrmacs (DCI) compara les concentracions efectives per a la inhibició del X% de la viabilitat cel·lular de cada fàrmac individualment i de la combinació. Es considera un DCI_X per sota de 0.85 com a sinèrgic, per sobre de 1.2 antagonístic, mentre que qualsevol valor intermig representa additivitat ($0.85 > DCI_X \leq 1.2$).

En general, tenint en compte les combinacions antineoplàstiques i les compassives en totes les línies cel·lulars, vam obtenir un 29.7% de combinacions sinèrgiques, un 25% d'additives i el 40.6% amb un efecte antagònic. Atesa l'heterogeneïtat de càncer de mama, no esperàvem que totes les combinacions fossin sinèrgiques en totes les línies cel·lulars, de manera que aquests valors són molt encoratjadors, ja que s'ha descrit prèviament que experiments "high-throughput" sense l'aplicació prèvia d'aproximacions

computacionals són capaços de trobar només entre un 4-10% de combinacions sinèrgiques (Borisy et al., 2003, Zhang et al., 2007).

Curiosament, en les combinacions antineoplàstiques es va observar que el 75% eren sinèrgiques almenys en una línia cel·lular i un terç en almenys dues línies cel·lulars diferents. No obstant això, per a les combinacions compassives només vam identificar una combinació clarament sinèrgica.

Pel que fa a la distribució del DCI a través de les diferents línies cel·lulars, gairebé el 60% de les combinacions van mostrar un comportament sinèrgic en la línia cel·lular triple negativa (MDA-MB-231), mentre que en la triple positiva (BT-474) el 85% eren antagòniques. Està descrit que el solapament de vies de senyalització entre els receptors HER2 i ER promou la resistència a les teràpies (Bender and Nahta, 2008), motiu pel qual es podria justificar l'elevat nombre de combinacions antagòniques observades en la línia cel·lular BT-474 que expressa tots dos receptors HER2 i ER.

Efecte de les combinacions de fàrmacs seleccionats sobre l'apoptosi i el cicle cel·lular

Degut a que els fàrmacs contra el càncer estan dirigits directament o indirectament contra la modulació de l'apoptosi i/o del cicle cel·lular (Ghobrial et al., 2005, Munagala et al., 2011), el nostre proper objectiu va ser determinar si els efectes sinèrgics induïts per les combinacions de fàrmacs es deuen a la inducció d'apoptosi o a la detenció del cicle cel·lular.

Ja que la línia cel·lular MDA-MB-231 (triple negativa) va mostrar el major nombre de combinacions antineoplàstiques sinèrgiques, d'acord amb els valors de la DCI, es van seleccionar les 5 millors combinacions en aquesta línia per als posteriors experiments, a més de l'única combinació compassiva que va mostrar un comportament sinèrgic, en aquest cas en la línia HER2+ (SKBR-3).

Subseqüentment, vam triar les concentracions corresponents a la IC_{50} per a cada fàrmac en el tractament de combinació, per realitzar a continuació els

assajos d'apoptosi (determinació dels nivells de proteïna PARP escindida i anàlisi de la població de cèl·lules apoptòtiques mitjançant citometria de flux) i anàlisi del cicle cel·lular.

Encara que totes les combinacions seleccionades van presentar resultats prometedors en els assajos de MTT, les combinacions que involucren inhibidors de mTOR (everolimus i BEZ235) i moduladors selectius dels receptors d'estrogens (raloxifè), no van mostrar cap efecte significatiu ni en la inducció de l'apoptosi ni en la progressió del cicle cel·lular comparat amb els fàrmacs per separat. Possiblement serien necessàries tècniques addicionals centrades en la detecció de l'autofàgia per tal de capturar l'efecte d'aquestes combinacions, ja que en tots dos tipus de fàrmacs s'ha descrit que poden conduir a la inducció de la mort cel·lular a través de l'autofàgia (Albert et al., 2006, Kim et al., 2015). Per tant, les següents seccions es centren en les combinacions antineoplàstiques que involucren els inhibidors de VEGFR, cediranib i sorafenib, combinats amb l'inhibidor de JAK1/2 (ruxolitinib) o el de MEK1/2 (trametinib), respectivament.

Tal i com està descrit en la bibliografia, excepte el trametinib, cap dels altres tractaments amb els fàrmacs individuals van ser capaços d'induir apoptosi a les baixes concentracions utilitzades en els nostres experiments (Liu et al., 2013, Yang et al., 2014), però, sorprenentment, totes dues combinacions van promoure significativament l'apoptosi tant pel que respecte a l'escissió de PARP com en el nombre de cèl·lules apoptòtiques detectades per citometria de flux (pic sub-G_0/G_1).

Addicionalment, per determinar si l'efecte sinèrgic observat era ocasionat també per efectes citostàtics, es va examinar la distribució del cicle cel·lular. De manera similar al ja observat en els assajos d'apoptosi, l'únic fàrmac que va tenir un efecte clar en els tractaments individuals va ser el trametinib, promovent un important arrest del cicle cel·lular en la fase G_1, juntament amb una disminució del nombre de cèl·lules en les fases S i G_2/M en

comparació amb el control negatiu. Curiosament, la combinació de cediranib amb ruxolitinib va promoure un efecte citostàtic que va conduir a un augment significatiu de cèl·lules en fase S acompanyat d'una reducció significativa en el nombre de cèl·lules en la fase G_1 en comparació amb cadascun dels fàrmacs per separat. Per altra banda, la combinació de sorafenib amb trametinib va induir un efecte citostàtic en G_1, mentre que en aquest cas va ser acompanyat per una disminució significativa tant en les fases S com G_2/M respecte al control negatiu i al sorafenib sol.

Prometedorament, el nostre estudi confirma que la combinació de cediranib amb ruxolitinb a baixes concentracions promou una clara inducció de l'apoptosi acompanyada d'una detenció del cicle cel·lular en la fase S, en cèl·lules de càncer de mama triple negatives. Aquest resultats concorden amb un estudi recent que suggereix que el tractament combinat amb anticossos contra VEGF i inhibidors de VEGFR-2 o JAK/STAT és una estratègia prometedora per reduir l'autorenovació cel·lular en línies cel·lulars de càncer de mama (Zhao et al., 2015). Per altra banda, la combinació de sorafenib amb trametinib també seria un tractament prometedor pel càncer de mama ja que els nostres resultats mostren que aquesta combinació promou efectes sinèrgics bàsicament a través de la inducció d'apoptosi. Fet que concordaria amb estudis fets per altres autors on es descriu que la combinació d'inhibidors de MEK i de VEGFR disminueix l'angiogènesi, el creixement tumoral i la metàstasi en models xenograft de càncer de pulmó (Takahashi et al., 2012).

Per tant, malgrat que estudis addicionals en models *in vivo* i estudis clínics serien necessaris per confirmar l'eficàcia real d'aquestes combinacions, els nostres resultats posen de manifest que ambdues combinacions són estratègies terapèutiques molt prometedores pel càncer de mama triple negatiu, les quals disminuirien a més els efectes secundaris degut a les baixes concentracions emprades.

7.3.2.2 Validació de combinacions de fàrmacs predites a través de la quantificació d'activitat de la xarxa

Col·laboració amb el Dr. Miquel Àngel Pujana, Institut Català d'Oncologia

Donat que els gens i les proteïnes s'organitzen funcionalment dins de xarxes moleculars complexes (Barabasi and Oltvai, 2004) i que en les cèl·lules canceroses els processos biològics i vies de senyalització són robustos a pertorbacions (Breitkreutz et al., 2012, Serra-Musach et al., 2012, Shiraishi et al., 2010, Teschendorff and Severini, 2010, van Wieringen and van der Vaart, 2011, Zadran et al., 2013), en el present estudi es va plantejar la hipòtesi de que la mesura de l'activitat de la xarxa (NA) podria capturar la sensibilitat a una teràpia determinada.

La mesura de NA pot ser utilitzada per predir sinergisme

Aquesta qüestió es va abordar mitjançant la integració de la xarxa d'interaccions protèiques humanes (interactoma) amb la mesura de l'expressió gènica basal en centenars de línies cel·lulars de càncer, la sensibilitat de les quals a diversos fàrmacs havia estat determinada prèviament (Garnett et al., 2012). Tenint en compte totes aquestes dades, es va calcular un algoritme ponderat per a cada línia cel·lular obtenint uns valors de NA que potencialment capturen els mecanismes associats al càncer i la sensibilitat de les cèl·lules respecte a una teràpia determinada.

Posteriorment, per tal de reflectir les possibles associacions entre la NA i la sensibilitat a una determinada teràpia, es van establir els coeficients de correlació de Pearson entre la NA i les IC_{50} per a cada fàrmac, calculats a través de totes les línies cel·lulars, o bé respecte a les línies complint una certa condició, com per exemple l'estatus de mutació d'un gen conductor del càncer. D'aquesta manera es van calcular i analitzar els coeficients de correlació respecte diverses condicions com per exemple mutacions gèniques, vies de senyalització o tipus de teràpies, demostrant que certament,

els perfils de NA poden distingir tipus de fàrmacs segons les seves característiques i també segons l'estatus de mutació dels gens conductors del càncer.

A partir d'aquestes dades es va plantejar la hipòtesi que mitjançant la mesura de NA es podria identificar la combinació de compostos que maximitzés la pertorbació de la xarxa. Donat que les mesures NA semblen capturar l'efecte produït pels processos biològics, aquestes mesures podrien predir sinèrgies entre les combinacions de fàrmacs. D'aquesta manera es va plantejar la hipòtesi que parells de compostos amb perfils de IC_{50} no correlacionats afectarien diferents vies de senyalització a través de les línies cel·lulars, proporcionant una major pertorbació de xarxa, aconseguint així efectes sinèrgics més significatius.

Validació de combinacions sinèrgiques mitjançant assajos de MTT

D'acord amb la hipòtesis prèviament descrita, l'estudi es va centrar en la senyalització de PI3K/AKT, ja que té un paper clau en la carcinogènesi i en la resposta a les teràpies en el càncer de mama (Lai et al., 2015). Per aquest motiu en el nostre laboratori es van utilitzar les següents línies cel·lulars: MCF-7 i BT-474 com a línies cel·lulars de càncer de mama les quals presenten una mutació oncogènica en *PIK3CA (http://www.atcc.org, She et al., 2008)* i la línia cel·lular d'osteosarcoma U2O2 per avaluar la nostra estratègia en altres tipus de càncer. Paral·lelament, altres línies cel·lulars de càncer de mama que alberguen mutacions oncogèniques en PIK3CA (MDA-MB-453 i HCC1954) o alteracions moleculars lligades a una major activitat de AKT (MDA-MB-231 i SKBR-3) (She et al., 2008) van ser testades en el laboratori del Dr. Pujana.

D'altra banda, pel que respecte al grup de fàrmacs dirigits contra PIK3CA/R1 (identificats a través de la correlació entre la NA i IC_{50}), es van considerar aquells amb IC_{50} no correlacionades en les diferents línies cel·lulars de càncer. Seguint aquests criteris, es seleccionà la metformina en

combinació amb AZD-8055, olaparib o SL-0101 pels posteriors assajos de citotoxicitat.

L'índex DCI revela sinèrgies significatives en les combinacions seleccionades

A continuació, es va avaluar l'efecte inhibitori de cada combinació per mitjà d'assajos MTT, seguits de la determinació dels respectius DCIs per tal d'analitzar les corresponents activitats sinèrgiques (DCI<0.85) tal i com s'explica en la secció 3.2.1.

En total, sis de les nou combinacions (66.6%) van mostrar un efecte sinèrgic en totes les línies cel·lulars. Les combinacions de metformina (activador de AMPK) amb AZD-8055 (inhibidor de mTOR) i olaparib (inhibidor de PARP) van donar lloc a un efecte sinèrgic en totes les línies cel·lulars, mentre que la combinació amb SL-0101 (inhibidor de la kinasa S6) va promoure un efecte sinèrgic clar només en la línia cel·lular d'osteosarcoma.

La metformina és un medicament antidiabètic aprovat el qual també està sent testat en assajos clínics pel tractament de càncer de mama (Bonanni et al., 2012, Grenader et al., 2009), però en cap de les combinacions proposades en aquest treball. El nostre estudi mostra que la combinació de metformina amb AZD-8055 presenta un efecte sinèrgic molt marcat, fet que concorda amb estudis recents en els quals s'han observat resultats prometedors en models *in vivo* i *in vitro* de càncer de mama, combinant la metformina amb un altre inhibidor de mTOR (everolimus) (Liu et al., 2012, Wang et al., 2015).

Tenint en compte els nostres resultats i els obtinguts pels nostres col·laboradors en altres línies cel·lulars de càncer de mama, podem suggerir que els models cel·lulars dependents de la senyalització PI3K/AKT poden ser tractats específicament amb una combinació de metformina i AZD-8055 o olaparib, i possiblement amb combinacions d'altres compostos que actuïn sobre les mateixes dianes. Aquests resultats són coherents i expandeixen estudis prèvies on s'observava un efecte sinèrgic al combinar inhibidors de

PI3K i PARP pel tractament de càncer de mama BRCA1-dependents (Juvekar et al., 2012).

En conjunt, els nostres resultats demostren que la mesura de NA és útil per guiar la identificació de combinacions de compostos eficaços, específics i sinèrgics per a la teràpia del càncer.

7.4. Conclusions

En la present tesis s'han utilitzat estratègies basades en la biologia de xarxes per tal de d'explorar amb detall els mecanismes moleculars subjacents al càncer de mama, conduint-nos així a les següents conclusions:

• En la primera part d'aquesta tesi s'han proporcionat noves evidències sobre determinats gens passatgers relacionats amb el càncer de mama, PSMC3IP i EPSTI1, demostrant que ambdós presenten un marcat paper anti-apoptòtic en cèl·lules de càncer de mama, a través de la interacció física amb la caspasa-8, suggerint així aquests dos gens com a potencials dianes terapèutiques preeminentment per la seva capacitat de sensibilització a l'apoptosis.

• En la segona part, la utilització de dues aproximacions diferents basades en la biologia de xarxes ens ha permès identificar noves combinacions de fàrmacs sinèrgiques amb gran potencial pel tractament del càncer de mama.

En particular, s'ha demostrat que les combinacions de fàrmacs que combinen cediranib amb ruxolitinib i sorafenib amb trametinib, presenten un sinèrgic efecte apoptòtic en cèl·lules de càncer de mama triple negatives, suggerint-les així com a prometedores estratègies pel tractament del càncer de mama triple negatiu.